UNIVERSITÀ DI PARMA

UNIVERSITÀ DEGLI STUDI DI PARMA

DOTTORATO DI RICERCA IN INGEGNERIA INDUSTRIALE

CICLO XXXVI

Smart management tools for integrated Power-to-Gas systems

Coordinatore:
Chiar.mo Prof. Gianni Royer Carfagni
Tutore:
Chiar.mo Prof. Mirko Morini

Dottorando:
Emanuela Marzi

Anni Accademici 2020/2021 - 2022/2023

Human life lasts but an instant.
One should spend it doing what one pleases.
In this world, fleeting as a dream, to live in misery
doing only what one dislikes is foolishness.
Yukio Mishima

Acknowledgements

At the end of this PhD, I deeply thank my supervisor Prof. Mirko Morini, for his constant support and supervision, that provided me the opportunity for personal growth, and I thank Prof. Gambarotta, for his valuable guidance. I thank Costanza for her constant presence and indispensable assistance. Finally, I thank Stavros, Valentina and Konstantinos, for their supervision during my research period in Sweden.

I thank my colleagues, those I've only met virtually and those I've had the pleasure of meeting in person, for their pleasant company. In particular, I thank Andrea for sharing part of the PhD journey and being a supportive listener, and I thank the lunchtime mates for bringing a bit of cheerfulness to the corridor.

I thank all the people I have met in Sweden. Most of all, I thank my two friends Dimitra and Jerol, for providing me with some warmth in that cold part of the world, and Smruti, for her kindness and presence. I thank all the researchers I have met in these years, with whom I had fruitful discussions. Perhaps our paths will cross again in the future.

Aside from academia, these three years wouldn't be the same without sharing them with wonderful people who made me always feel loved. First of all, I thank Monica for always believing in me and for the love that helped me grow, I thank Dario for the inspiration and for instilling in me the passion for science and I thank Eugenia for allowing me to see things from other perspectives.

I thank Gabriele from the deep of my heart, for always be there supporting and believing in me.

I thank my housemates of these three years. Thank you for the talks, the shared meals and for the love that made me always feel at home.

Last but not least, I thank all my friends, whether near or far, for being a constant source of vitality in my life. Thank you for the moments we shared, the nice talks, the laughter, the adventures across mountains and sees, the wood weeks and the new projects grown in these years.

Abstract

The growing penetration of renewable energies, which have a fluctuating nature, requires the enhancement of energy system flexibility. This can be achieved through sector integration, which encompasses the conversion of energy into the most convenient vectors. Within this context, the utilization of highly integrated energy systems, known as Multi-Energy Systems (MES), where different energy vectors optimally interact with each other, becomes imperative. Power-to-Gas (PtG) technologies, i.e. the production of gaseous fuels from electricity, emerge as a promising solution when considering sector integration, by allowing surplus renewable electricity to be directly transformed into green hydrogen or methane, which can be utilized or stored. Furthermore, these fuels exhibit excellent long-term storage capabilities, making them a promising option for seasonal energy storage. However, the full potential of PtG systems can be unlocked only if the waste heat released by electrolysis and methanation processes is recovered and fed, for instance, into a district heating network to be supplied to an end-user. A smart energy system, however, which includes these innovative solutions and allows for full integration of the fuel, electrical, and heating sectors, requires advanced management and control tools for optimizing its operation. The scope of this thesis is to investigate the operational strategies of energy systems integrated with PtG solutions by developing novel planning and control tools that enable optimal system management. The core of this research involves three main analyzed problems.

First, an innovative optimization model for the system is introduced, formulated as a Mixed-Integer Linear Programming (MILP) problem. The model tackles the uncertain nature of future disturbances, such as energy needs, generation, and price through a two-stage stochastic programming approach. The algorithm is tested on grid-connected and positive energy districts case studies, allowing for more robust optimization compared to a deterministic approach. Furthermore, the integration of PtG solutions ensures the energy security of the systems and

acts as a buffer to forestall unpredictable behavior of the disturbances.

Second, a control strategy based on Model Predictive Control (MPC) is presented. The controller aims to operate the production of methane from a PtG system and the supply of waste heat to a district heating network with minimal cost. The MPC makes use of a detailed MILP algorithm, able to optimize the system over a future time horizon. The feasibility of the controller is demonstrated through a Model-in-the-Loop simulation platform, and its performances are compared to those obtained with a conventional controller. The novel controller enables a 54 % increase in operating margin and more than halves carbon dioxide emissions. A better exploitation of renewable energy is also obtained (+4.6 %), as well as an increase in the share of heat recovered from the PtG plant.

Lastly, a novel control architecture is proposed that combines the first two developed tools into a more comprehensive and exhaustive tool for coordinating multiple MES integrated by means of a shared natural gas seasonal storage. Each individual MES has its own short-term control logic based on MPC, managing the day-ahead energy exchanges, while a long-term MPC controller, employing a two-stage stochastic programming MILP algorithm, takes into account yearly dynamics and the interactions among the different energy systems, managing the seasonal storage. It provides additional constraints to the short-term controllers, ensuring that yearly goals are met. With the developed control architecture, a multi-temporal and multi-spatial control is obtained. The proposed management is validated in a Model-in-the-Loop configuration, and the benefits of the novel control strategy are quantified. Notably, a smart management for the system is achieved, and the controller is able to optimally control the system by making use of the seasonal storage to balance the seasonal mismatch between production and demand. Indeed, the surplus renewable generation is stored when available, and used in periods of shortage, resulting in a higher utilization of renewable energy and lower emissions and costs.

Overall, the tools proposed in this thesis offer innovative solutions for the effective integration of PtG systems and their optimal management. They are versatile tools, and their utilization for different case studies is straightforward as they were developed in a general way. By optimizing energy management, enhancing efficiency, and ensuring sustainability of energy systems, the novel proposed tools allow taking some steps forward in the realization of smarter and more resilient energy systems for a sustainable future.

Abstract

La crescente penetrazione delle energie rinnovabili, che hanno natura non programmabile, richiede il potenziamento della flessibilità del sistema energetico. Ciò può essere ottenuto attraverso l'integrazione di diversi settori (sector coupling), ovvero la conversione dell'energia nei vettori energetici più convenienti. In questo contesto, diventa imperativo l'utilizzo di sistemi energetici altamente integrati, noti come Sistemi Multi-Energia (Multi-Energy Systems - MES), in cui diversi vettori energetici interagiscono in modo ottimale tra loro. Le tecnologie Power-to-Gas (PtG), ovvero la produzione di combustibili gassosi a partire da energia elettrica, emergono come una soluzione promettente quando si considera il sector coupling, poiché consentono di trasformare direttamente l'elettricità rinnovabile in eccesso in idrogeno verde o metano, che possono essere utilizzati o immagazzinati. Inoltre, questi combustibili presentano eccellenti proprietà per lo stoccaggio a lungo termine, il che li rende un'opzione promettente per lo stoccaggio stagionale dell'energia. Tuttavia, il pieno potenziale dei sistemi PtG può essere sfruttato solo se il calore di scarto generato dall'elettrolisi e dalla metanazione viene recuperato e immesso, ad esempio, in una rete di teleriscaldamento per essere fornito a un utente finale. Un sistema energetico intelligente, tuttavia, che include queste soluzioni innovative e consente la piena integrazione di diversi settori energetici quali i combustibili, l'elettricità e il riscaldamento, richiede strumenti avanzati di gestione e controllo per ottimizzarne il funzionamento. Lo scopo di questa tesi è quello di indagare strategie operative di sistemi energetici integrati con soluzioni PtG sviluppando nuovi strumenti di pianificazione e controllo che consentano una gestione ottimale del sistema. Il nucleo di questa ricerca coinvolge tre principali problemi analizzati.

Innanzitutto viene introdotto un modello di ottimizzazione innovativo del sistema, formulato come problema di Programmazione Lineare Intera Mista (MILP). Il modello affronta la natura incerta dei disturbi futuri, come il fabbisogno energetico, la generazione e il prezzo attraverso un approccio di programmazione

stocastica a due stadi. L'algoritmo è testato su diversi casi studio, che comprendono sia distretti energetici positivi, sia sistemi connessi alla rete elettrica, consentendo un'ottimizzazione più robusta rispetto a un approccio deterministico. Inoltre, l'integrazione di soluzioni PtG garantisce la sicurezza energetica dei sistemi ed è in grado di mitigare gli effetti derivanti da comportamenti imprevedibili dei disturbi.

In secondo luogo, viene presentata una strategia di controllo basata sul Model Predictive Control (MPC). Il controllore mira a gestire la produzione di metano da un sistema PtG e la fornitura del calore di scarto a una rete di teleriscaldamento con costi minimi. L'MPC si avvale di un algoritmo MILP dettagliato, in grado di ottimizzare il sistema su un orizzonte temporale futuro. La fattibilità del controllore viene dimostrata attraverso una piattaforma di simulazione Model-in-the-Loop e le sue prestazioni vengono confrontate con quelle ottenute con un controllore convenzionale. Il nuovo controllore consente un aumento del 54 % del margine operativo e di ridurre di più della metà le emissioni di anidride carbonica. Si ottiene inoltre un migliore sfruttamento delle energie rinnovabili (+ 4,6 %), nonché un aumento della quota di calore recuperato dall'impianto PtG.

Infine, viene proposta una nuova architettura di controllo che utilizza i primi due strumenti sviluppati, combinandoli in uno strumento più completo ed esaustivo per il coordinamento di più MES integrati mediante uno stoccaggio stagionale condiviso di gas naturale. Ogni singolo MES ha una propria logica di controllo a breve termine basata sul MPC, che gestisce gli scambi di energia in tempo reale, mentre un controllore MPC a lungo termine, che utilizza un algoritmo MILP di programmazione stocastica a due stadi, tiene conto delle dinamiche annuali e delle interazioni tra i diversi sistemi energetici, gestendo lo stoccaggio stagionale. Esso fornisce ulteriori vincoli ai controllori a breve termine, che garantiscono il raggiungimento degli obiettivi annuali. Con l'architettura di controllo sviluppata si ottiene un controllo multitemporale e multispaziale. La gestione proposta viene validata in una configurazione Model-in-the-Loop e vengono quantificati i vantaggi della nuova strategia di controllo. In particolare, si ottiene una gestione intelligente del sistema e il controllore è in grado di controllare in modo ottimale il sistema sfruttando lo stoccaggio stagionale per bilanciare lo squilibrio stagionale tra produzione e domanda. Infatti, la produzione rinnovabile in eccesso viene immagazzinata quando disponibile e utilizzata in periodi di carenza, con conseguente maggiore utilizzo dell'energia rinnovabile e abbassamento delle emissioni e dei prezzi.

Nel complesso, gli strumenti proposti in questa tesi offrono soluzioni innovative per l'efficace integrazione dei sistemi PtG e la loro gestione ottimale. Gli strumenti sviluppati sono versatili e il loro adattamento a diversi casi di studio è semplice perché sono stati sviluppati con un approccio generalizzato. Ottimizzando la gestione energetica, migliorando l'efficienza e garantendo la sostenibilità dei sistemi energetici, i nuovi strumenti proposti consentono di compiere alcuni passi avanti nella realizzazione di sistemi energetici più intelligenti e resilienti per un futuro sostenibile.

Contents

List of Figures

List of Tables

Nomenclature

Acronyms

AC	Absorption Chiller
Al	Algebraic
BES	Battery Energy Storage
CHP	Combined Heat and Power
COP	Coefficient of Performance
DHN	District Heating Network
DRL	Deep Reinforcement Learning
DT	Down-Time
Dy	Dynamic
EER	Energy Efficiency Ratio
EU	European Union
FC	Fuel Cell
GC	Grid-Connected
GHG	Greenhouse Gas
GHSV	Gas Hourly Space Velocity
GT	Gas Turbine
HP	Heat Pump
HRC	Heat Recovery Circuit
HS	Hydrogen Storage
IQR	Interquartile Range
KPI	Key Performance Indicators
LCA	Life Cycle Assessment
LCC	Life Cycle Cost
LP	Linear Programming
MES	Multi-Energy Systems
MiL	Model-in-the-Loop
MILP	Mixed-Integer Linear Programming

MINLP	Mixed-Integer Nonlinear Programming
MPC	Model Predictive Control
MS	Methane Storage
NLP	Nonlinear Programming
PDF	Probability Density Function
PE	Positive-Energy
PEM	Proton Exchange Membrane
PID	Proportional Integrative Derivative
PtG	Power-to-Gas
PV	Photovoltaics
RES	Renewable Energy Sources
RIA	Research and Innovation Action
SoC	State of Charge
SP	Set-point
TES	Thermal Energy Storage
TRL	Technology Readiness Level
UT	Up-Time

Subscripts

bo	bought
c	charging
d	discharging
def	deficit
el	electricity
exp	exported
f	fuel
g	gas
in	input
LT	Long-Term
MAX	maximum
MIN	minimum
ng	natural gas
nom	nominal
out	ouput
p	polytropic
r	rotor
s	index for scenario

sd	self-discharge
so	sold
ST	Short-Term
$stor$	stored
th	thermal
u	uncertain parameter
w	water

Greek symbols

α_i	Variable $\in [0,1]$ associated with breakpoint x_i in the piecewise linear approximation of functions of one variable
α_{ij}	Variable $\in [0,1]$ associated with breakpoint (x_i, y_j) i in the piecewise linear approximation of functions of two variables
β_j	Performance parameter for conversion system linearization related to output energy vector j
Δt	Time-step length, (h)
δ	Switch on/off binary variable associated with a conversion unit
ϵ_{in_i}	Variables added for softening the long-term constraints regarding the energy to inject in the seasonal storage
ϵ_{out_i}	Variables added for softening the long-term constraints regarding the energy to withdraw from the seasonal storage
η	Efficiency, -
γ	Standby binary variable associated with a conversion unit
λ	Parameter $\in [0,1]$ used for the definition of the piecewise linear approximation of functions of one variable
μ	Mean of normal distribution
ϕ	Valve opening ratio
Π	Compressor pressure ratio, -
ρ	Density, (kg/m^3)
σ	Standard deviation of normal distribution
ξ_s	Symbol for scenario

Latin symbols

$\mathbf{x}$	First-stage decision variables of two-stage stochastic programming problem
$\mathbf{y}$	Second-stage decision variables of two-stage stochastic programming problem
$\dot{H}$	Enthalpy flow, (J/s)

$\dot{m}$	Mass flow rate, (kg/s)
$\dot{Q}_w$	Heat loss through wall, (J/s)
$\dot{V}$	Volumetric flow rate, (m^3/s)
Q1	First quartile of a data set
Q3	Third quartile of a data set
A	Area, (m^2)
A_{ij}	Matrix coefficients of a general MILP problem, $i = 1, ..., n$, $j = 1, ..., m$
b_j	Constant values of a general MILP problem, $j = 1, ..., m$
c	Energy cost, (EUR/kWh) or (EUR/MWh)
C_c	Correction factor for COP calculation, -
$C_p(u)$	Power coefficient of wind turbine with wind velocity equal to u
c_p	Specific heat at constant pressure, (J/(kgK))
c_v	Specific heat at constant volume, (J/(kgK))
c_i	Objective function coefficients of a general MILP problem, $i = 1, ..., n$
$C_{t,j}$	Thrust coefficient of turbine j
D_{in}	Inner diameter of pipeline, (m)
$DT(i, j)$	Distance between scenarios ξ_i and ξ_j
E	Energy, (kWh) or (MWh)
e_{CO_2}	Carbon dioxide emission factor, (gCO_2/kWh)
$f(x)$	Function of one variable x
$f(x, y)$	Function of two variables x and y
f	Friction factor, -
F_k	Ratio between k of gas and k_{air}, -
f_{obj}	Objective function
$g(\mathbf{x}, \mathbf{y})$	Cost function of the two-stage stochastic programming problem
H	Pressure head, (m)
h_i	Binary variable associated with interval $[x_i - x_{i+1}]$ in the piecewise linear approximation of functions of one variable
h_{ij}^l	Binary variable associated with lower triangle in the rectangle defined by the breakpoints $[x_i, x_{i+1}, y_i, y_{i+1}]$ in the piecewise linear approximation of functions of two variables
h_{ij}^u	Binary variable associated with upper triangle in the rectangle defined by the breakpoints $[x_i, x_{i+1}, y_i, y_{i+1}]$ in the piecewise linear approximation of functions of two variables
HHV	High Heating Value, (kJ/kg)
L	Length of pipeline, (m)

M	Molar mass, (g/mol)
m	Mass, (g) or (kg)
n	Rotational speed, (rpm)
N_c	Corrected compressor rotational speed, (rpm)
P	Power, (kW) or (MW)
p	Pressure, (Pa)
p_k	Probability of interval k of the probability distribution
$PD(i,j)$	Distance between scenarios ξ_i and ξ_j times probability of scenario ξ_i
$Pr(s)$	Probability of scenario ξ_s, -
$Q(\mathbf{y}, \xi_s)$	Cost function part associated with second-stage decision variables $\mathbf{y}$
R	Gas constant, (J/(mol K))
r_{down}	Ramp down limit associated with a conversion unit
r_{up}	Ramp up limit associated with a conversion unit
S	Set of generated scenarios
SU	Start-Up variable associated with a conversion unit
T	Temperature, (K) or (°C)
u	Velocity, (m/s)
V	Volume, (m^3)
$v^i_{t,u}$	Value of the scenario ξ_i at time t for uncertain parameter u
w_i	Mass fraction of the i-th species, -
X	Ratio between valve pressure drop and inlet pressure, -
x	Mole fraction, -
x_i	Decision variables of a general MILP problem, $i = 1, ..., n$
Y	Valve expansion factor, -
y	Yield of reaction, -
Z	Total concentrated pressure drop through pipeline, (Pa)

Chapter 1

Introduction

The complete decarbonization of the energy sector is one of the main challenges faced today and, to address it, energy systems are becoming increasingly complex. This thesis aims at taking some steps forward in the search for possible future management strategies and new solutions to handle this complexity and help the energy sector on the path towards decarbonization. This chapter outlines the motivations and challenges that led to the formulation of this thesis, gives a background of the tools employed, and delineates the contribution of the research presented.

1.1 Motivation and challenges

Addressing environmental issues arising from the current use of fossil fuels is a central concern within research. The ambitious goals set by Europe to combat global warming entail a substantial reduction in greenhouse gas (GHG) emissions in the coming decades, ultimately achieving a carbon-neutral economy by 2050. To meet these targets, radical transformations must take place within the existing energy sector [1]. The urgency of replacing fossil fuel-based energy sources is at the center of the energy transition, and using Renewable Energy Sources (RES) is seen as the most promising solution, primarily due to their capacity to provide an abundant and environmentally friendly energy supply. However, one of the main challenges associated with renewable energy is its intermittent nature, particularly evident in sources such as wind and solar. Managing this variability is essential to maintain the stability of the electricity grid. Consequently, there is a pressing need for long-term, high-capacity electricity storage solutions and

backup production capacity [2]. Furthermore, the successful exploitation of RES such as wind, solar, sustainable biomass and hydropower in decarbonizing the power sector has been demonstrated, achieving promising results [3]. However, there are other sectors, often referred to as hard-to-abate, where electrification (i.e. the replacement of a different energy vector with electricity) is not a viable option, presenting particular challenges in achieving decarbonization.

Within this context, emerging fuel technologies, such as electrofuels, have the potential to assume a pivotal role. These fuels are a category of fuels synthesized directly from electricity. The fundamental concept involves storing electrical energy within the molecular structure of either gaseous or liquid fuels. When produced using renewable electricity sources, these fuels can be considered to be carbon-neutral. Electrofuels serve a dual purpose: they can be employed as energy storage solution and subsequently converted back into electricity, or they can be utilized in combustion systems such as conventional fuels. The production process is based on water electrolysis, with which, by separating water molecule in oxygen and hydrogen, it is possible to obtain pure hydrogen. However, there are notable challenges associated with managing and utilizing hydrogen as a fuel, and for this reason, molecular hydrogen is frequently employed to create more easily manageable liquid or gaseous fuels. Examples include the synthesis of methane and longer-chain hydrocarbons from carbon dioxide, or the generation of ammonia from nitrogen [4].

When integrating the production of such fuels into existing energy systems, besides being themselves a product, their production also involves additional benefits [5]:

- *Addressing power grid balancing*: the transition to a low-carbon energy system driven by the introduction in the system of RES involves technical challenges linked to the fluctuating nature of their supply and their impact on maintaining a balance between energy supply and demand across time and space [1]. Electrofuels production presents an opportunity to enhance the flexibility of the power grid, both spatially and temporally, thus mitigating the need to curtail renewable energy. Furthermore, when considering the Power-to-Gas (PtG) process, which allows the conversion of electricity into methane, and sector coupling of electricity and gas networks, a significant increase of renewable energy share in the overall energy generation mix is allowed [6].

- *Carbon dioxide 'sequestration'*: when the carbon dioxide (CO_2) used for the production of electrofuels is captured from industrial processes or other sources, it can be viewed as temporarily avoided emissions.

- *Storing electrical energy into chemical form*: countries facing intermittent weather conditions, such as those with substantial renewable energy production during the summer season and high electricity demand during winter (or vice versa), necessitate large-scale energy storage solutions. Electrofuels offer a viable option for long-term storage of renewable energy and provide a solution to this challenge [7]. Additionally, electrofuels can serve as a storage solution when power generation is geographically distant from end-users, such as offshore wind turbines or electricity production in remote areas like deserts, as they can be transported for long distances. Figure 1.1 illustrates the advantages of electrofuel technology for storage, including its substantial energy capacity and large discharge time at rated power compared to other existing technologies [8]. These features make these fuels a particularly suitable solution for seasonal energy storage.

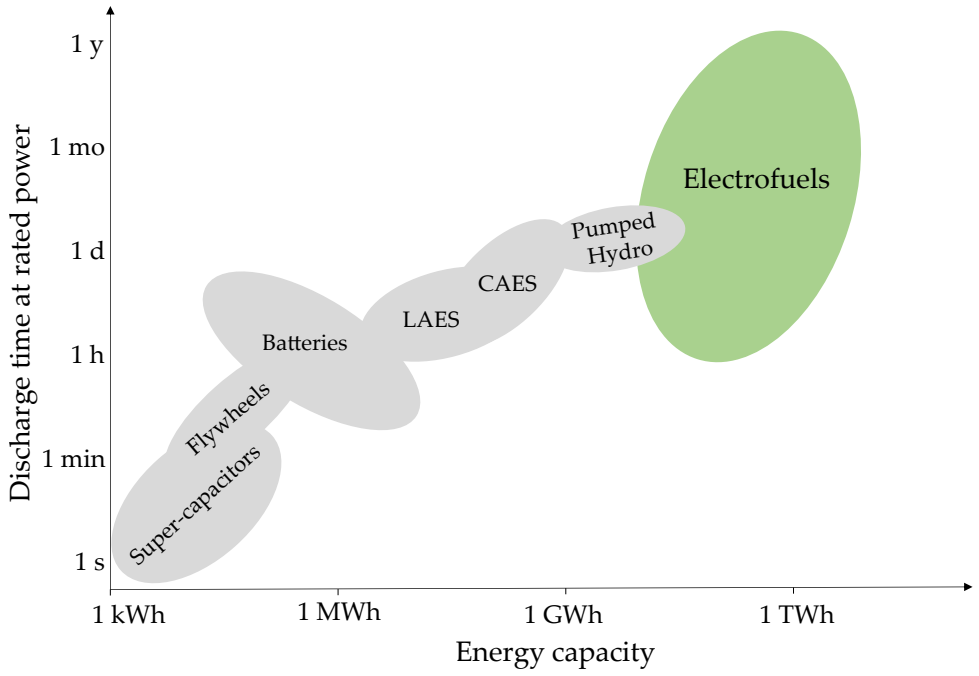

Figure 1.1: Mapping storage technologies according to performance characteristics (CAES = Compressed Air Energy Storage, LAES = Liquid Air Energy Storage).

Technologies

The core of electrofuel production is the conversion of electrical into chemical energy, primarily accomplished through water electrolysis. During this process, water undergoes a split into its constituent elements, hydrogen and oxygen, by the application of electrical current between two electrodes. The electrolyzer, which is used for this process, consists of the following components: a cathode, an anode, an electrolyte that conducts ions and a diaphragm or separator, crucial for preventing the recombination of hydrogen and oxygen [9]. There are many existing electrolyzer technologies, that differs in terms of electrolyte, membrane and operating conditions. The main characteristics of the most notable technologies for electrolysis are shown in Table 1.1 [10–14].

Table 1.1: Main characteristics of different electrolyzer technologies.

	AEC (Alkaline Electrolysis Cell)	**PEM (Proton Exchange Membrane)**	**AEM (Anion Exchange Membrane)**	**SOEC (Solid Oxide Electrolysis Cell)**	**PCEC (Proton Ceramic Electrolysis Cell)**
State of development	Mature	Mature	Under developing	Under developing	Research status
Electrolyte	Alkaline solution	Proton exchange ionomer	Anion exchange ionomer	Solid electrolyte	Ceramic solid electrolyte
Cell separator	Diaphragm	Electrolyte membrane	Electrolyte membrane	Electrolyte membrane	Ceramic membrane
Temperature (°C)	65 to 100 [14]	70 to 90 [14]	50 to 70 [14]	700 to 1000 [10]	300 to 600 [12]
Advantages	Available for large plant sizes, low costs, long lifetime	High efficiency, high dynamics	Low costs, high dynamics	High efficiency, possible integration of waste heat	Dry hydrogen produced, low costs
Disadvantages	Low current density, low dynamics, corrosive environment	Expensive, low durability	Not mature technology, expensive, low durability	Expensive, low durability, corrosive environment, low dynamics	Not mature technology, low durability

As previously mentioned, hydrogen can be further converted into more complex fuels. For example, using methanation process, it is possible to generate synthetic methane: by employing the exothermic Sabatier reaction, hydrogen and carbon dioxide combine to generate methane (CH_4). Methane, in comparison to hydrogen, offers advantages in terms of transportation and utilization. Indeed, by using existing infrastructures, its integration into the current energy system is facilitated.

In addition, long-chain hydrocarbons can be generated through Power-to-Liquid processes. With this approach, a portion of the renewable hydrogen pro-

duced is used to convert carbon dioxide into carbon monoxide. This carbon monoxide is then mixed with additional hydrogen to create syngas, which, in turn, serves as the precursor for Fischer-Tropsch synthesis [4]. Alternatively, the Power-to-Ammonia pathway offers a means to produce carbon-free liquid fuel. This process relies on an abundant atmospheric component, nitrogen, which reacts with hydrogen via the Haber-Bosch reaction to produce ammonia. However, it is worth mentioning that ammonia presents certain drawbacks, including a relatively low energy density, as well as corrosive and toxic properties [4, 15].

Significant efforts are presently underway to develop new technologies and cost-effective solutions for the generation of these fuels. Nevertheless, it is also of paramount importance to investigate their integration into existing energy systems. Indeed, if properly integrated, electrofuels have the potential to fully harness the benefits of renewable energy sources. This integration not only enhances the stability of the energy grids but also reduces greenhouse gas emissions by enabling the use of clean energy for various sectors, including transportation and hard-to-abate industries. In addition, the integration of electrofuels can lead to greater energy security of stand-alone energy systems, reducing the reliance on fossil fuels. The ongoing research and development in this field, coupled with the effective integration of these solutions into existing energy systems, are crucial steps towards accelerating the transition to a cleaner and more sustainable energy system.

Multi-Energy Systems

Achieving ambitious environmental targets while ensuring secure and affordable energy for current and future generations requires comprehensive strategies that address all energy sectors. Within this framework, the conversion of electricity into fuels reveals to be a source of flexibility and gives the possibility to interconnect several sectors. In particular, when considering the PtG pathway, numerous possibilities emerge, including the sector coupling between electricity, gas and heating sectors.

Traditionally, energy sectors have been treated separately in terms of operation and planning. Still, they are becoming increasingly interconnected. For instance, electricity, heating, cooling, and gas networks often interact through distributed technologies such as Combined Heat and Power (CHP), trigeneration systems, Heat Pumps (HP) or PtG systems. Similarly, interactions between the electricity sector and the transportation sector are growing, with the advent of

electric vehicles. Therefore, there is a need to better understand and develop systems that can tackle these challenges: the concept of Multi-Energy Systems (MES) have gained prominence over the past decade as they offer a comprehensive approach to decarbonizing the energy systems. A MES is an energy system that allows the optimal interaction between different energy vectors such as electricity, heat, cooling, fuels, and transportation at various geographical levels. This approach aims to reduce carbon emissions while simultaneously mitigating the economic impact and ensuring efficient energy utilization [16]. Compared to conventional energy systems that treat each energy carrier independently, MES offer notable advantages in terms of technical performance, economic viability, and environmental sustainability. The identification of these benefits led to numerous research efforts dedicated to exploring and advancing the concept of MES [17].

Nevertheless, given their complexity, when dealing with highly interconnected MES, optimal strategies for their management, as well as smart controllers must be investigated and developed, in order to fully exploit their potential [18].

1.2 Solutions employed

In this thesis, some of the available tools and methodologies to perform the optimal management of highly integrated MES are investigated. These methodologies include the Model Predictive Control strategy, the use of optimization algorithms and the Model-in-the-Loop control verification. The tools employed are briefly exposed in the following paragraphs, and they will be presented in detail in the chapters of this thesis, together with applications in which they are tested and verified.

Model Predictive Control

Model Predictive Control (MPC) is a smart control strategy, and its utilization has been tested and evaluated for many applications, demonstrating to be a successful tool [19]. Such controllers include three main steps: model prediction, rolling optimization and feedback correction. Indeed, in these controllers an optimization algorithm is used, that is able to optimize the system to control, by employing a simplified model of the system. Every time-step of the optimization, the algorithm receives the necessary information on the actual behavior of the system, and calculates an optimal trajectory for the control variables over a future time-horizon, known as prediction horizon, which is discretized in a certain

number of time-steps. From this trajectory, only the first control action is implemented in the real system (e.g. as a set-point in low-level controllers). Then, after a time-step is passed, the system states are estimated and given again, together with the forecast of the disturbances, to the controller, which repeats the calculation for a new prediction horizon. In this way, through rolling the optimization horizon and feedback correction, the controller can update the state of the system in real time and the system error caused by inaccurate prediction is minimized [20]. A schematic representation of this control strategy is displayed in Figure 1.2.

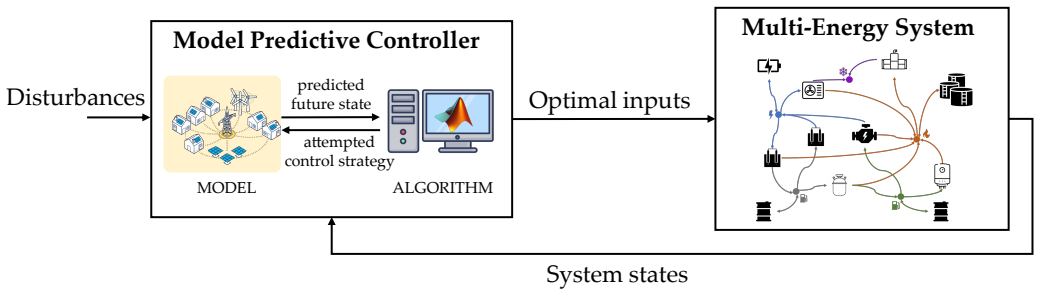

Figure 1.2: Schematization of a Model Predictive Controller applied to a general Multi-Energy System.

The advantages of using this technique, such as the possibility to handle constraints, the consideration of the predicted disturbances and the concomitant optimization make MPC a suitable control technique for MES. With this control strategy, an optimal control of the system is allowed: the controller communicates the optimal control actions to the system every time-step (e.g. 30 minutes), and there is an implicit feedback and feed-forward on the disturbances. However, a suitable algorithm is required to develop such controllers. Among the available optimization algorithms, Mixed-Integer Linear Programming algorithms allow obtaining an accurate result in a calculation time acceptable to the controller, and therefore their utilization is suitable for the use in MPC controllers.

Optimization

As seen in the previous paragraph, an optimization algorithm is necessary when developing MPC controllers. The application of optimization in the field of energy system management is fundamental for the efficient use of resources and the achievement of sustainability objectives. The primary purpose of optimization is to determine the values of system variables that minimize or maximize a function,

often referred to as objective function or cost function, and the selection of these optimal values is influenced by a set of constraints, which represent the physical or operational limitations of the system.

The optimal management of an energy system can be formulated as an optimization problem, with all the power flows and energy stored being the decision variables, while the constraints being the physical and operational limitations of the system, such as energy conservation equations, which ensure that the solution aligns with the real-world boundaries, and the objective of the optimization being for instance minimizing energy costs, maximizing efficiency, or achieving other defined objectives. The optimization problems can be formulated in many ways, being the constraints of the problems, as well as the optimization variables, dependent on the problem considered. For instance, variables can be continuous or integer, and the constraints can be linear equations or nonlinear ones. Therefore, it is possible to obtain Linear Programming algorithms (LP), or Nonlinear Programming ones (NLP) when using only continuous variables, while Mixed-Integer Linear Programming (MILP) and Mixed-Integer Nonlinear Programming (MINLP) algorithms are used if also integer variables are included in the problem.

When optimizing energy systems, the equations that describe them are intrinsically nonlinear, because of the inherent nonlinear nature of energy transformations and conversions. Nonlinearity comes into play when modeling components like conversion units, which often exhibit nonlinear behavior at different load levels. However, techniques such as piecewise linearization can be employed to approximate the nonlinearities and reformulate them as linear or piecewise linear problems. As outlined by Taccari et al. [21], for optimizing MES linear algorihms, such as MILP, are preferred, since the linearized problems can generally be solved more efficiently than their MINLP counterparts, and they appear to be fairly accurate. Indeed, while the MILP formulation introduces a higher level of approximation error when approximating the nonlinear aspects of the problems using linearized correlations, it offers several advantages. First, the global optimality of the solution is guaranteed: indeed, MILP considers all time periods simultaneously within a single, large-scale problem, providing global optimality guarantees. Second, there are many available effective solvers, both open-source solvers (e.g. CBC [22]) and commercial ones (e.g. Gurobi [23]) which are highly efficient and capable of handling large-scale MILP problems with thousands of variables, making them suitable for real-world applications. These solvers have evolved to meet the demands of real-world energy systems, making them indis-

pensable tools for engineers, energy analysts, and policymakers striving to design, manage, and optimize energy systems in a rapidly changing and increasingly complex framework.

The general formulation of a MILP problem comprises the minimization of a linear objective function, subject to linear constraints, while the variables involved being both continuous and integer. The formulation can be expressed in matrix way as in Equation 1.1, with $x_0, ...x_n$ being the variables of the problem:

$$\begin{cases} min_x \begin{bmatrix} c_0 \\ \vdots \\ c_n \end{bmatrix}^T \begin{bmatrix} x_0 \\ \vdots \\ x_n \end{bmatrix} \\ s.t. \\ \begin{bmatrix} A_{00} & \dots & A_{0n} \\ \vdots & \ddots & \vdots \\ A_{m0} & \dots & A_{mn} \end{bmatrix} \begin{bmatrix} x_0 \\ \vdots \\ x_n \end{bmatrix} \leq \begin{bmatrix} b_0 \\ \vdots \\ b_m \end{bmatrix} \\ x_0, ..., x_i \in \mathbb{Z} \\ x_{i+1}, ..., x_n \in \mathbb{R} \end{cases} . \tag{1.1}$$

Model-in-the-Loop application

The novel control strategies need to be tested and verified before the application on real-world case studies. One method to do that is to apply them in a Model-in-the-Loop (MiL) configuration. This means to test the developed controllers on a detailed model of the system, also known as *digital-twin*, that emulates the behavior of the real system. By using this approach, a real system is not affected during the testing phase of the controller, and it is possible to validate the effectiveness of the control action, even by comparing it with traditional rule-based strategies.

A schematization of this procedure is displayed in Figure 1.3 for an MPC controller. Every time-step, the controller receives the forecast of the disturbances, and the initialization variables from the model (e.g. the component or storage states), it performs the optimization and returns to the system digital-twin the control variables (e.g. set-points for low-level controllers).

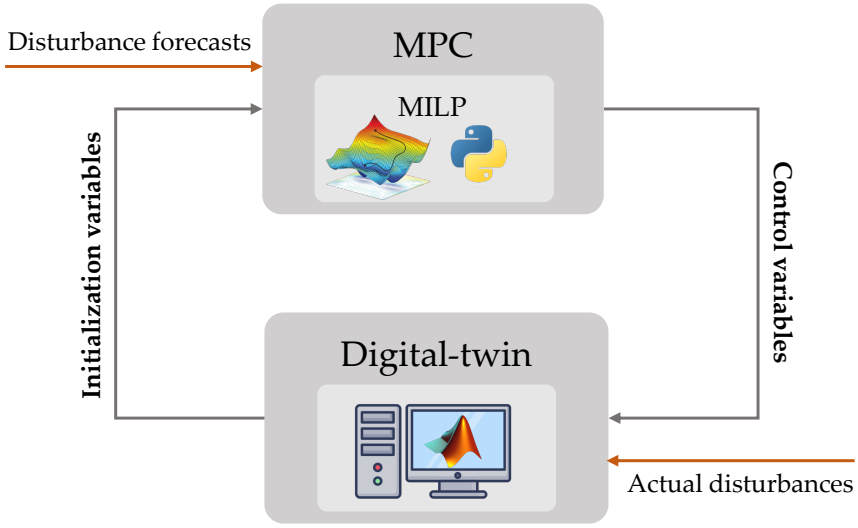

Figure 1.3: Schematization of a Model Predictive Controller applied in a Model-in-the-Loop application.

1.3 Thesis contribution

As outlined above, due to the complexity of these systems, when designing, operating and planning a MES, mathematical models, capable of reproducing the behavior of the system and optimizing it, are essential. However, depending on the purpose of the study, several approaches can be employed.

In this thesis, the integration of new fuel technologies into MES was investigated, and in particular the PtG pathway. Indeed, the production of hydrogen through water electrolysis, and its further transformation into methane was considered. On one hand, hydrogen generation is the most effective and the easiest electrofuel pathway, since it only encompasses the electrolysis process, and the long-term storage of hydrogen was investigated through the development of a *novel two-stage stochastic programming algorithm*, capable of optimizing the operation of the system over the year by considering the uncertain characteristics of external disturbances such as energy prices, needs and renewable generation. The algorithm was tested on different case studies, both grid-connected and positive energy districts, located in regions with different weather conditions. In this way, its ability to optimize the systems under several external conditions was verified.

However, when methane is generated, full integration of the electricity and gas sectors is enabled, and in addition, if the heat recovery from the process is exploited, the integration of the heating sector is also unlocked. Therefore, this process was also studied and innovative control strategies are proposed for

the smart management of the system. In particular, a *novel controller based on MPC* is proposed for the optimal management of a PtG system integrated with a DHN through waste heat recovery. The controller is developed and tested on a case study in a MiL configuration, and the results obtained with the innovative control strategy are compared with those obtained using a traditional rule-based strategy, showing the ability of the innovative controller to outperform compared to rule-based strategies.

In addition, an *innovative control architecture* for the management of a synthetic methane seasonal storage is designed. It is composed of two MPC module levels: a long-term supervisory module that communicates to short-term modules additional information that allow the optimal management of a shared seasonal storage, by taking into account future uncertainties in the disturbances. The novel multi-temporal and multi-spatial control approach is tested in a MiL configuration on two different periods of the year, and the architecture is validated.

The proposed solutions are based on MILP optimization algorithms which were appositely developed: a long-term algorithm which uses two-stage stochastic programming is developed to tackle the uncertain behavior of external disturbances over the year and manage a seasonal storage, and a detailed MILP algorithm is used for short-term MPC controllers, which aim at the real-time optimal management of MES. The developed tools proved to be effective in efficiently managing integrated PtG systems, both in the long-term and on shorter time scales. Furthermore, by integrating the two time scales in a smart control architecture, an optimal management approach for the systems and seasonal storage was achieved.

The thesis focuses on the integration of PtG solutions, nevertheless the approaches can be employed for general MES.

1.4 Outline of the thesis

The present thesis is structured as follows.

In Chapter 2, a research on European projects regarding electrofuel production funded under the Horizon 2020 Framework Programme is first proposed, which helped to define the key drivers that lead the integration of these fuels in the energy framework. Second, it presents the literature which was relevant for the drafting of this work, and in particular the current status on the optimal planning and the smart control of MES is presented, with a focus on PtG optimal

integration in such systems.

The remaining of the thesis regards the three problems analyzed:

- Chapter 3 presents the development and the application of a planning tool for the optimal management of complex energy systems with hydrogen seasonal storage, which considers uncertainties in the external optimization parameters using two-stage stochastic optimization.
- In Chapter 4, a novel Model Predictive Control is presented, developed for the optimal management of a Power-to-Gas system for synthetic natural gas generation, integrated with a District Heating Network though waste heat recovery. The controller is applied in a Model-in-the-Loop configuration and the benefits of the novel control action are quantified by comparing it with a traditional rule-based strategy.
- Chapter 5 introduces an innovative control architecture for managing in an optimal way a natural gas seasonal storage, shared among multiple energy systems. The control strategy is based on Model Predictive Control and it is has a hierarchical architecture, with a double time-scale that allows for the consideration of both yearly dynamics and day-ahead energy exchanges. This application combines the methods used for the other two applications to obtain a more complete tool.

Finally, the conclusions of this dissertation and the future possible developments of the research are presented in Chapter 6. The outline of the thesis is presented in Figure 1.4.

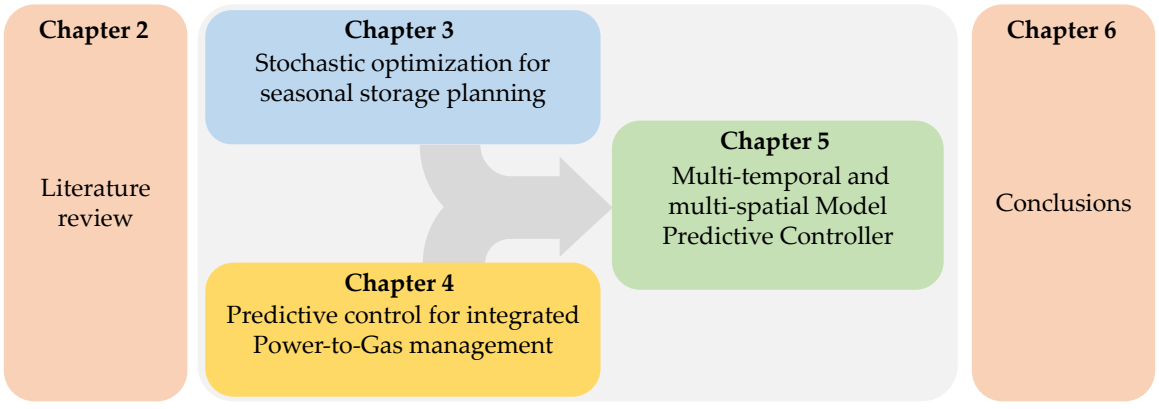

Figure 1.4: Outline of the present thesis.

Chapter 2

Literature review

In this chapter, a literature review of the works which are relevant to this thesis is proposed. This preliminary study served to identify the key motivations that guided the formulation and development of this thesis. First, a research on projects funded by the European Union (EU) in the framework of the Horizon 2020 Programme for Research and Innovation is introduced to define the current state-of-the-art of electrofuel technologies. Then, relevant papers regarding PtG integration into MES are presented, with focus on the optimal management and smart control of the systems. The aim is to identify research works that address these topics and determine fields that require further advancement to improve knowledge.

2.1 Research on European projects dealing with electrofuels

A research has been carried out with the aim to make an overview of all the projects funded under the Horizon 2020 Programme (the EU research and innovation funding program for the period 2014-2020) which deal with the production of electrofuels. The projects were selected, analyzed in terms of key features and an overview of the European state-of-the-art concerning electrofuels production has been achieved.

An extensive internet search was performed with the scope to find actions dealing with electrofuel production, as a solution for decarbonizing different sectors, for balancing the power grid or for storing surplus energy. The main tool used for this search was the CORDIS (Community Research and Innovation Ser-

vice) portal [24], which is the primary source of results of all projects funded by the EU's programs for research and innovation. It includes information such as project factsheets, participants, deliverables, and links to open-access publications. In addition, also the Fuel Cell and Hydrogen Joint Undertaking (FCH JU) [25] and the ERA-Net Smart Energy Systems (SES) [26] websites were used for the research.

The investigation led to the selection of 56 projects, with the mentioned characteristics. To evaluate them, a profile sheet was generated for each of them, which reported the main characteristics of the projects: name, website, logo, grant agreement ID, start and end date, EU contribution, coordinating country, participants, funding scheme, goals, features, demonstration sites and current status. An extensive explanation of the results obtained is available in [5]. Many results have been drawn, and the most relevant are summarized below.

In Figure 2.1, the final utilization of the electrofuels in the selected projects is depicted, namely the application for which the fuels are generated. Several projects encompass multiple final utilizations for the fuel, demonstrating the potential of these fuels to enhance flexibility and integration across diverse sectors. For 18 projects, instead, the final utilization was unspecified: these projects typically involved technologies that were still at the development phase and not yet mature enough for market deployment, such as Research and Innovation Actions (RIAs).

It is notable that a significant number of projects consider transportation as final utilization. Specifically, 17 projects focus on road transport, five on marine transport, and an additional five on aviation. This reflects the substantial effort directed towards decarbonizing the transportation sector. Moreover, 14 projects explore integration into industrial processes, particularly in sectors such as steel, refineries, and fertilizer production. These industries, often referred to as hard-to-abate sectors, see electrofuels as a promising solution for achieving decarbonization. Finally, 13 projects consider re-electrification, underscoring the viability of electrofuels as a storage solution. Sector coupling with the natural gas grid is contemplated in seven projects, while another four projects leverage electrofuels for heating systems.

Figure 2.2 presents the number of projects divided per type of electrofuel generated. Although hydrogen presents certain drawbacks in terms of transportation and utilization, it remains a prevalent choice in the majority of projects, accounting for 39 projects (69.6 %). In these projects, hydrogen is generated through

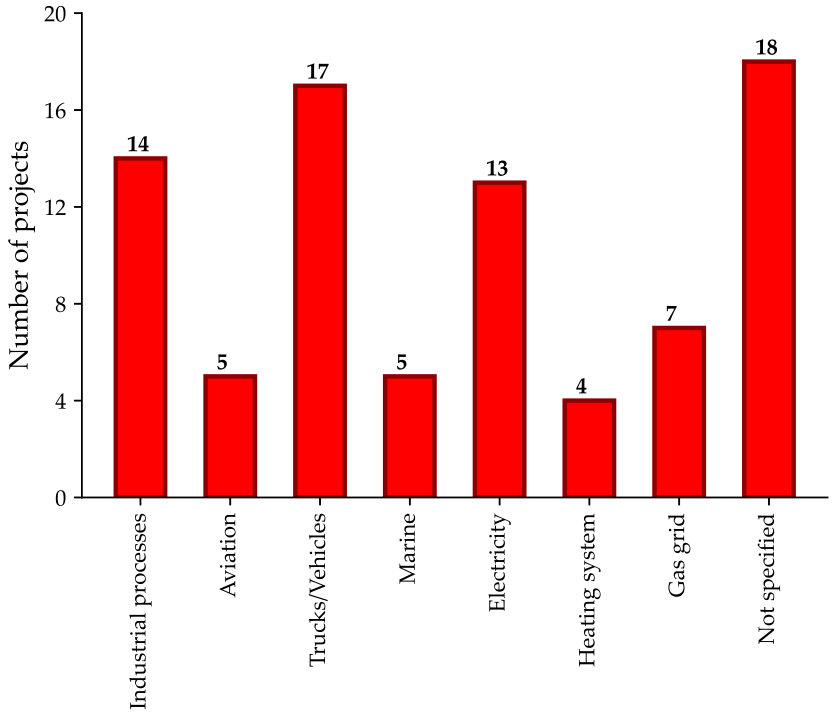

Figure 2.1: Number of projects per final utilization of the electrofuel produced.

water electrolysis and serves as ultimate product. Additionally, in eight projects, hydrogen production is combined with the production of other electrofuels. In 25 projects (44.6 %) other electrofuels are considered, such as methane, ammonia, methanol, kerosene/jetfuel.

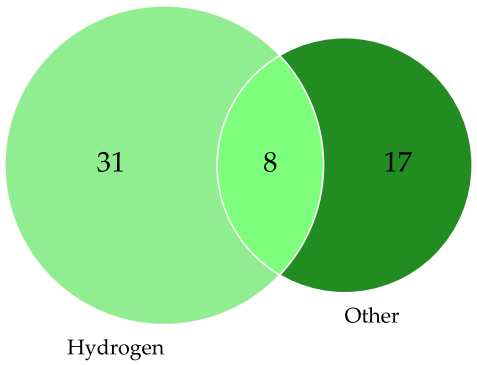

Figure 2.2: Number of projects per type of electrofuel produced.

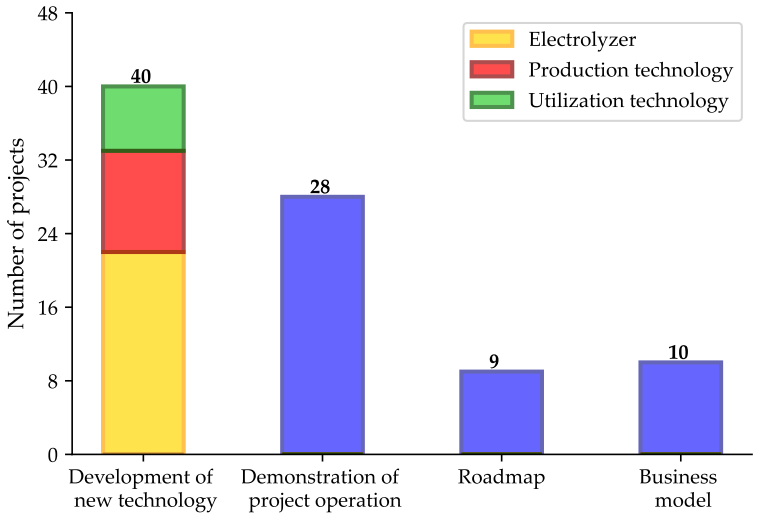

Figure 2.3: Number of projects per project purpose.

The distribution of projects based on their primary aim, which is in some cases more than one for each project, is depicted in Figure 2.3. The majority of projects (71.4 %) are centered around the development of new technologies. Specifically, 22 projects are dedicated to developing novel electrolyzers, while 11 projects investigate alternative production technologies such the methanation process. Additionally, seven projects are focused on pioneering new technologies for the utilization of the fuels. This highlights that there is still a long way to go for the commercialization and full market integration of such technologies. Furthermore, 28 projects (50 %) are oriented towards demonstrating innovative solutions and processes, and 10 projects involve the formulation of business models. The substantial number of projects focusing on business models underscores the growing economic interest in these technologies. This emphasis reflects the imperative to enhance the affordability and cost-effectiveness of electrofuels as a decarbonization solution. Lastly, nine projects are dedicated to supporting future developers and researchers, with the aim of providing guidance and potentially drafting a roadmap for future developments.

In Figure 2.4, the distribution of projects concerning other identified outcomes is illustrated. It is noteworthy that 22 projects (39.3 %) incorporate a Life Cycle Assessment (LCA) or Life Cycle Cost (LCC) analysis, highlighting the significance given to these assessments as valuable tools to better understand the strengths and limitations of the studied technologies. Eight projects are dedi-

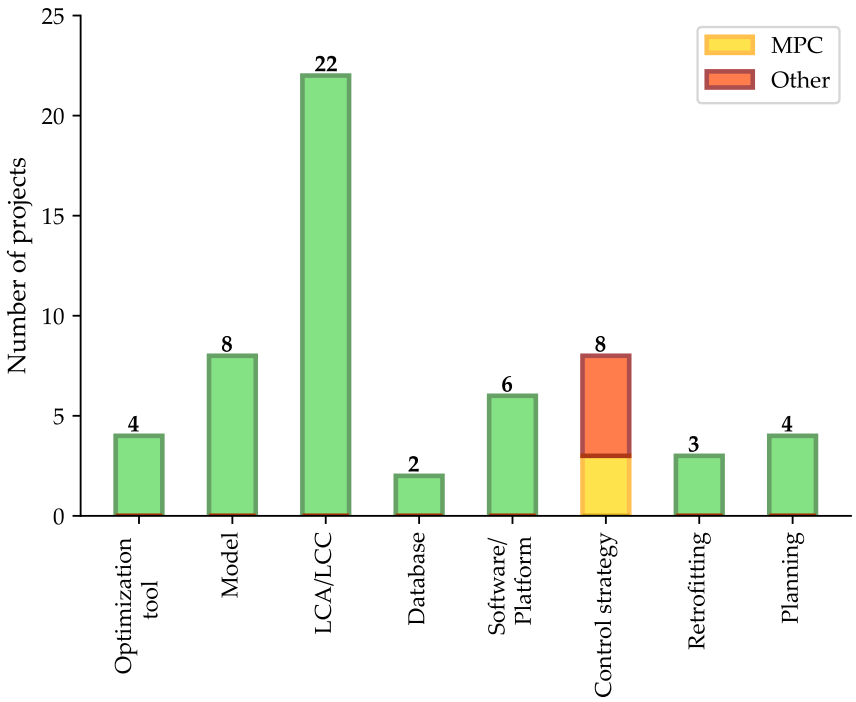

Figure 2.4: Number of projects per outcomes.

cated to the development of control strategies, with three of them utilizing Model Predictive Control (MPC), a notable technique emerging within the context of energy system digitalization. Furthermore, eight projects involve the creation of models, six projects a software or platform, and four projects contribute to the development of optimization tools. Additionally, planning is considered in four projects, retrofitting in three, and two projects yield databases as result. These diverse outcomes collectively contribute to a comprehensive understanding of electrofuel technology, and show that still big effort must be put in the development of planning, optimization and control tools for the exploitation of these technologies.

The presented study gives an overview on the status of European Research and Innovation Actions on electrofuels, and led to the definition of four key drivers, which can serve as guidelines for researchers and stakeholders to identify the pathway to follow.

- **Industrialization.** Many of these technologies have achieved a low Technology Readiness Level (TRL), indicating that there is a substantial distance to cover before they become practical solutions for decarbonizing various sectors. It is of paramount importance to maintain ongoing research

efforts to transform them into market-ready technologies.

- **Barrier abatement.** The absence of well-defined legislation regarding the commercialization and recognition of electrofuels contributes to the difficulty to spread them. It is imperative that policymakers take action to dismantle legal obstacles, facilitating the widespread adoption of these fuels by offering incentives and actively promoting their utilization [27].

- **Flexibility and sector coupling.** Electrofuels, by serving as storage solutions, grid-balancing tools, and enabling technology for sector-coupling, inherently provide a valuable source of flexibility within the energy sector. This flexibility should be recognized as an added value when planning a future resilient and sustainable energy system.

- **Smart management.** On the road towards the ambitious goal of achieving carbon neutrality by 2050 and transition from fossil to renewable energy sources, the energy systems will undergo substantial transformations. These transformations will involve the implementation of various innovative solutions, and an increasing complexity of the systems, that will need innovative and intelligent management strategies to optimize their performance. This necessitates further research and exploration within this field to develop and refine the necessary tools and strategies.

These factors are intended to serve as guiding principles to help stakeholders make more informed decisions. They are mainly directed at policymakers (who have the ability to eliminate legal barriers and introduce incentives to promote the adoption of electrofuels), to researchers (who are encouraged to persist in their investigations in this field) and to industries (which need to study and put efforts to raise the TRLs and achieve commercialization of these technologies).

2.2 Optimal management of integrated PtG systems

The previously exposed applied research projects provided insights into technologies that are on the verge of reaching commercialization, and highlighted the main drivers that can be used by researchers and stakeholders to force the penetration of these new technologies. The present dissertation falls within the scope of the

last two drivers identified: *flexibility and sector coupling* and *smart management*. Indeed, it aims at investigating new ways to enable the integration of PtG technologies for allowing a higher level of flexibility in the system, through the use of novel smart management tools that rely on MILP optimization algorithms and Model Predictive Control.

In the following, a scientific literature review is proposed, that shows the latest advances and cutting-edge researches that served as starting point for the draft of this thesis.

2.2.1 PtG integration in MES

In response to the imperative of reducing carbon dioxide emissions in the energy sector, substantial efforts are currently underway to facilitate the adoption of renewable energy sources, and this transformation is changing the structure of current energy systems. Indeed, the mismatch between energy generation and consumption presents challenges that introduce complexity and necessitates the incorporation of novel technologies and technical solutions. Consequently, this is modifying the traditional approach to energy system management and underscores the importance of exploiting the concept of MES. This entails viewing energy systems as a whole and performing an overall optimization of energy exchanges, encompassing the integration of different sectors.

Within this context, PtG technologies have gained substantial importance by enabling the integration of various sectors through the production of synthetic fuels derived from renewable electricity [28]. These fuels can serve not only as conventional energy sources but they can also be converted back into electricity when needed, thus serving as an effective energy storage solution that mitigates the wasteful curtailment of renewable energy resources. The integration of PtG solutions into integrated energy systems further enhances this potential. This approach facilitates bidirectional interconnections between the electrical and gas networks, by using the excess renewable electricity to generate sustainable fuels [29]. Over the past years, numerous studies in the field of PtG have been conducted, as well as pilot and demonstration projects [30, 31]. Concurrently, there is a growing emphasis on improving the thermal management of these technologies to unlock opportunities for combined heat and power generation while enhancing infrastructure interconnectivity. System-level investigations of these systems have also been undertaken, highlighting their positive impacts on electrical and gas transmission networks. These efforts not only facilitate the long-term

chemical storage of surplus renewable energy, thereby reducing the need for curtailment and decarbonizing the gas sector, but also alleviate congestion in both gas and electricity networks [32].

Despite the current lack of economic efficiency of PtG plants, advances in these technologies and their operation within integrated energy systems are expected to change this landscape. As global awareness of sustainable energy transformation grows, PtG technologies will benefit significantly from evolving energy policies. Furthermore, multiple coordinated energy systems, with well-planned PtG implementations, are promising in providing alternative solutions for future decarbonized energy systems [33].

2.2.2 Planning and scheduling considering uncertainties

As highlighted, when integrating PtG solutions in MES, the optimal management of the integrated system is possible only by employing strategies which include the optimization of the system as a whole. Besides, in the process of modeling and optimizing an energy system over a future time horizon, it is essential to take into account the forecasts of the future external conditions in which the energy system will operate. Typically, deterministic methods are employed, and the forecasts of future disturbances are considered as predetermined. Indeed, due to the complexity of models and the higher computational effort needed to tackle uncertainties, many models tend to give limited consideration to them. However, it is of crucial importance to account for the inherently uncertain behavior of physical systems when forecasting future disturbances (such as user demands, energy price or renewable energy generation) and when performing optimal scheduling. Consequently, evaluating and addressing uncertainties has emerged as one of the main challenges of energy system optimization models.

In the literature, there are many studies that focus on the development of planning and scheduling tools for the management of MES, in which uncertainties in energy needs, prices or production are considered, to obtain a more robust result. Several techniques are used to include the uncertainty in planning and optimization of energy systems: according to Chen et al. [34], the most popular optimization methods are robust optimization [35], stochastic programming [36] and chance constrained programming [37].

Stochastic programming takes the form of a scenario-based mathematical model in which uncertainties are represented through their probability distribution function (PDF). This approach allows for recourse actions to mitigate

infeasibility. In contrast, robust optimization operates without requiring probability distribution information about uncertainties. Its key feature lies in ensuring problem feasibility across all potential realizations of uncertain parameters within a predefined uncertainty set. However, it is often criticized for its conservative nature, as it considers the worst-case scenario within the set. Lastly, chance constrained programming permits some degree of constraint violation without penalizing the objective function, provided that the probability of meeting these constraints is assured with a specified confidence level. To apply this method, the PDF associated with uncertainties must be known [34]. Each method has advantages and limitations, and the main features of them are exposed in Table 2.1 [34, 38].

Table 2.1: Main features of the three optimization methods presented.

Optimization method	Stochastic programming	Robust optimization	Chance constrained programming
PDF	Needed	Not needed	Needed
Advantages	Sequential decision making	Computationally tractable	Relaxation of constraints
Limitations	Computationally expensive if large number of scenarios considered	Overconservative, cannot provide unified strategy	Computationally challenging
Applications	Long-term production planning and design	Short-term scheduling	Production planning, design and operation

For the purpose of this thesis, to investigate the integration of PtG into a MES for seasonal storage, it was decided to employ a two-stage stochastic programming approach. The algorithm was developed with the final aim to be used in a MPC which is able to calculate the best management strategy for a complex MES with an integrated electrofuel seasonal storage. Indeed, with this type of algorithms, it is possible to formulate a problem that considers long prediction horizons (e.g. one year), which is computationally tractable if the number of scenarios is properly selected. By using this approach, the algorithm can be embedded in a predictive controller and run at each time-step, to update the control action in according to current external conditions.

In two-stage stochastic programming models, decision variables are categorized into two groups: first-stage and second-stage variables. The first-stage variables have a deterministic behavior, and must be the same for all scenarios considered, which represent diverse realizations of uncertain parameters. In contrast, the management of second-stage variables is dependent on the specific realization of the uncertain parameters. Some relevant studies that utilize this technique for optimizing the operation and design of MES are presented below.

Two-stage stochastic programming is used in many studies to perform the optimal design of MES, where multiple uncertainties are taken into account, such as energy demand, price and production. In these studies, commonly the first-stage variables represent the selection and size of technologies, while the second-stage variables are associated with the operational aspects of the system. For instance, linear formulations are used in [39], where the optimal design of PV and battery is performed to minimize the economic cost, in [40], where the aim of the optimization is to find optimal sizes for the installation of RES production, and in [41], where the authors build a multi-region stochastic programming model to generate the technology portfolio to be installed, minimizing the total cost over a multi-year optimization horizon. Nonlinear formulations have been used in [42], with the aim to find the optimal energy storage size and bilateral contracts to sign, and in [43], where the optimal size of the system is found, with a 20-year planning horizon. Nevertheless, none of these studies investigate the integration of PtG or the possibility to use this technology to perform long-term seasonal storage.

However, this technology has been included in other works, in which two-stage stochastic optimization has been used, to perform day-ahead scheduling of MES or microgrids, with the aim to find the optimal operation under multiple uncertainties. For instance, Eghbali et al. [44] present a linear stochastic management algorithm for the optimal operation of a smart microgrid, including a wind turbine, photovoltaic unit, fuel cell, electrolyzer, microturbine, and energy storage (such as battery and hydrogen storage tank), which considers the participation of smart homes in demand response management. They include multiple uncertainties that are modeled creating scenarios by discretizing their PDFs. PtG technologies are also investigated in [45], where the authors propose a two-stage linear stochastic programming problem, in which day-ahead scheduling for the electricity system is modeled in a first-stage problem, and the scheduling for the natural gas system is performed as a second-stage problem. They find that, with the integration of PtG, more wind energy can be exploited, additional flexible ramp capabilities are provided, and the gas supply from gas suppliers is reduced, as well as gas load shedding.

In other works, two-stage stochastic programming is used to perform the optimization of MES under multiple uncertainties, even without considering the integration of PtG technologies in the system. For instance, a linear formulation is used in [46], where the authors develop a stochastic scheduling problem for a

virtual power plant, with the aim to maximize the net profit, and they develop a new approach for modeling the uncertainty in wind speed. A linear formulation is also used in [47, 48], where the energy management of a microgrid is investigated, including demand response programs and several system configurations, and considering multiple uncertainties. The results of these activities include the quantification of the benefits of using demand response strategies in terms of cost reduction, and of using a stochastic approach for the optimization.

Shabazbegian et al. [49] use two-stage stochastic programming for the coordinated operation of natural gas and electricity networks, creating a MINLP problem, where the nonlinearities are due to the equations used to model the gas systems. One of their results is to quantify the value of flexibility options, namely the electrical storage systems, to tackle the uncertainties. Other nonlinear formulations exist in the literature to perform multi-objective optimization of microgrids, minimizing both operational cost and voltage deviation [50] or costs and emissions [51]. Finally, Correa et al. [52] analyze the interaction of different sources of flexibility, such as electrical and thermal storages, taking the cycling aging cost of the battery into account, and they show the benefits of using a stochastic approach compared to a deterministic one.

Although many nonlinear formulations exist in the literature, as shown in [21], in many cases it is beneficial to maintain problem linearity. Indeed, for energy system scheduling and planning, nonlinear formulations may offer higher accuracy, but they present a significantly higher computational burden compared to their linear counterparts and it may fail struggle to identify a feasible solution. In contrast, a well-designed linear formulation can reach a good level of accuracy while an optimal solution is ensured.

In Table 2.2, the characteristics of the aforementioned papers are summarized, namely the optimization algorithm used, the aim of optimization, the uncertainties considered, the length of the optimization horizon, the scenario generation method used and if the works also included PtG solutions.

Reference	Algorithm	Aim of optimization		Uncertainties			Opt. horizon	Scenario generation	PtG
		design	planning	needs	RES	prices			
[40]	MILP	✓		✓	✓	✓	day-ahead	roulette wheel mechanism	
[43]	NLP	✓		✓	✓	✓	year	Frank-Copula function	
[42]	NLP	✓		✓	✓	✓	year	moment matching[1]	
[39]	MILP	✓		✓	✓		year	k-means clustering	
[41]	LP	✓		✓			more years	decision tree[2] and Monte Carlo simulation	
[47]	MILP		✓	✓	✓	✓	day-ahead	Kernel Density Estimation	
[46]	MILP		✓	✓	✓	✓	day-ahead	errors from PDF[3]	
[44]	MILP		✓	✓	✓	✓	day-ahead	errors from PDF[3]	✓
[48]	MILP		✓	✓	✓	✓	day-ahead	errors from PDF[3]	✓
[45]	MILP		✓	✓	✓		day-ahead	Monte Carlo simulation	✓
[52]	NLP		✓	✓	✓		day-ahead	based on quantile[4]	
[50]	NLP		✓	✓	✓	✓	day-ahead	roulette wheel mechanism	
[51]	NLP		✓	✓	✓		day-ahead	roulette wheel mechanism	
[49]	MINLP		✓	✓	✓		day-ahead	Monte Carlo simulation	

Table 2.2: Literature linked to two-stage stochastic optimization applied to MES or microgrids

[1]The set of scenarios generated must match the key statistical properties (e.g. mean or standard deviation) of the original distributions.

[2]The scenarios are generated using a set of nodes and branches. Each node is a possible state for the uncertainty at a specific time and a position where a decision can be made. An arc starting from a node is a possible realization of the uncertainty from that state.

[3]To generate the scenarios, the forecasted data is considered as the average value and variable errors are added to the average value of each variable to generate new scenarios.

[4]The median of the forecast is used to select a central value for the forecast. Quantiles 10 % and 90 % are taken as the lower and upper bounds of forecast values. All central and deviated values of uncertainties are combined to form a set of scenarios, representative of all potential combinations of minimum, maximum and central values according to realistic information from measurements and predictions.

2.2.3 Smart control of the system

In light of the imperative to decarbonize existing energy systems, there is currently significant interest among researchers and industries in studying and applying new control strategies and optimization tools in practical systems. This is crucial for enabling the integration of emerging technologies and facilitating sector coupling. Indeed, effectively managing the interaction among gas, electricity, and district heating networks to achieve the decarbonization of energy systems is not solely a matter of installing sufficient capacity. Instead, it is imperative to coordinate and operate the various plants intelligently, since the way different components are integrated into the system and how they are operated profoundly influences their potential. Traditional controllers, based on fixed time schedules, are not able to address these challenges, as they do not offer tailored solutions adapted to real-time conditions and therefore smart control tools are needed.

According to Alabi et al. [53], the main innovative energy management techniques that are able to consider the dynamic behavior of energy systems and control them are Model Predictive Control (MPC) and Deep Reinforcement Learning (DRL). As aforementioned, MPC is an advanced control technique which allows the optimal control of complex systems by making use of an optimization algorithm that contains a simplified model of the system to control [54, 55]. DRL instead, is a technique based on machine learning, recently emerged in the context of managing MES [56]. It combines deep learning and reinforcement learning by using a reinforcement learning agent to interpret the system, learn dynamically using a deep learning approach and alter its action based on feedback from the system. Usually, model-free approaches are used in the context of MES control, and the algorithm learns through the interaction with the environment and update its parameters. In this way, without the use of a system model, it is possible to handle nonlinearities of the problems.

However, while DRL may seem advantageous compared to traditional optimal controllers, its literature remains relatively undeveloped compared to MPC and presents drawbacks such as the high offline computational cost for training it and difficulties in handling constraints [57]. In Table 2.3, a comparison of the two control methods identified is proposed [57, 58].

DRL enables system optimization without relying on a model, but it requires extensive training. Moreover, evaluating its performance and understanding the decision-making processes used by the algorithm can be challenging. Conversely, the implementation of a detailed model within an MPC algorithm allows for

Table 2.3: Comparison of the two advanced control strategies identified.

Control technique	Reinforcement Learning	Model Predictive Control
Performance	Close to optimal	Optimal with perfect model
Model	Not required	Required
Online computational cost	Low	High
Offline computational cost	High	Low
Constraint handling	Difficult	Inherent

more straightforward evaluation. In addition, for complex systems, offline training of the reinforcement learning agent may require long computational time. In contrast, model-based controllers like MPC can be easily customized for the specific case study and, with the use of an appropriate optimization algorithm, online computational efficiency can be achieved. For these reasons, the use of MPC controllers was preferred in this thesis. Its implementation on several case studies was investigated and the relevant literature regarding this technique is presented in the following, in order to highlight the state-of-the-art and the benefits of this technique for managing the integration of PtG processes in MES. To enhance understanding of the optimal integration of these technologies into energy systems, particular emphasis has been placed on studying the heat recovery from the process, and its utilization in DHN, as well as on exploring seasonal energy storage optimal management.

MPC was proven to be an effective control method for optimizing the operation of PtG technology, particularly when integrated in complex MES. Turk et al. [59] explored the application of MPC in a system involving PtG and gas storage to enhance system flexibility and address various uncertainties. Their research demonstrated that MPC reduced wind curtailment and improved the economic performance of the system when compared to traditional control strategies. Additionally, they investigated how the prediction horizon length in MPC influenced computational efficiency, suggesting that the selection should align with the computational efficiency of the application and storage capacity. Abdelghany et al. [60] delved into the implementation of a two-stage MPC for integrating a PtG plant with a wind farm for hydrogen production, intended for use in hydrogen-fueled vehicles or grid injection. Through the use of a two-stage predictive controller, they effectively managed diverse objectives and different time-scales while optimizing the interactions between the wind farm, end-users, and the power grid. Similarly, Fischer et al. [61] successfully applied MPC to enhance the operation of a PtG unit and on-site storage, while considering the constraints of energy networks and fluctuating electricity prices.

PtG for decarbonizing DHN

The studies presented above highlight the importance of employing intelligent control strategies in managing PtG systems. However, the waste heat recovery from PtG plants issue is little covered in the literature. Since the overall efficiency of PtG processes is relatively low, their potential can be unlocked by making a fruitful use of the waste heat generated by their components. Indeed, being an exothermic process, a PtG plant can be integrated into an energy system to provide additional heat that can be utilized by end-users.

Huang et al. [62] conducted research on waste heat recovery: they analyzed the advantages of employing MILP-based economic MPC for real-time control of complex MES integrated with hydrogen production. Specifically, they considered the waste heat recovery from a high-temperature alkaline electrolyzer and its utilization in a DHN. The MPC management led cost savings and improved utilization of RES compared to traditional rule-based strategies. In another research [63], an enhanced MPC is proposed, that incorporates a scheduling correction algorithm into the basic MPC structure in order to achieve a superior trade-off between the scheduling accuracy and the computational efficiency, making it a promising solution for real-time control. The controller effectively optimizes the operation of an hydrogen-based microgrid, with heat recovery from an alkaline electrolyzer, under normal and emergency conditions.

A study conducted by Böhm et al. [64] examined the potential benefits of combining Power-to-Hydrogen with a DHN. Their research revealed several synergies and efficient interactions between these technologies. While high-temperature electrolysis allows heat recovery in alignment with industrial waste heat, the integration of low-temperature electrolysis can be more complex. Nonetheless, modern low-temperature DHN systems provide an opportunity to capture and effectively utilize the waste heat generated by such processes. Indeed, low-temperature DHN are expected to play a pivotal role in the ongoing energy transition by enhancing the energy efficiency of future sustainable energy systems, as many district heating systems in Europe are still predominantly reliant on fossil fuels.

From the perspective of a district heating company, the use of a PtG plant has multiple advantages. It acts as a fuel producer, a carbon dioxide sink, and a valuable source of heat, as outlined in the study by Ikaheimo et al. [65]. In a related study, Weiss et al. [66] demonstrate that it is feasible to decarbonize energy systems when a sufficient capacity of Power-to-Heat and PtG is integrated into the district heating system, and an adequate wind and solar power capacity

is installed to entirely replace the use of fossil fuels. Consequently, by fully exploiting sector integration in the development of smart energy systems, there is a promising potential for achieving complete decarbonization of DHNs and PtG. However, to fully unlock the potential of these technologies, a smart management for the system is needed.

PtG for seasonal storage

Numerous studies in the existing literature have highlighted the prospective energy savings that can arise from the employment of predictive controllers, that allow the system to be optimally managed. A challenge in this framework is the ability for the control action to incorporate information regarding the long-term changes in external factors impacting the behavior of the system. This is of key importance when a seasonal storage is included in the system, and it is clear that effectively optimizing the seasonal storage capabilities of the system is a complex task [67]. Nevertheless, the use of PtG technologies to perform seasonal storage is promising and need to be investigated. For hydrogen storage, there are many examples of MPC applications for MES, that focus on the electrical load and do not consider seasonal unbalances of renewable energy production.

However, Thaler et al. [68] included the seasonal dynamics related to the hydrogen storage through the addition of an hydrogen cost term in the optimization objective function. Indeed, when integrating a PtG system for seasonal storage it is essential to take into consideration the yearly dynamics that regulate its management. Nonetheless, the computational effort of optimizing the whole year with time-steps that allow the real-time control of the system is too large. For this reason, Weber et al. [69] developed a control architecture based on MPC using two controllers with different time scales for the management of a seasonal termochemical storage in buildings. The considered a higher-level annual scheduling objective-based controller, and a lower-level tracking-MPC that flexibly track the trajectory given by the high level controller. Similarly, in [70] the authors developed a novel control strategy for the optimal management of microgrids with high penetration of renewable energy sources and different energy storage systems. A supervisory MPC generates an optimal scheduling using a statistical approach to tackle weather and load forecasting uncertainties. In particular, long-term optimization of the various microgrid components is obtained by the adoption of an optimal generation scheduling, while the real-time management of the system is determined by a short-term MPC module, which uses the results obtained by the

optimal generation scheduling in the optimization. In this way, both long and short-term optimal planning scheduling are achieved by the usage of an MPC.

Zhang et al. [20] propose a multi time-scale optimization strategy, that includes both multi-day forecast information and an intra-day MPC. Within the day, the MPC is performed considering multi-day forecasts, employing hierarchical rolling optimization to track and correct the day-ahead scheduling, and utilizing MPC to account for uncertainties in renewable energy sources and loads. Darivianakis et al. [67] introduce a data-driven stochastic predictive control scheme designed to efficiently manage energy hubs with seasonal storage capabilities. This approach captures long-term system operation through a value function, evaluating historical data to assess system uncertainties and building bounds, that confine the optimal charging trajectory of seasonal storage devices. A multi-stage stochastic optimization problem is formulated to minimize both total energy consumption over a finite horizon and the value function of the seasonal storage at the end of the horizon.

Addressing the challenge of optimizing both short-term and long-term decisions, Cuisinier et al. [71] propose two innovative approaches that rely on adaptive time-step aggregation. These methods maintain continuity between state variables over the long term while ensuring short computation times. The first approach simplifies long-term data and decisions, aggregating them with a simplified long-term model. The second approach incorporates long-term decisions through cost functions, estimated using representative future data periods and the original detailed model. Both approaches are evaluated in the context of a heat production problem, demonstrating promising performance and potential for integration into rolling horizon approaches.

Finally, Castelli et al. [72] introduce a novel approach based on an Affine Adjustable Robust Optimization model, combining day-ahead scheduling, commitment, and economic dispatch with real-time operation adjustments in a rolling horizon algorithm. This model considers various inputs, including day-ahead forecasts, performance expectations, and target charge levels for seasonal storage, optimizing over representative years derived from historical data. This approach addresses the management of energy systems subject to yearly performance constraints and seasonal storage while accounting for short-term forecast uncertainties. Results indicate the efficacy of the proposed rolling horizon algorithm in meeting yearly constraints, managing seasonal storage, and ensuring energy demand fulfillment.

2.3 Novelties of the thesis

From the literature review exposed, it can be concluded that suitable management tools are of key importance to carry out a transition towards a fully decarbonized energy sector. When developing new tools, their versatility, i.e. their ability to be easily adapted for various applications, is essential for their utilization in multiple situations, encompassing energy systems of different sizes and configurations.

In light of this, this thesis aims to develop innovative tools for the optimal management of integrated MES, with particular focus on the integration of PtG solutions. Notably, the following novelties are introduced:

- A *stochastic optimization algorithm* able to tackle the uncertain behavior of future external disturbances such as energy price, demand and renewable production, that can serve as a valuable planning tool.
- A computationally fast *MILP optimization algorithm*, formulated for general MES, easily adaptable to different case studies, and capable of computing the optimal day-ahead energy schedule for the system.
- A scalable and adaptable *MPC controller* that can optimally control a MES in which multiple energy carriers interact at various scales.
- A novel *multi-temporal and multi-spatial control architecture* based on MPC, which is able to take into account both yearly dynamics related to the management of seasonal storage, and short-term unit commitment.

All these tools are exposed in the next Chapters, along with applications in which they are implemented and tested.

Chapter 3

Stochastic optimization for seasonal storage planning

The first problem analyzed in this thesis regards the development of a stochastic optimization algorithm, able to tackle the uncertain behavior of future disturbances by the use of a set of scenarios, and its application to various energy systems with different architectures to test the benefits of using seasonal hydrogen storage [73]. In this chapter, the method used is firstly explained, then the application is introduced, i.e. the case studies analyzed and how the method was implemented, and finally the results are presented and discussed.

3.1 Method

This section outlines the mathematical model, the optimization technique, and the method used to include the uncertainties in the optimization.

3.1.1 Optimization algorithm

As mentioned in Chapter 2, many algorithms exist, that can be used for the optimization of MES. Nonetheless, it was found that linear programming (LP) algorithms are preferred for these applications, compared to nonlinear models. Indeed, the latter can be very challenging in terms of computational effort, and linear algorithms, if properly tailored to the case study, appear to be fairly accurate [21].

A MILP algorithm was used for this application, and it was developed in python using the PuLP library [74]. In such problems, the constraints of the

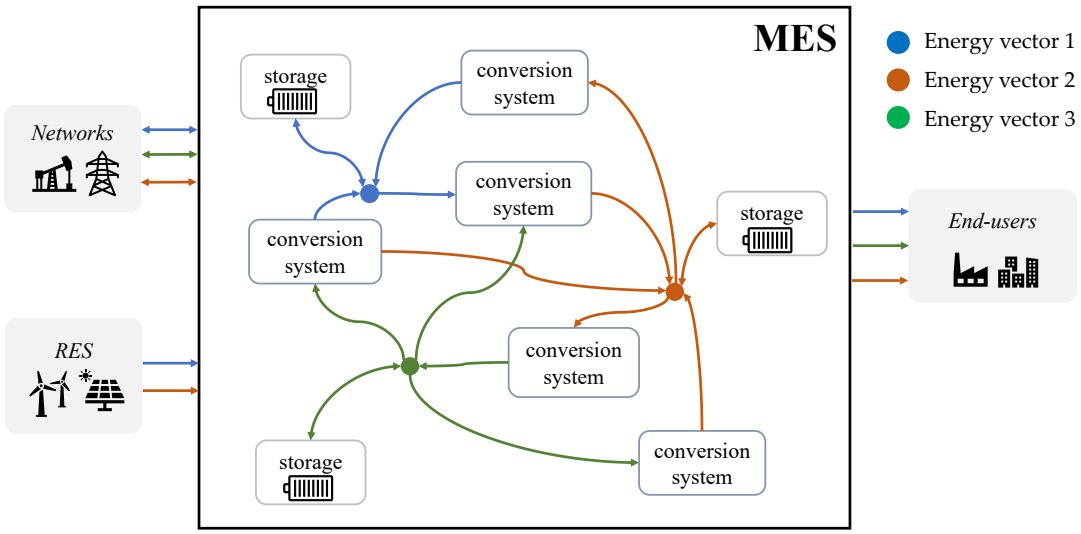

Figure 3.1: Schematic diagram of a general MES.

problem are linear relationships and the variables involved can be both continuous and integer.

The algorithm was developed for a generic MES, as the one schematically shown in Figure 3.1: in this way, it is straightforward to use it for different case studies and applications, only by changing external files (such as .json and .csv files) without modifying the main code. The components involved, which are the different parts of the energy system that interact with each other, are listed below.

Networks: the energy networks involved, for instance electricity grid or gas network. In the model they are described as entities with which the system can exchange energy, and the energy purchased from or injected into the networks can be associated with a certain economic cost, or bounded to a maximum value.

End-users: all those who have a certain energy need in the energy system. They are described as energy consumers, with the energy request given as input to the algorithm, corresponding to the user needs that must be fulfilled.

RES: the renewable energy sources involved. They are described as energy producers, and are associated with a certain amount of energy generated at each time-step, which enters the MES without additional costs.

Conversion systems: all components involved in the system, which can convert one or more energy vectors into one or more other energy vectors: for instance, heat pumps, combined heat and power plants or absorption chillers. They are described by linear equations that correlate the input and output energy flows

of each plant, with specified performance parameters. The general equation that describes the input-output performance curve of a generic conversion system is the following:

$$P_{out,j}(t) = \beta_j P_{in,l}(t)\,, \tag{3.1}$$

where j and l are different energy vectors, t is the time-step, and β_j is the performance parameter associated with the output energy vector j. In addition, the input power at each conversion system is constrained between a maximum and minimum value

$$P_{in,l_{MIN}}\delta(t) \leq P_{in,l}(t) \leq P_{in,l_{MAX}}\delta(t)\,, \tag{3.2}$$

where $\delta(t)$ is the switch on/off binary variable related to the conversion system. A binary variable is a variable of the problem that can only assume the value 0 or 1. In this case, when $\delta(t) = 0$ the plant is switched off, while when $\delta(t) = 1$ the plant is on. It is worth noting that one conversion system can have more than one output energy carrier, with different performance parameters (as in the case of a cogeneration plant, which generates both electricity and heat and, therefore, has electrical and thermal efficiencies).

Storages: all the components that can perform energy storage, such as thermal storages, batteries or fuel storages. The energy stored at each time-step is related with the energy stored at the previous time-step through the following linear equation, which is valid for the energy vector l:

$$E_l(t) = \eta_{sd} E_l(t-1) + \left(\eta_c P_{in,l}(t) - \frac{P_{out,l}(t)}{\eta_d}\right)\Delta t\,, \tag{3.3}$$

where E_l is the energy stored in the form l, η_{sd} is the self-discharge efficiency of the storage, while η_c and η_d are the charge and discharge efficiencies, and they model the energy losses when charging and discharging the storage, respectively.

For all the variables, lower and upper bounds are also set, according to the design of the energy system modeled. In addition, other constraints of the model are represented by the energy balances at each node of the system, indicated by dots in Figure 3.1. For a general energy vector l, the balance is described by the following equation:

$$\sum_{n=1}^{N_{in}} P_{in,l}(n,t) = \sum_{m=1}^{N_{out}} P_{out,l}(m,t)\,, \tag{3.4}$$

where N_{in} and N_{out} are the number of energy flows in the form l entering and exiting the node, respectively. They also include the energy exchanged with the

networks, the energy produced by the RES and the energy used by the end-users.

3.1.2 Two-stage stochastic programming

When optimizing the management of energy systems over a future period, the optimization involves parameters, such as end-user needs, weather conditions, energy prices, or renewable energy generation, which are to some extent uncertain. Indeed, their future behavior can be forecasted, but it is clear that the forecasts are not entirely precise. In this work, two-stage stochastic programming was used to address these uncertainties.

Stochastic programming is a powerful framework for modeling optimization problems that deal with uncertainty. It achieves this by creating a finite number of scenarios that represent different realizations of the uncertain parameters over the time-span considered, and each scenario is related with a probability of occurrence. In the case of two-stage stochastic programming problems, the decision variables are divided into two groups: first-stage and second-stage decision variables. The first-stage variables are the same for all scenarios and must fulfill the constraints for each of them. On the other hand, the second-stage variables are repeated for each scenario, and their management depends on the specific scenario being considered. The cost function in two-stage stochastic programming is built by summing the costs associated with all the scenarios ($f(\mathbf{x})$) and those associated with each possible future scenario considered ($Q(\mathbf{y}, \xi_s)$). Each term in the summation is multiplied by the probability of occurrence of the corresponding scenario, as described in the following equation:

$$\min g(\mathbf{x}, \mathbf{y}) = \sum_{s=1}^{N_s} Pr(s)[f(\mathbf{x}) + Q(\mathbf{y}, \xi_s)] = f(\mathbf{x}) + \sum_{s=1}^{N_s} Pr(s)[Q(\mathbf{y}, \xi_s)]\,, \quad (3.5)$$

where ξ_s are the future scenarios, $Pr(s)$ is the probability of occurrence of scenario ξ_s, N_s is the total number of scenarios considered, $\mathbf{x}$ represent the first-stage decision variables while $\mathbf{y}$ the second-stage decision variables.

For this application, since the initial deterministic problem is a MILP, the resulting two-stage stochastic programming problem remains a MILP, with the cost function being the one described in Eq. (3.5). In addition, the constraints of the problem involve all the constraints related to the first- and second-stage variables. In this way, all the stochastic parameters will be dependent on the

considered scenario.

3.1.3 Uncertainty modeling

The optimization model can effectively handle uncertainties and provide meaningful results for decision making regarding the optimal operation of the energy system by employing scenarios. As introduced in Section 2.2.2, the scenarios to use in these applications can be generated and reduced by means of several methodologies. The methods used in this thesis are explained in the following paragraphs.

Scenario generation

A scenario generation method based on Monte Carlo sampling combined with the roulette wheel mechanism was utilized for the present application [51, 75]. This method requires knowledge of the probability density function (PDF) of the uncertain parameters and their forecast over the prediction horizon. The steps involved in scenario generation are the following:

- **Discretization**: each time-step, the PDF of each uncertain parameter is discretized into a finite number of intervals, centered around the mean value, which corresponds to the forecast of the uncertainty at the considered time-step, as shown in Figure 3.2. The length of each interval is the standard deviation of the distribution σ. For the purpose of this work, to model the uncertain parameters, the normal PDF is used [48], which is described by Eq. (3.6)

$$PDF(x) = \frac{1}{\sigma\sqrt{2\pi}} e^{\left(-\frac{(x-\mu)^2}{2\sigma^2}\right)} . \tag{3.6}$$

- **Probability calculation**: for each interval k, an associated probability is calculated by integrating the PDF within the interval:

$$p_k(x) = \int_{x_{start}}^{x_{end}} PDF(x)dx . \tag{3.7}$$

- **Probability normalization**: the probabilities p_k are normalized in such a way that their summation becomes equal to one, and an accumulated probability is associated with each interval, as depicted in Figure 3.2.

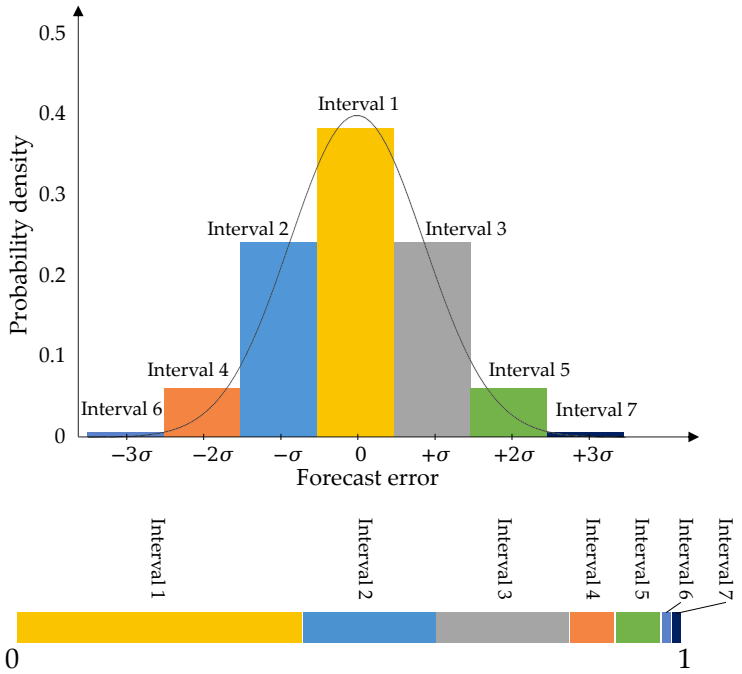

Figure 3.2: Discretization of the PDF for the uncertain parameters, and accumulative normalized probabilities.

- **Scenario creation**: for each time-step of the prediction horizon and for each uncertain parameter, a random number in range $[0, 1]$ is generated, and the corresponding interval is consequently picked. The value for the random parameter becomes equal to the mean value associated with the interval selected, while the associated probability is set as equal to that of the interval selected.

- **Scenario probability**: assuming that the uncertain parameters are independent from each other, the probability of each scenario ξ_s is calculated based on the probabilities of the selected intervals for all uncertain parameters, as follows

$$Pr(s) = \frac{\prod_{u=1}^{N_u} \prod_{t=1}^{N_t} p_k(u,t)}{\sum_{s=1}^{N_s} \prod_{u=1}^{N_u} \prod_{t=1}^{N_t} p_k(u,t)}, \tag{3.8}$$

  where N_t is number of time-steps, N_u is the number of uncertain parameters, N_s is the total number of scenarios generated and $p_k(u,t)$ is the probability associated with the value of the uncertain parameter u of the scenario at the time-step t.

Scenario reduction

To effectively represent uncertainties through scenarios and reproduce their probabilistic behavior, a large number of scenarios is initially generated. However, for the sake of tractability in the optimization problem, the number of scenarios needs to be reduced while maintaining an accurate representation of the uncertain behavior of the system, and an appropriate scenario-reduction method must be chosen. In the present thesis, a simultaneous backward reduction method is employed, which considers both the probability of the scenarios and their similarity to other existing scenarios [51, 76].

Considering N_s scenarios $\xi_i\,(i = 1, ..., N_s)$, each with a probability equal to $Pr(i)$, let $DT(i, j)$ indicate the distance between two different scenarios ξ_i and ξ_j, calculated as follows

$$DT(i,j) = \sqrt{\sum_{t=1}^{N_t}\sum_{u=1}^{N_u}\left(v_{t,u}^{i} - v_{t,u}^{j}\right)^2}, \tag{3.9}$$

where $v_{t,u}^{i}$ is the value of scenario ξ_i for the uncertain parameter u at the time-step t, N_t is the number of time-steps and N_u is the number of uncertain parameters. The scenario reduction method employed is shown in Figure 3.3, and it is composed of the following steps:

Step 1: Let S be the initial set of scenarios to be reduced, which initially contains all the scenarios. For all the scenario pairs (ξ_i, ξ_j), the distances $DT(i, j)$ are calculated.

Step 2: For each scenario $\xi_k \in S$, the scenario ξ_r with the minimum distance $DT(k, r(k))$ from it is found.

Step 3: For each scenario $\xi_k \in S$, the value $PD(k, r(k)) = Pr(k) * DT(k, r(k))$ is calculated and the scenario ξ_d with $PD(d, r(d)) = \min PD(k, r(k))$ is selected.

Step 4: The scenario ξ_d is deleted from the set of scenarios S and the probabilities of the scenarios are updated, by adding the probability of the deleted scenario ξ_d to the probability of ξ_r: $Pr(r) = Pr(r) + Pr(d)$.

Step 5: The procedure from Step 2 to Step 4 is repeated until the desired number of scenarios is reached.

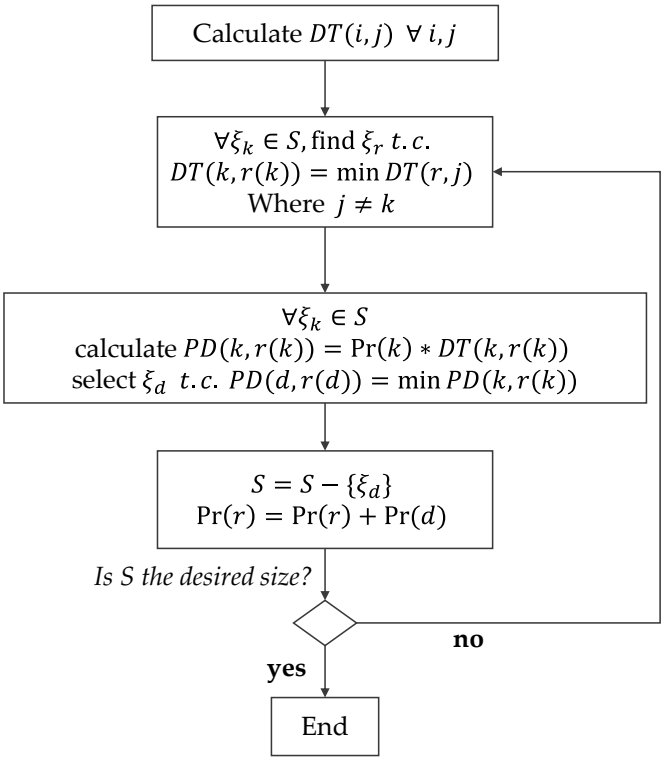

Figure 3.3: Simultaneous backward scenario reduction method.

A schematic representation of the process is displayed in Figure 3.4: here, the circles represent the scenarios, and the distance among circles the distance among scenarios. The scenarios are initially a large number (a), and they are are reduced by incorporating the least probable ones with the most probable scenarios close to them (b), resulting in a lower number of scenarios (c).

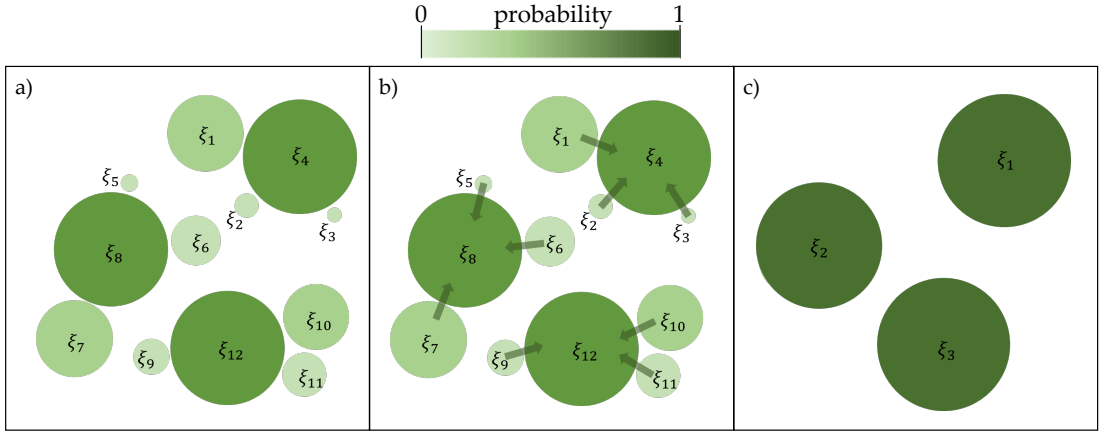

Figure 3.4: Schematic representation of the simultaneous backward scenario reduction method.

By applying this scenario-reduction method, the number of scenarios is effectively reduced while preserving a meaningful representation of uncertainties and maintaining the probabilistic behavior of the system.

3.2 Application

This section presents the case studies to which the method described was applied, and all the characteristics of the optimizations performed.

3.2.1 Case studies description

The MILP-based stochastic optimization algorithm presented in Section 3.1 was tested on four case studies: two grid-connected and two positive energy districts. These case studies served as virtual test benches to test the algorithm, and the results were compared with the ones obtained using a deterministic approach, with the same boundary conditions. In the following sections, the four case studies are described.

Grid-connected case studies

The city of Västerås was chosen as a first case study, which is a municipality in the south of Sweden. The energy system of the city can exchange electricity with the electrical grid, therefore it is grid-connected (GC). The needs of the city are fulfilled using three combined heat and power plants (CHPs), which convert residential waste, biofuels and recycled fuels into heat and electricity. In addition, an absorption chiller (AC) and two heat pumps (HPs) contribute to the supply of the district heating network (DHN) of the city together with the CHPs, and to the fulfillment of the cooling needs. The energy system is also equipped with a water tank that serves as thermal energy storage (TES), while another bigger underground thermal storage will be built in the near future (TES-u), to perform seasonal storage, and it was included in the optimization model. This first case study was called GC_Västerås.

With the aim to analyze the impact of the introduction of hydrogen seasonal storage on the existing MES, a second case study was developed starting from the reference system (GC_Västerås_H2). It was assumed to install a PEM electrolyzer (PEM), a hydrogen storage tank (HS) and a fuel cell (FC) to convert the hydrogen into electricity and heat. The configuration of this second case study is displayed

in Figure 3.5. It was also assumed to use part of the produced hydrogen to fulfill the needs of a steel mill in the area (the Hallstahammar steel mill [77]). The characteristics of the plants involved are listed in Table 3.1.

Table 3.1: Characteristics of the technologies of the GC case study.

Technology	Nominal inlet power	Performance parameters	Reference
CHP 5	200 MW	$\eta_{th} = 63\,\%$, $\eta_{el} = 27\,\%$	[78]
CHP 6	167 MW	$\eta_{th} = 63\,\%$, $\eta_{el} = 27\,\%$	[78]
CHP 7	150 MW	$\eta_{th} = 63\,\%$, $\eta_{el} = 27\,\%$	[78]
HP 1	5 MW	$COP = 3$, $EER = 1.4$	[79]
HP 2	4 MW	$COP = 3$, $EER = 2.5$	[79]
AC	9 MW	$EER = 0.78$	[79]
PEM	200 MW	$\eta_{H_2} = 60\,\%$, $\eta_{th} = 16.1\,\%$	[80]
FC	200 MW	$\eta_{th} = 25\,\%$, $\eta_{el} = 55\,\%$	[81]
HP-el	32.2 MW	$COP = 4$	[82]
Technology	Nominal capacity	Performance parameters	Reference
TES-u	13 000 MWh	$\eta_{sd} = 99.5\,\%$, $\eta_c = \eta_d = 95\,\%$	[83]
TES	1 200 MWh	$\eta_{sd} = 99.9\,\%$, $\eta_c = 95\%$, $\eta_d = 95\,\%$	[83,84]
HS	66 644 MWh	$\eta_{sd} = \eta_c = \eta_d = 100\,\%$	[84]

It needs to be mentioned that the PEM efficiency also includes the electricity used by the compressor, needed to compress the hydrogen until the storage pressure (max 100 bar) [85]. In addition, HP-el represents an additional heat pump which is introduced in order to upgrade the temperature level of the heat recovered from the electrolyzer (around 55 °C), to the temperature level needed for the DHN of the city (80 °C). For a clearer representation, the HP-el is not included in Figure 3.5. Moreover, given the state of knowledge and the purpose of the analyzes performed, it was decided to consider a self-discharge efficiency η_{sd} equal to one for the hydrogen storage, as it has been done in other works [84,86]. Although for some storage technologies, due to the small size of the hydrogen molecule, the self-discharge efficiency might be lower, this assumption does not affect the reliability of the developed algorithm.

The three CHPs of the city burn different fuels: CHP 5 uses biofuel, which costs 19 EUR/MWh [87], CHP 7 uses renewable fuels, which have a cost of 9.5 EUR/MWh [87], while CHP 6 uses residential waste, which utilization entails a revenue of about 16 EUR/MWh [88]. Indeed, the residential waste is also imported from other cities in Europe, and it has a negative price since the plant owners get a revenue for managing it. Part of the electricity demand of the city is covered by the CHPs; nevertheless, the CHPs are heat-driven rather than

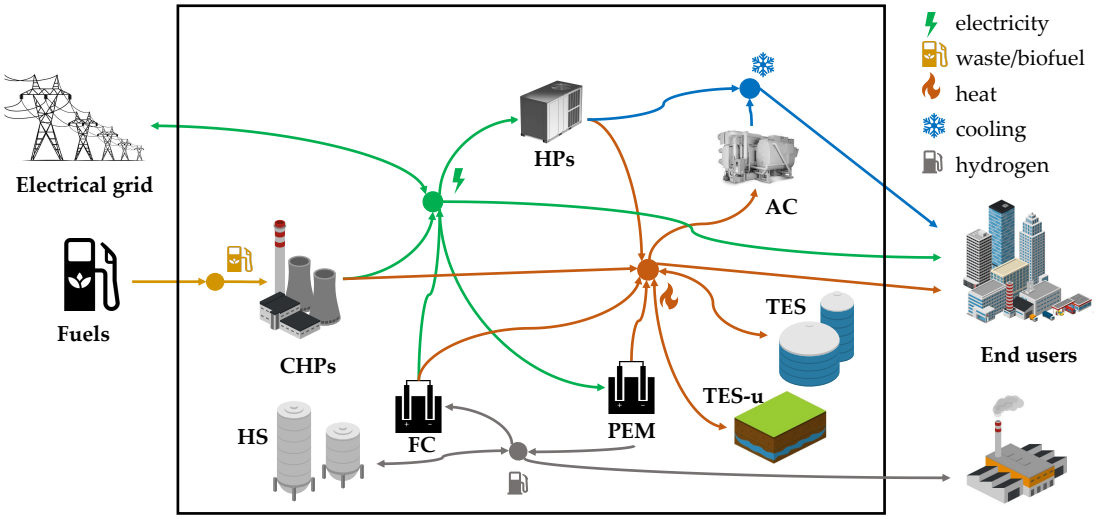

Figure 3.5: Layout of the GC case studies (PEM, HS and FC are only present in the GC_Västerås_H2 case study).

electricity-driven, therefore the remaining part of electricity needs are fulfilled by using electricity from the national electrical grid. The prices of electricity in Sweden are regulated by Nord Pool, which manages power exchange in the Nordic countries [89].

The disturbances given to the optimization algorithm are the energy needs of the entire city, namely electrical, thermal, cooling and hydrogen needs, (shown in Figures 3.6a and 3.6b) and the energy prices (which are fixed for fuels and variable for electricity). The electrical and thermal needs are estimated using historical data, while the district cooling demand is calculated based on [90]. In addition, the forecast over the year for the electricity price is estimated based on historical price data and it is displayed in Figure 3.7.

In the stochastic optimization, the management of the first-stage variables is defined a priori and cannot be changed depending on the future realization of the scenario. Instead, the second-stage variables represent a source of flexiblity for the system, as their behavior is calculated based on the realization of the scenario. For this case study the variables associated with the PEM electrolyzer, CHPs, and AC management are selected as first-stage variables, while the ones related to the FC, HPs, storages and electricity bought are taken as second-stage variables, and therefore the undesirable effects of the uncertain parameters can be adjusted through their management.

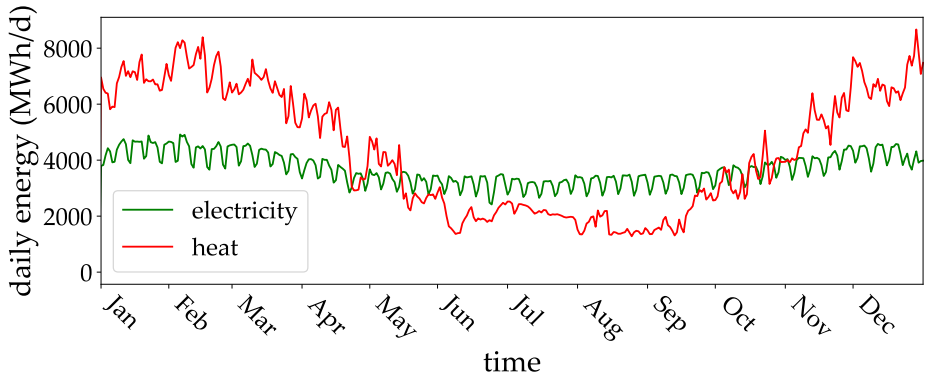

(a)

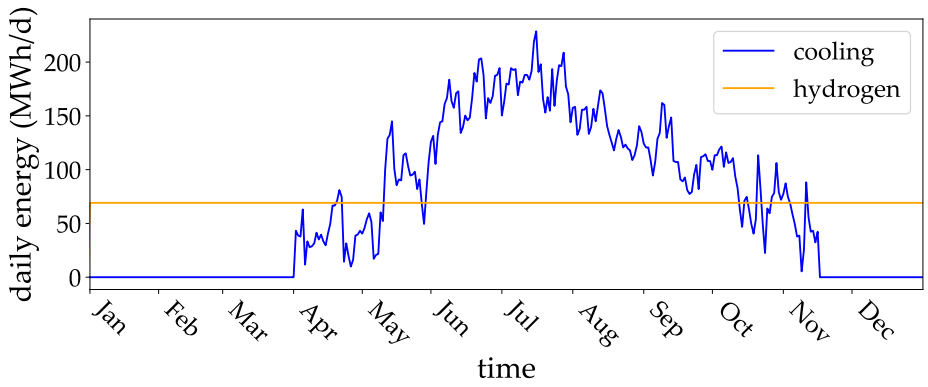

(b)

Figure 3.6: Forecast of the energy needs for the GC case studies (the hydrogen need is only present in the GC_Västerås_H2).

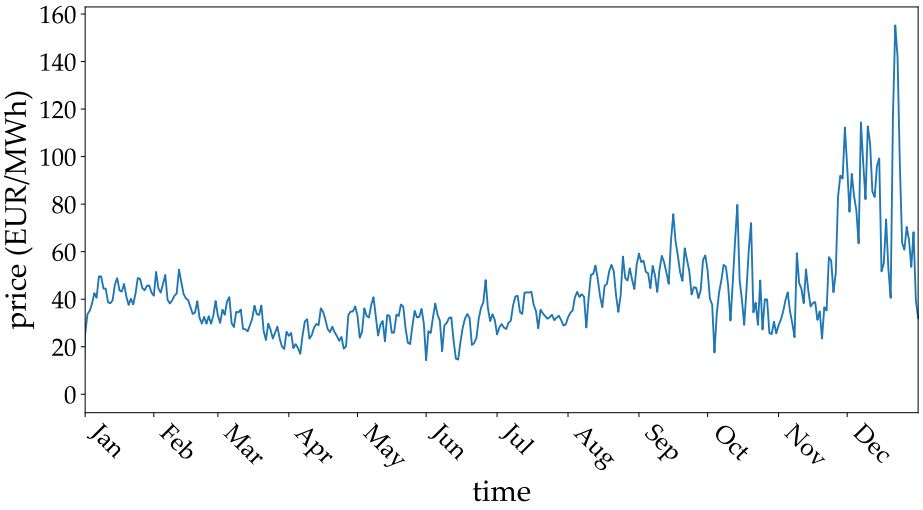

Figure 3.7: Forecast of the electricity prices for the GC case studies.

Positive-energy district case studies

The other two case studies analyzed are taken from a study from Bahlawan et al. [86]. They are two districts with the same architecture but different ambient conditions: in particular, the same MES was assumed to be located in Italy and in China, respectively in Rome (PE_Rome_H2) and in Guangzhou (PE_Guangzhou_H2). The layout of these case studies is shown in Figure 3.8. They comprise a PEM electrolyzer (PEM), a gas turbine (GT), which works with hydrogen, a photovoltaic plant (PV), a heat pump (HP), an absorption chiller (AC), and storages for heat (TES), hydrogen (HS) and electricity (BES). The HS is supposed to be used for seasonal storage, while TES and BES are meant for daily energy fluctuations. The energy systems are designed in [86] and sized to be stand-alone, i.e. not connected to the electrical grid. However, in this work, it was assumed that the system can inject into the grid the surplus electricity produced by the PV (although the electricity cannot be bought), in this way the system can be considered as a positive-energy (PE) district. Table 3.2 displays the sizes of the plants involved in the systems.

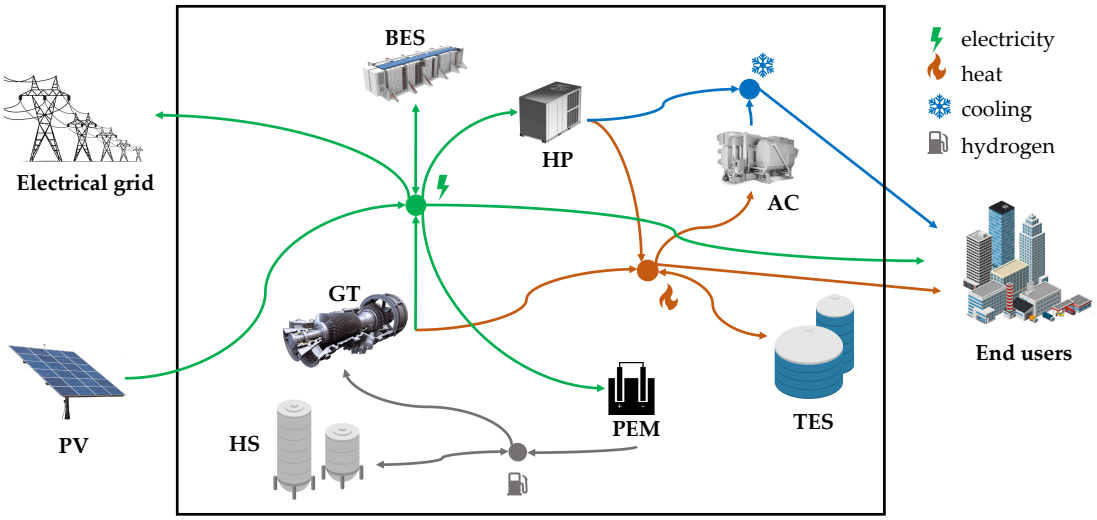

Figure 3.8: Layout of the PE case studies.

It needs to be mentioned that in these case studies the waste heat of the electrolyzer is not recovered, in order to allow the comparison of the results with those obtained in [86], where this is not considered. In this way, it is possible to test the quality of the solution of the novel algorithm.

Both case studies have an electricity demand of 10 GWh/year, that corresponds to approximately 300 buildings, and the forecast of the energy needs for

Table 3.2: Characteristics of the technologies of the PE case studies.

Technology	Nominal inlet power		Performance parameters	
	Rome	Guangzhou	Rome	Guangzhou
GT	7.61 MW	5.28 MW	$\eta_{el} = 26\%$	$\eta_{el} = 25\,\%$
			$\eta_{th} = 60\,\%$	
HP	5.5 MW	7 MW	$COP = 3.3$, $EER = 2.8$	
AC	0.8 MW	2 MW	$EER = 0.75$	
PEM	11 MW	13 MW	$\eta_{H_2} = 55\,\%$	
Technology	Nominal capacity		Performance parameters	
	Rome	Guangzhou	Rome	Guangzhou
HS	3314 MWh	2038 MWh	$\eta_{sd} = \eta_c = \eta_d = 100\,\%$	
TES	92 MWh	66 MWh	$\eta_{sd} = \eta_c = \eta_d = 99.5\,\%$	
BES	10 MWh	30 MWh	$\eta_{sd} = 100$, $\eta_c = \eta_d = 95\,\%$	

the two locations is shown in Figures 3.9 and 3.10. The profiles were taken from Bahlawan et al. [86], where the authors calculated the energy demands and the renewable energy generation using the TRNSYS® software and monthly average data.

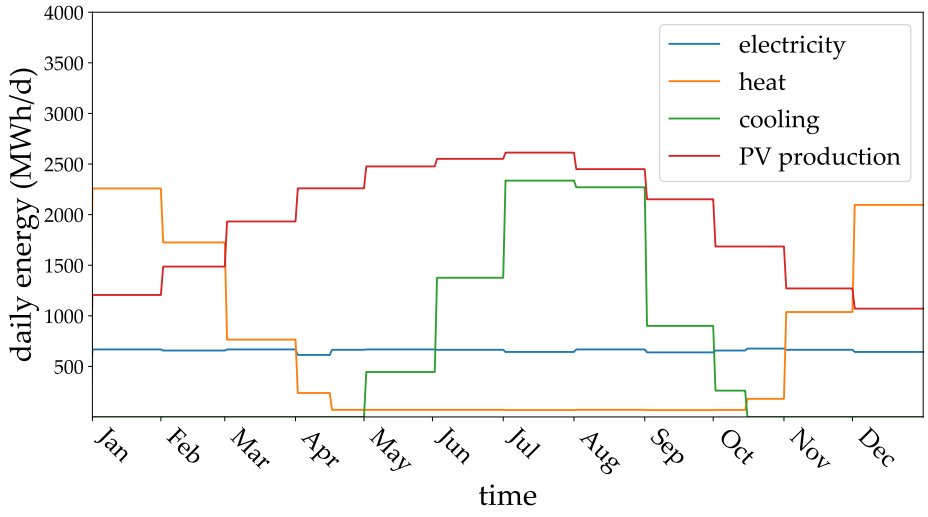

Figure 3.9: Forecast of the energy needs and production for the PE_Rome_H2 case study.

In these case studies, the energy stored in the BES and the management of AC, PEM and HP are the first-stage variables in the stochastic approach, while the energy stored in the HS and TES, the energy at the GT and the electricity exported are selected to be second-stage variables and help to mitigate the effects of the uncertainties.

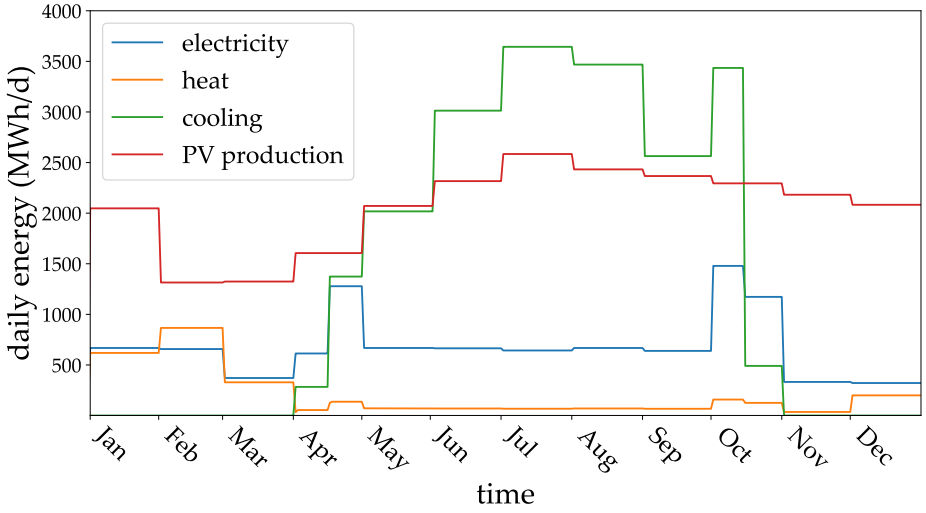

Figure 3.10: Forecast of the energy needs and production for the PE_Guangzhou_H2 case study.

3.2.2 Implementation

This section presents how the optimization algorithm was applied to the case studies and how the uncertain parameters were modeled. The deterministic and stochastic optimization algorithms described in detail in Section 3.1.1 were adapted to the four case studies, leading to the eight case studies listed in Table 3.3.

Table 3.3: Case studies simulated.

Case study	Approach
GC_Västerås	Deterministic
GC_Västerås	Stochastic
GC_Västerås_H2	Deterministic
GC_Västerås_H2	Stochastic
PE_Rome_H2	Deterministic
PE_Rome_H2	Stochastic
PE_Guangzhou_H2	Deterministic
PE_Guangzhou_H2	Stochastic

The optimization algorithm was developed in the Python environment, using the PuLP library and the problem was solved through the open-source solver CBC [22]. The simulations time-span is one year, with a daily time-step. It is worth pointing out the reason why such parameters have been chosen: although this algorithm is now tested on virtual test-benches to test its performances, it

was developed with the intent of being used to optimize and control real energy systems, by being employed in a supervisory MPC module. Therefore, the algorithm should have a long-term vision of the system to be optimized, with the scope to give additional constraints to short-term controllers which operate the real-time control of the system. In this way, it is possible to have a control which also considers long-term objectives and performs better over time, as done e.g. by Saletti et al. [91]. To use the algorithm in such application, it needs to be fast, since it must be run every day and communicate the optimized strategy to the real-time controllers. For this reason, the model was simplified and a daily time-step was used. In addition, only an average efficiency was implemented for each plant, as the daily average power is considered.

For the GC case studies, the cost function implemented is the minimization of the total economic operating cost, which can be expressed for the stochastic approach by the following equation:

$$\min f_{obj_{GC}} \,, \tag{3.10}$$

with

$$f_{obj_{GC}} = \sum_{t=1}^{N_t} \left[\sum_{f=1}^{N_f} c_{f,bo} P_{f,bo}(t) + \sum_{s=1}^{N_s} Pr(s) \Big(c_{el,bo,s}(t) P_{el,bo,s}(t) - c_{el,so,s}(t) P_{el,so,s}(t) \Big) \right] \Delta t \,, \tag{3.11}$$

where $c_{f,bo}$ is the cost of buying the fuel f, while $c_{el,bo,s}(t)$ and $c_{el,so,s}(t)$ are the costs of purchasing and selling electricity at time-step t for scenario ξ_s, expressed in EUR/MWh. In addition, $P_{f,bo}(t)$ represents the amount of fuel f used by the CHPs, $P_{el,bo,s}(t)$ is the amount of electricity bought at time-step t for scenario ξ_s, and $P_{el,so,s}(t)$ is the electricity sold at time-step t for scenario ξ_s, in MW, N_t is the total number of time-steps considered in the optimization, N_f is the number of fuels involved, N_s is the number of scenarios, ξ_s is the scenario considered and $Pr(s)$ is its probability of occurrence.

In the PE case studies, it was supposed that the energy systems cannot buy or sell energy with external networks. Instead, it was assumed that the energy systems can export the surplus renewable electricity internally generated. The objective implemented in the PE case studies represents the maximization of the total electrical energy exported by the MES. By imposing this objective, the system is forced to use the renewable energy in the most efficient way. The

stochastic cost function is the following

$$\max f_{obj_{PE}} \,, \tag{3.12}$$

with

$$f_{obj_{PE}} = \sum_{t=1}^{N_t} \sum_{s=1}^{N_{scen}} Pr(s) P_{el,exp,s}(t) \Delta t \,, \tag{3.13}$$

where $P_{el,exp,s}(t)$ is the amount of excess electrical power at time-step t for scenario ξ_s, that can be exported and possibly injected into the grid, $Pr(s)$ is the probability of occurrence of scenario ξ_s, Δt is the time-step length, N_t is the total number of time-steps in the prediction horizon and N_s is the total number of scenarios considered.

The cost function for the deterministic approaches is easily obtained starting from the stochastic one, by considering a single scenario with probability equal to one.

The uncertainties were accounted for by creating scenarios for the uncertain parameters. First, the PDF of the uncertain parameters was divided into seven intervals centered around the forecasted value, each interval having a width equal to the standard deviation σ, as illustrated in Figure 3.2 [50, 51]. Subsequently, a large number of scenarios was generated using the roulette wheel mechanism (i.e. 2000 initial scenarios), and then this number was reduced to be used in the optimization model, following the procedure outlined in Section 3.1.3. The uncertain parameters considered in the GC case studies are the electricity price and user needs, while in the PE case studies, PV production and user needs are considered to be uncertain. These parameters were treated as independent of each other, although, in real-life situations, this may not always be true. Nevertheless, this assumption does not compromise the robustness of the approach.

Although Weibull or Beta PDFs are commonly used for wind speed and solar irradiance, the roulette wheel scenario generation method generates scenarios based on the difference between the forecasted and actual values, rather than the quantity itself. Therefore, as previously mentioned, the normal PDF was adopted to model the deviation in the forecasted value for all the uncertain parameters, similarly to what it has been done in [50]. The standard deviation was estimated from historical data.

As an example, Figure 3.11 shows the scenarios for electricity needs in the GC case studies for a one-month period, alongside the deterministic forecast

(represented by the black line).

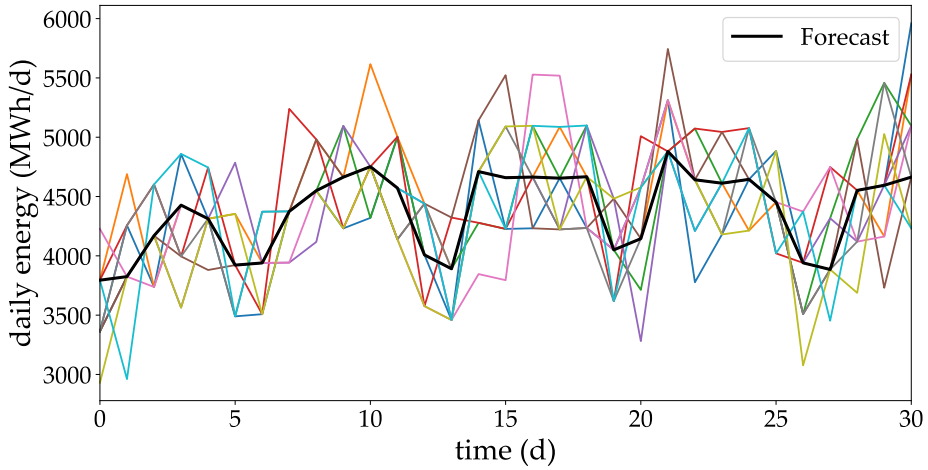

Figure 3.11: Scenarios for electricity needs over one month, for the GC case studies.

3.3 Results

The novel stochastic algorithm was tested by applying it to the case studies presented above. The simulations have been performed both with deterministic and stochastic approaches, with the aim to compare the results obtained with the two. This section presents the results of this study. First, the outcomes of a sensitivity analysis are presented, performed to analyze the impact of using different number of scenarios when employing the stochastic approach and find the most appropriate one; second, the results obtained performing yearly simulations and the comparison between the different case studies are discussed.

3.3.1 Sensitivity analysis

When solving a stochastic optimization problem, the more scenarios are employed, the more the solution is robust. However, the complexity of the problem increases with high number of scenarios, as well as the computational effort to find an optimal solution, since the number of decision variables increases, and thus one key issue is to find a proper number of scenarios that allows a reliable solution to be find in a appropriate computational time. For this reason, a sensitivity analysis was performed for the case study of the city of Guangzhou, with

the aim of determining the number of scenarios to use for further simulations. The sensitivity analysis considered the computational time needed to find an optimal solution and the relevance of the solution, and the number of scenarios that permits a compromise between the two was selected.

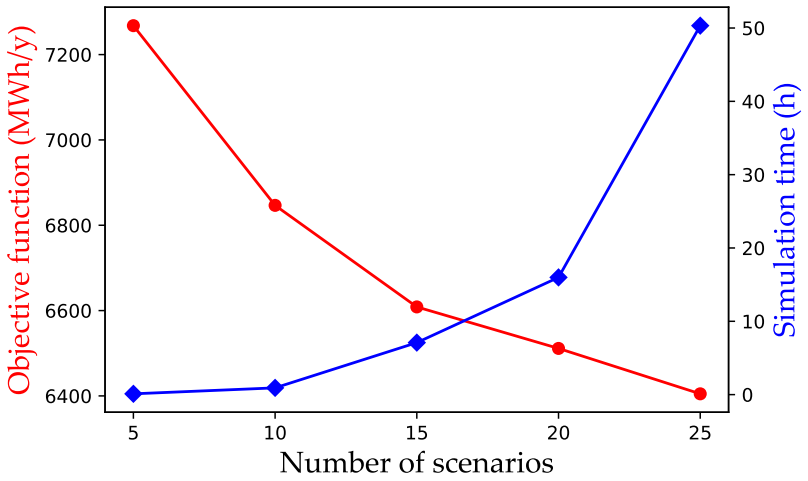

Figure 3.12: Results of the sensitivity analysis for the PE_Guangzhou_H2 case study.

The simulations have been run with 5, 10, 15, 20 and 25 scenarios and the objective function value obtained, as well as the computational time needed to find the optimal solution are displayed in Figure 3.12. The tests were performed using a Core i7 system with 2.80 GHz CPU and 16 GB of RAM. The aim of the analysis is to find the most suitable number of scenarios for the simulations with the stochastic approach, taking into account both computational time needed to find a solution and relevance of the solution.

By analyzing the results obtained, the best solution for the scope of this work was found to be in the number of 10 scenarios for the stochastic simulations, which allows to have a reasonable computational time for solution (around one hour). Indeed, this time is acceptable if the algorithm is meant to be used for updating every day the yearly scheduling, and it was noticed that even by increasing the number of scenarios, the solution obtained was not affected in a relevant way.

3.3.2 Results for the grid-connected case studies

This section presents the results obtained from the simulations conducted for the GC case studies. Figures 3.13a and 3.13b depict the amount of electricity bought

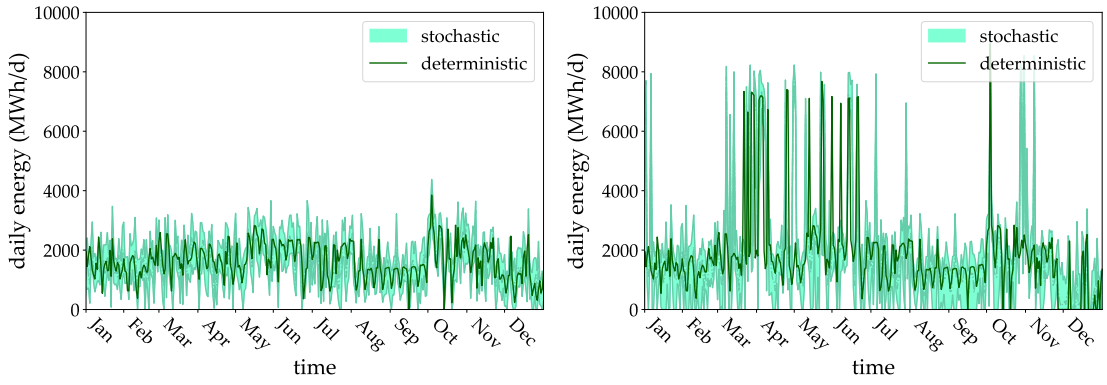

Figure 3.13: Electricity bought from the grid in the (a) GC_Västerås and (b) GC_Västerås_H2 case studies in the deterministic and stochastic approach.

from the electrical grid in the two cases. The results obtained with the stochastic approach are displayed in the form of bands, that represent the range of values obtained with the different scenarios. In the GC_Västerås case study, the imported electricity exhibits some variations, but it remains consistently lower than 4000 MWh/day. Instead, in the GC_Västerås_H2 case study, there are peaks of electricity purchased when the electricity price is lower. This happens thanks to the introduction of the electrolyzer in the system, that allows hydrogen production during periods of low electricity prices. Consequently, the integration of hydrogen production enhances flexibility within the energy system. Moreover, comparing the deterministic and stochastic approaches, it can be observed that the deterministic results are mostly contained within the stochastic bands, demonstrating coherence between the two methods.

Given the considerable variability of electricity prices in this region of Sweden, the integration of such technologies can be beneficial in cost savings and leveraging the large availability of renewable energy in the country during certain periods of the year, which leads to low electricity prices. As shown in Table 3.4, in the GC_Västerås_H2 case study, the value of the objective function, i.e. the economic cost for the system, is lower, despite part of the produced hydrogen being used to meet additional hydrogen needs. It is worth mentioning that it was possible to compare the results of the two approaches in terms of the value of the cost function as the percentage difference between the data used for the deterministic simulations and the weighted values obtained with the scenario approach over the entire year was not significant.

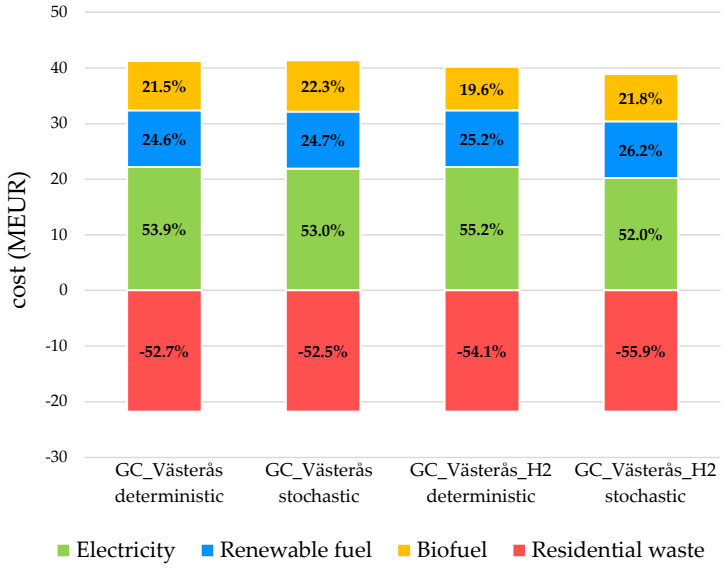

Figure 3.14: Economic analysis for the GC_Västerås and GC_Västerås_H2 case studies in the deterministic and stochastic approach.

In Figure 3.14, the cumulative costs and revenues of the system over the course of the year in the four simulations are shown. For the stochastic approach, a weighted value for the cost of electricity was calculated and the percentage indicated refers to the total positive economic cost (excluding revenues). It can be seen that the cost of electricity represents more than half of the total cost for all simulations, followed by renewable fuels and biofuels. On the other side, great savings are allowed by the use of residential waste, since the revenues deriving from its usage cover more than half of the expenses. Moreover, it can be seen that the cost of electricity is the main cost saving factor for the GC_Västerås_H2 case studies. Indeed, as already mentioned, it is possible to better exploit periods of low electricity prices and avoid purchasing electricity at high prices with the introduction of the electrolyzer.

Figure 3.15 shows the management of hydrogen storage in the GC_Västerås_H2 case study using both approaches. It is noteworthy that with the deterministic approach, the storage is kept empty during the initial months of the year, when it is not utilized, leading to reduced system flexibility. In addition, the hydrogen stored is not always greater in the stochastic approach than in the deterministic approach, indeed the system is connected to the power grid and therefore the energy security of the system does not need to be guaranteed.

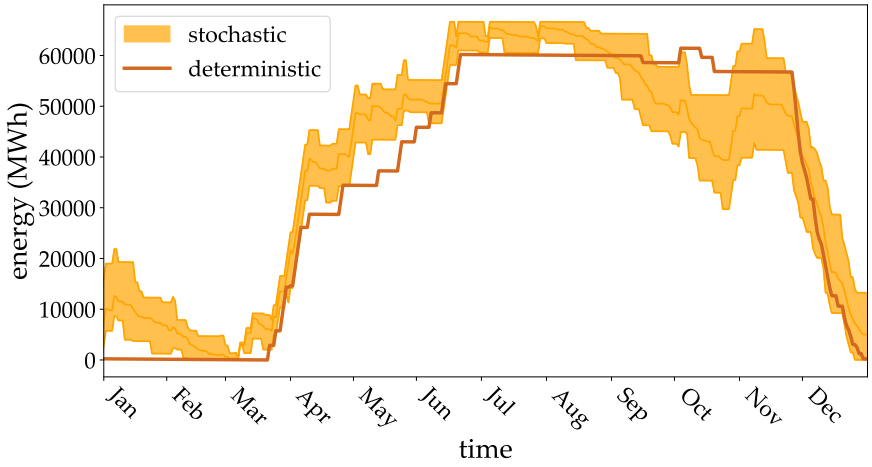

Figure 3.15: Management of the hydrogen storage in the GC_Västerås_H2 case study in the deterministic and stochastic approach.

Table 3.4: Objective function obtained for the GC case studies.

Simulation approach	Cost function value (EUR)		Cost reduction
	GC_Västerås	GC_Västerås_H2	
Deterministic	19 496 164	18 475 391	5.2 %
Stochastic	19 636 593	17 164 267	12.6 %

Among the other findings, it was observed that the HP-el, that recovers the waste heat from the hydrogen production process, contributes 0.7 % of the heat for the DHN supply in the deterministic approach, whereas this number increases to 1.4 % in the stochastic approach. This demonstrates that the waste heat from the PtG plant, although in modest quantities, also contributes to thermal energy usage in the city DHN.

3.3.3 Results for the positive-energy case studies

Also for the PE case studies, simulations over one year have been performed, and the results were analyzed. The electricity exported to the grid during the simulated year is displayed in Figures 3.16 and 3.17: for the stochastic approach, the results are shown in the form of bands of operation, as it was done for the GC case study. It needs to be mentioned that the maximum amount of electricity exported was constrained to be less than 24 MWh per day for two main reasons: firstly, if the maximum amount of exported electricity is not constrained, since maximization of exported electricity is the objective of the optimization, the seasonal hydrogen storage could be used less, mainly with the deterministic

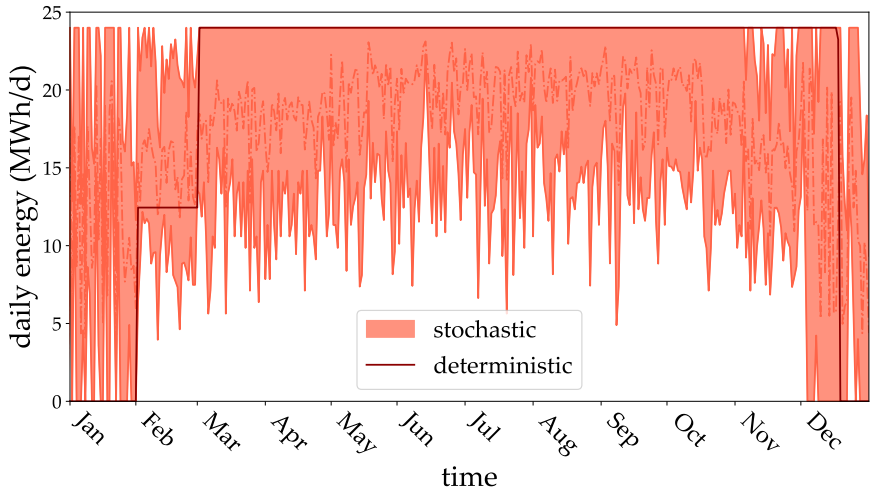

Figure 3.16: Electricity exported in the PE_Rome_H2 case study in the deterministic and stochastic approach.

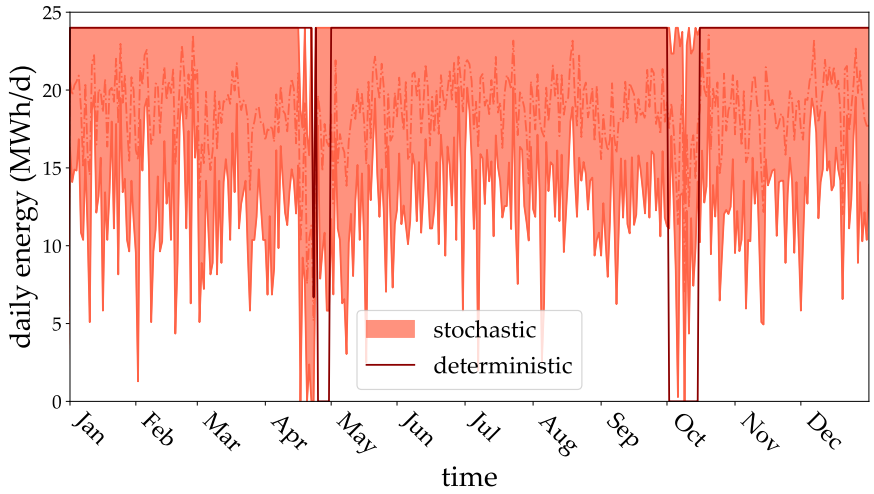

Figure 3.17: Electricity exported in the PE_Guangzhou_H2 case study in the deterministic and stochastic approach.

approach, reducing the energy security of the system; secondly, considering the integration of these positive energy districts with the electrical grid, this allows for a lower impact on the stability of the grid. The systems, in fact, are considered self-sufficient, with the possibility of feeding (if available) surplus renewable electricity into the electrical grid. It is clear that, to integrate such positive energy systems into the existing energy networks, they need to maintain their self-sufficient characteristics while not impacting negatively on external networks.

The results show that in both cases the average amount of electricity sold using

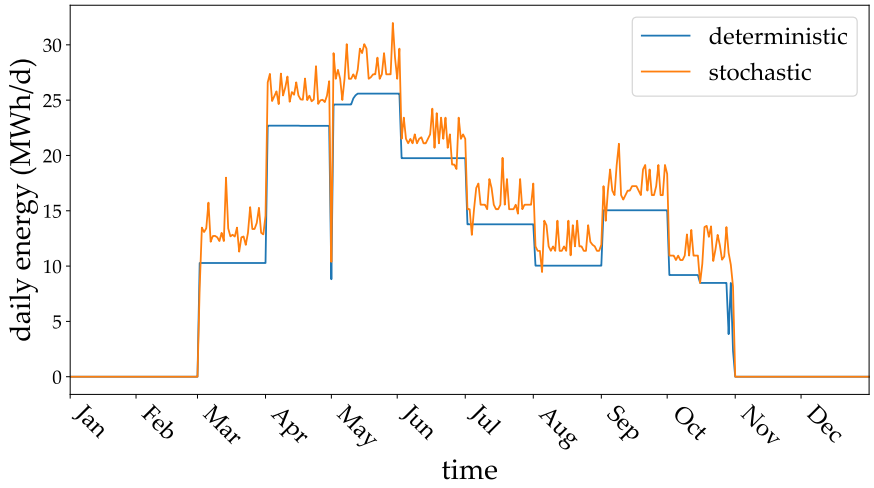

Figure 3.18: Management of the PEM electrolyzer in the PE_Rome_H2 case study in the deterministic and stochastic approach.

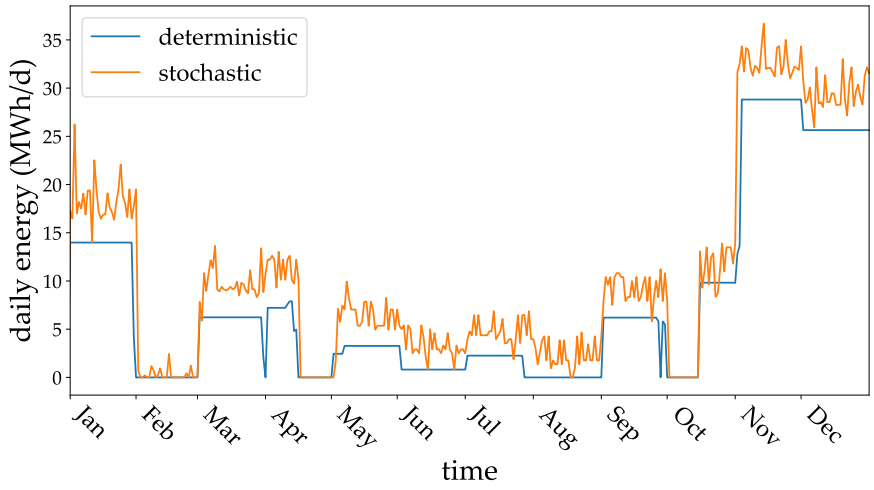

Figure 3.19: Management of the PEM electrolyzer in the PE_Guangzhou_H2 case study in the deterministic and stochastic approach.

the stochastic approach (the dotted line) is lower than the electricity sold using the deterministic approach, which also leads to a lower cost function value for the stochastic approach (see Table 3.5). This management is due to the variability added through the scenarios both in energy production and utilization, which causes a more conservative behavior of the system, a lower export of electricity and therefore the storage of a greater amount of energy.

By looking at Figures 3.18 and 3.19, where the management of the PEM electrolyzer in both approaches is displayed, it can be seen that with the stochastic

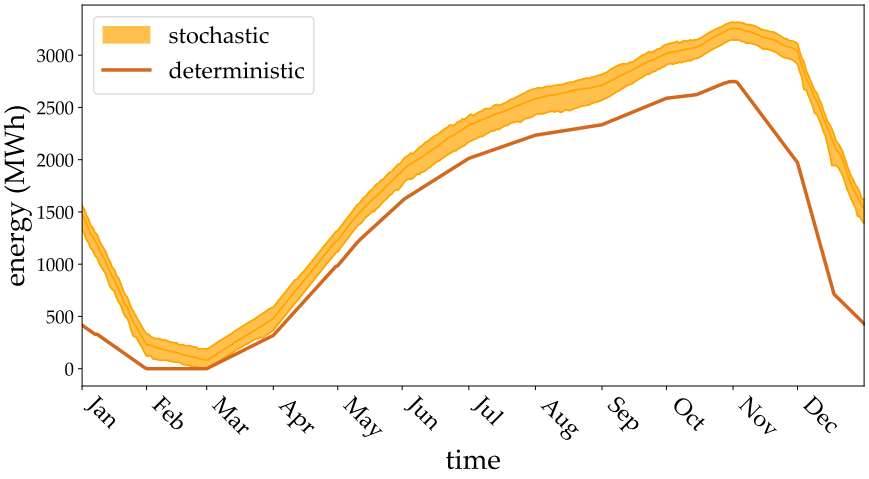

Figure 3.20: Management of the hydrogen storage in the PE_Rome_H2 case study in the deterministic and stochastic approach.

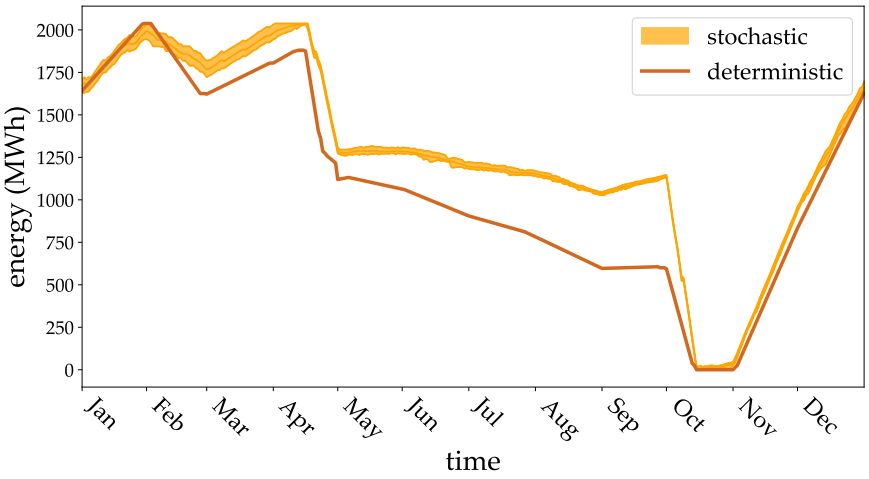

Figure 3.21: Management of the hydrogen storage in the PE_Guangzhou_H2 case study in the deterministic and stochastic approach.

approach, a higher amount of hydrogen produced in both case studies is obtained, leading to a higher amount of stored hydrogen (Figures 3.20 and 3.21). This contributes to a more robust management of the system against uncertainties, enhancing energy security by ensuring a fuller storage capacity to handle unpredictable events (such as an unexpected high energy request from the end-user or a sudden decrease in energy production).

Another noteworthy result is the different hydrogen storage management in the two locations. In Rome, the storage is emptied during the spring (see Figure 3.20), in order to use the stored hydrogen to fulfill the thermal needs during the

winter season. On the other hand, in Guangzhou, the storage is filled during the winter and the hydrogen is used to meet high cooling demands during the summer (see Figure 3.21). Especially, the seasonal storage is emptied rapidly during the first half of October: here, as it is shown in Figure 3.10, the electrical and cooling demands are high, while the renewable generation starts to decrease because of the coming of the winter season. This demonstrates that the novel optimization algorithm has successful results regardless of different geographical locations and external conditions, which lead to varying energy demands, as displayed in Figures 3.9 and 3.10.

Analyzing the management of the GT (shown in Figures 3.22 and 3.23), which was considered a second-stage variable and behaves differently for each scenario, it is observed that the results obtained with the deterministic approach are mostly contained within the bands of operation derived from the stochastic approach.

However, a comparison between the two approaches reveals that the deterministic solution can be misleading. Indeed, the stochastic approach, considering uncertainties, results in less electricity sold to the grid, leading to a higher operational energy cost. This highlights the vulnerability of the deterministic approach to uncertainty and the potential for unrealistic outcomes. On the contrary, if any of the scenarios considered in the stochastic approach happen, the management of the MES is possible with the solution obtained using the stochastic approach.

Furthermore, the results obtained using this optimization strategy align with the findings of Bahlawan et al. [86]. Nonetheless, using both approaches, the

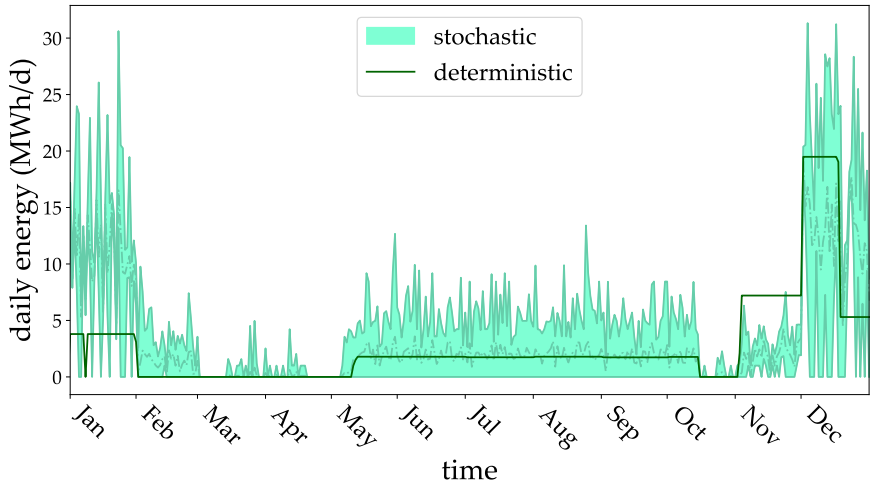

Figure 3.22: Management of the GT in the PE_Rome_H2 case study in the deterministic and stochastic approach.

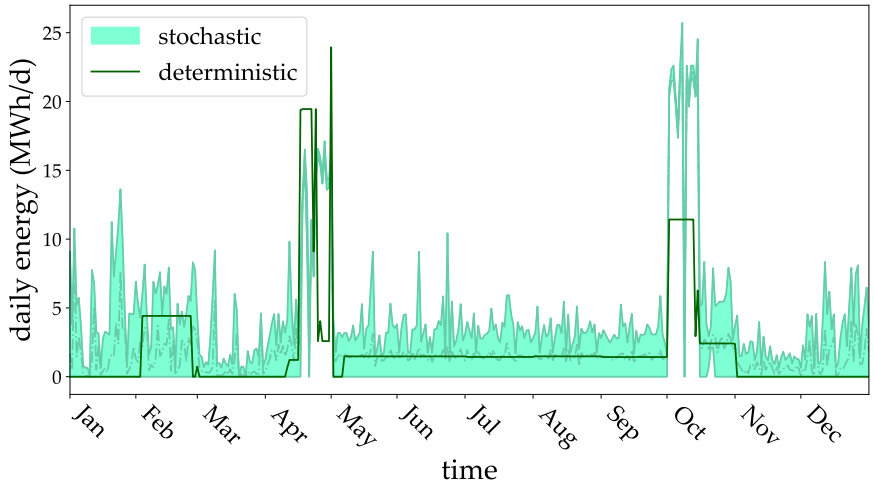

Figure 3.23: Management of the GT in the PE_Guangzhou_H2 case study in the deterministic and stochastic approach.

Table 3.5: Objective function obtained for the PE case studies.

Case study	Cost function value (MWh)		Difference
	Deterministic	Stochastic	
PE_Rome_H2	7356	6443	-12.4 %
PE_Guangzhou_H2	8263	6847	-17.1 %

results show that part of the electricity is always exported and then that the system is oversized. Additionally, the AC is not used in the PE_Rome_H2 case study, indicating that it is more cost-effective to fulfill cooling needs through the HP using renewable electricity. In the PE_Guangzhou_H2 case study, the AC is used for around 25 days per year in both approaches, during April and October, which is a relatively short amount of time. It is demonstrated that even when the AC is removed from the energy system, its management remains feasible, implying that it could be omitted from the system design in both locations.

3.4 Discussion

The method employed in this study involved the application of a novel MILP-based stochastic optimization algorithm to four distinct case studies, encompassing both grid-connected and positive energy district energy systems. These case studies served as virtual test benches to evaluate the algorithm performance, by comparing it with a deterministic approach under identical boundary conditions.

The novelty of the study proposed is to introduce the uncertainty in various external parameters in a conventional energy planning algorithm, to study the integration of a PtG solution for seasonal storage. Indeed, deterministic models have a notable limitation, as they are unable to account for uncertainties in optimization parameters, which stochastic programming can effectively address. The stochastic approach incorporated uncertainties by generating multiple scenarios for external disturbances such as electricity prices, user needs, and renewable energy production. A sensitivity analysis determined that the use of ten scenarios achieved an optimal balance between computational efficiency and solution reliability for the stochastic approach.

In the grid-connected case studies, the results demonstrated the potential benefits of introducing hydrogen seasonal storage to enhance system flexibility. This was particularly evident in the ability to take advantage of low electricity prices for hydrogen production and subsequent use during high-demand periods. The adoption of this technology can serve as a buffer against unpredictable disturbances, mitigating undesirable consequences arising from unexpected behavior. As a result, the system flexibility increases, and the impact of uncertainties on management is minimized.

In the positive energy district case studies, the stochastic approach demonstrated its robustness by allowing a lower electricity exports compared to the deterministic approach. This conservatism in electricity export, driven by the consideration of various scenarios, resulted in a more secure system operation with fuller hydrogen storage capacity. The study also highlighted the adaptability of the optimization algorithm to different geographical locations and external conditions, enabling effective long-term planning in diverse settings.

The algorithm has proven to be a reliable tools with different case studies and external conditions. Indeed, the seasonal storage was managed in different ways depending on external weather conditions and user demands, in order to exploit the seasonal storage to meet the predominant needs in seasons with a lack of renewable generation. In addition, even though the forecasting was not the focus of the research, the algorithm showed its efficiency both using historical data as forecasts, and using average monthly data and typical days for the reconstruction of energy demand and generation.

The developed algorithm can be easily applied to various other case studies, proving itself as a versatile tool for examining different applications at different scales. Depending on the specific case study, different business models can be

considered by adjusting goals and the implemented objective function. Overall, these findings underscore the value of the MILP-based stochastic optimization algorithm in addressing long-term planning challenges with seasonal storage, offering a promising tool for enhancing the sustainability and resilience of energy systems. Nevertheless, there are potential further improvements for the algorithm, such as addressing the interdependence of uncertainties or implementing multi-objective optimization to meet different objectives. In addition, it is acknowledged that further research is required to investigate the economic aspects of these systems, including investment costs, to provide a more comprehensive understanding of their viability.

Chapter 4

Predictive control for integrated Power-to-Gas management

This chapter presents the second contribution of this thesis: the development and validation in a Model-in-the-Loop (MiL) configuration of a smart controller based on MPC, applied to a PtG system integrated with a DHN through waste heat recovery. First, the methods used are described, i.e. the MPC concept and the optimization algorithm employed, then the case study is introduced and finally the application and the results are presented.

4.1 Method

This section presents the methods exploited in this work: the concept of MPC and the optimization algorithm developed for its implementation are described.

4.1.1 Model Predictive Control

The smart control of complex energy systems allows the system to be optimally managed, following the implemented objectives, which can be related to economic cost or energy consumption minimization, and it is becoming more and more common. As seen in Section 2.2.3, many advancements in the field of control of energy systems are being carried out. Diverse advanced control strategies exist, that help to manage and control in an optimal way energy systems, taking into account their growing complexity [92].

As mentioned earlier, in this thesis the control of the energy systems was achieved through the utilization of the Model Predictive Control (MPC) tech-

nique. MPC is an intelligent and adaptive control strategy that employs an optimization algorithm which is able to calculate the optimal trajectory for the system initialization variables over a future time horizon, also known as prediction horizon. The algorithm contains a simplified model of the system being controlled and makes use of predictions of future external factors that may influence the operation of the system. This approach allows for dynamic and forward-looking management of the system, allowing it to respond effectively to changing conditions and external disturbances, ultimately enhancing its performance and efficiency. This strategy is described in detail in Section 1.2 of this thesis.

4.1.2 Optimization algorithm

As explained above, to develop an MPC controller, an optimization algorithm is required, that calculates the optimal future trajectory for the control variables over the prediction horizon. Among the existing optimization algorithms, MILP algorithms have revealed to be successfully for optimizing the management of MES, if properly tailored to the case study. Indeed, they allow the systems to be optimized with a good accuracy and with a adequate computational complexity. In addition, the global optimality of the solution is guaranteed and allowed by the usage of available solvers. When using such approach, the equations that describe the physical behavior of the system need to be linearized in order to obtain linear constraints.

The constraints of the algorithm are able to model the dynamics of a general MES, which is composed by the following components:

- **Conversion units**: they are all the plants present in the system, which are able to convert energy from one (or more) form to another one (or more), e.g. cogeneration plants, electrolyzers, heat pumps. To obtain a linear model, the input-output relationship is linearized. Nevertheless, to take into account variations in the efficiency with the load, piecewise linearization can be used [93, 94]. Furthermore, each plant allows for the modeling of three operating modes (on, off, and standby), with the option to define start-up costs, as well as minimum up-time (UT), down-time (DT), and operating ramps. This can be achieved by introducing additional equations and binary variables into the problem.

- **Energy storages**: these encompass various energy storage methods, such as batteries, thermal energy storage systems, and gas storage tanks. The

equation governing these components relates the energy stored at the current time-step with that stored in the previous one, accounting for charge, discharge, and self-discharge efficiencies.

- **Energy networks**: these are depicted as energy sources or sinks, enabling the energy system to exchange energy by purchasing or selling it at specific costs. Examples include electricity grids and natural gas networks.

- **End-users and RES**: they are depicted as energy sources or sinks as well, with specified energy requirements that must be met or production rates that serve as disturbances to the algorithm.

- **Energy nodes**: while not representing physical nodes, energy nodes play a crucial role in ensuring that the energy balance for each energy vector is maintained during every time-step.

All power flows and energy stored constitute the optimization variables, and the algorithm computes their optimal control for each time-step. This is done with the aim of minimizing the defined objective function over the prediction horizon.

Constraints

As previously explained, the models of energy system components need to be implemented in the optimization algorithm as linear constraints. The details regarding how these constraints were developed are presented in the following.

Conversion units modeling: to model the conversion units in a MILP algorithm, the input-output relationship needs to be linearized. In order to tackle the nonlinearities, which are intrinsic of these systems, piecewise linearization was used for the components that needed it. This formulation needs the use of auxiliary variables and constraints. When the output power of the conversion unit only depends on the input power of the unit, a one-dimensional piecewise linear approximation can be implemented, as shown in Figure 4.1 [95]. This means to perform a piecewise linearization of a function of a single variable.

The mathematical formulation that describes the piecewise linearization of a function $f(x)$ of one variable is obtained by introducing a number n of coordinated $x_1, ..., x_n$ on the x axis, called breakpoints, on which the function is evaluated. Then, the function is approximated using linear segments which connect the

breakpoints $[(x_i, f(x_i)), (x_{i+1}, f(x_{i+1}))]$, with $i = 1, ..., n-1$. The equation that describes this formulation is the following, with $\lambda \in [0, 1]$ and $x_i \leq \bar{x} \leq x_{i+1}$.

$$\bar{x} = \lambda x_i + (1 - \lambda) x_{i+1} \,. \tag{4.1}$$

It follows that the approximated value of the function in a generic point $\bar{x}$ can be expressed as

$$f(\bar{x}) = \lambda f(x_i) + (1 - \lambda) f(x_{i+1}) \,. \tag{4.2}$$

To use this technique in a MILP algorithm, it is necessary to express it in terms of constraints that bound the decision variables. Therefore, to use piecewise linear approximations, it is necessary to introduce in the algorithm additional constraints and variables. In particular, for each breakpoint a continuous variable $\alpha_i \in [0, 1] \, (i = 1, ..., n)$ is needed, and a binary variable h_i is associated with each i-th interval $[x_i, x_{i+1}] \, (i = 1, ..., n-1)$, with dummy values at the extremes $h_0 = h_n = 0$. The piecewise linear approximation is formulated with the following constraints:

$$\sum_{i=1}^{n-1} h_i = 1 \,, \tag{4.3}$$

$$\alpha_i \leq h_{i-1} + h_i \quad (i = 1, ..., n) \,, \tag{4.4}$$

$$\sum_{i=1}^{n} \alpha_i = 1 \,, \tag{4.5}$$

$$x = \sum_{i=1}^{n} \alpha_i x_i \,, \tag{4.6}$$

$$f(x) = \sum_{i=1}^{n} \alpha_i f(x_i) \,. \tag{4.7}$$

Eq. (4.3) imposes that only one h_i can be equal to 1 at the same time-step, while Eq. (4.4) indicates that only α_i and α_{i+1} can be different from zero. In this way, a single interval is selected for the piecewise linearization. Finally, by referring to the formulation in Eq. (4.1), it is possible to deduce that Eqs. (4.5), (4.6) and (4.7) impose that $\alpha_i = \lambda$, while $\alpha_{i+1} = 1 - \lambda$, leading to the same formulation.

For modeling the conversion unit with this formulation, $f(x)$ represents the output power of the plant, while x is the input power. An additional feature was added to this formulation, since it is necessary to consider minimum load when

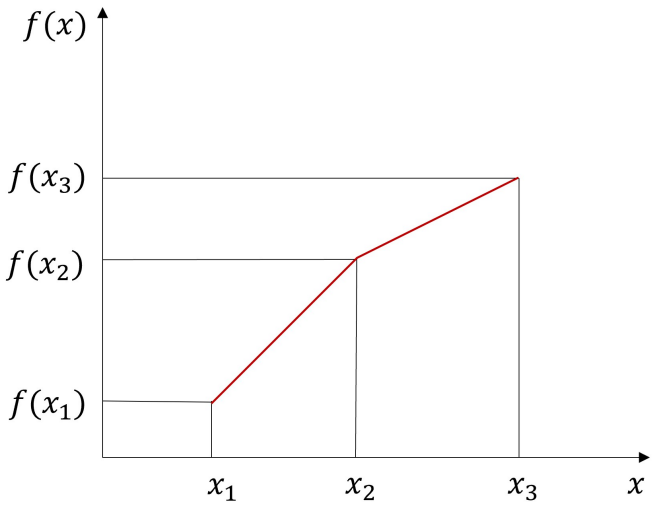

Figure 4.1: Representation of piecewise linearization in one dimension, with two intervals and three breakpoints.

modeling energy system components. Indeed, each plant presents a minimum load under which it is switched off, and this behavior was taken into account by adding a binary variable for each plant. By using the formulation presented above, α_0 was set to be binary (and not continuous, as other α_i variables), so that when the input power drops below the minimum value x_1, it follows that $\alpha_0 = 1$ immediately, as well as the output power. Therefore, it follows that the switch on/off variable for the plant at time t is

$$\delta(t) = 1 - \alpha_0(t)\,, \tag{4.8}$$

where $\delta(t) = 1$ when the plant is in operation while $\delta(t) = 0$ when the plant is switched off.

When the performance of a component depends on two external variables, the piecewise linearization has been performed on two dimensions (e.g. the electrical power used to drive the gas compressor depends both on the mass flow rate of the gas and on the pressure ratio, which depends on the storage pressure). While one-degree of freedom performance curves can be piecewise linearized relatively straightforwardly, the situation becomes more complex when attempting to perform a piecewise linearization on two variables, leading to the existence of several approaches for such piecewise linear approximations. Figure 4.2 schematically represents the two-dimensional piecewise linearization [95]. The process of approximating a function with a piecewise linear approach in two variables is more

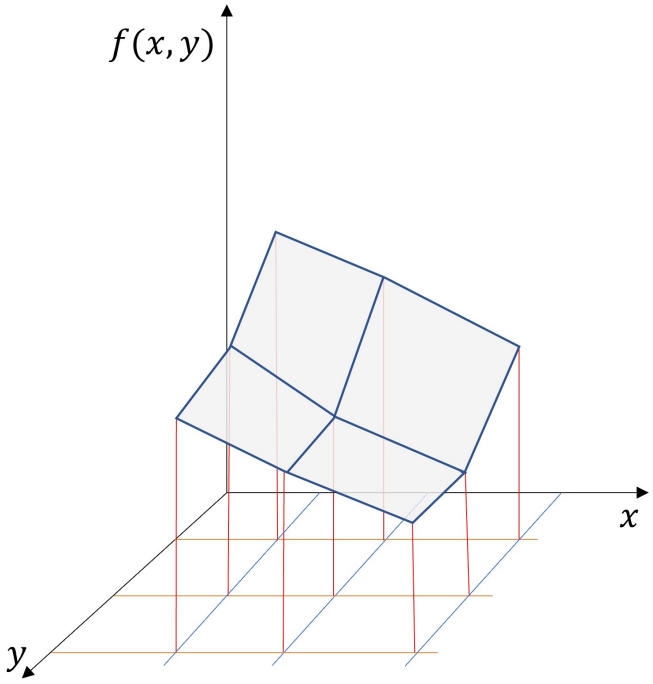

Figure 4.2: Representation of the piecewise linearization in two dimensions, with four rectangles and nine breakpoints.

complex than in one variable, and various methods can be employed. In this thesis, the triangle method was utilized, which is an extension of the one-dimensional piecewise linearization method previously described, adapted for two variables.

Considering the general function on two variables $f(x, y)$, it is assumed to divide the domain in n coordinates on the x axes $x_1, ..., x_n$ and in m coordinates on the y axes $y_1, ..., y_m$. As for functions of one variable, the domain is discretized using breakpoints $(x_i, y_j)\,(x = 1, ..., n; y = 1, ..., m)$ and the function is evaluated in each of them. For any given $(\bar{x}, \bar{y})$ point, such that $x_i \leq \bar{x} \leq x_{i+1}$ and $y_j \leq \bar{y} \leq y_{j+1}$, the rectangle and the triangle that contain it are used for the approximation of the function in the point, as shown in Figure 4.3. Then, the function value is approximated using a convex combination of the function values at the vertices of the triangle containing $(\bar{x}, \bar{y})$, similarly to what it has been done for the piecewise linearization in one dimension.

For the formulation of this approach in the MILP algorithm, additional variables and constraints are added, as done for the linear approximation of functions of one variable. In particular, $n \times m$ continuous variables $\alpha_{ij} \in [0, 1]$ are introduced, one for each breakpoint, and the following constraints describe the triangle approach:

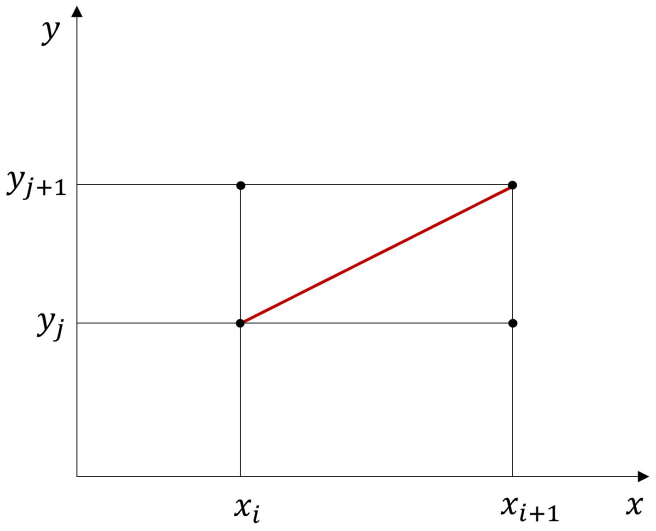

Figure 4.3: Schematization of the triangle method for the piecewise linearization on two variables.

$$\sum_{i=1}^{n}\sum_{j=1}^{m}\alpha_{ij} = 1\,, \tag{4.9}$$

$$x = \sum_{i=1}^{n}\sum_{j=1}^{m}\alpha_{ij}x_i\,, \tag{4.10}$$

$$y = \sum_{i=1}^{n}\sum_{j=1}^{m}\alpha_{ij}y_j\,, \tag{4.11}$$

$$f(x,y) = \sum_{i=1}^{n}\sum_{j=1}^{m}\alpha_{ij}f(x_i,y_j)\,. \tag{4.12}$$

Where Eqs. (4.9) - (4.12) represent the formulation on two variables of Eqs. (4.5) - (4.7), and therefore allow for the selection of one rectangle in the domain. As mentioned above, for this formulation it is also necessary to identify the right triangle to consider, in the rectangle selected, as shown in Figure 4.3. Therefore, for each triangle, a binary variable is introduced. In particular, considering the rectangle in Figure 4.3, the binary variables h^u_{ij} and h^l_{ij} are associated to the upper and lower triangles, respectively. Additional constraints are added, that impose that only the triangle in which the point $(\bar{x}, \bar{y})$ is located is used for the linearization. The additional constraints are the following

$$\sum_{i=1}^{n-1}\sum_{j=1}^{m-1}(h_{ij}^{u}+h_{ij}^{l})=1\,, \tag{4.13}$$

$$\alpha_{ij}\leq h_{ij}^{u}+h_{ij}^{l}+h_{i,j-1}^{u}+h_{i-1,j-1}^{l}+h_{i-1,j-1}^{u}+h_{i-1,j}^{l}\quad (i=1,...,n;j=1,...,m)\,. \tag{4.14}$$

Similarly to what it has been done for the one-dimensional piecewise linearization, an additional binary variable is added for the switch on/off.

When modeling the conversion units with the presented approach, $f(x,y)$ represents the output power of the conversion unit, x the input power, while y is an external variable which the output power also depends on.

For each conversion unit, the possibility to model three operating modes (on, off, standby) was added, as well as a cost to switch on the plant when is off (start-up cost) due to the necessity, when present, to reach operating temperature or pressure. The additional constraints introduced to model them are explained below.

Being $\delta(t)$ the switch on/off binary variable at time-step t ($\delta(t)=0$ plant switched off and $\delta(t)=1$ plant switched on), $\gamma(t)$ the standby binary variable ($\gamma(t)=0$ plant not in standby and $\gamma(t)=1$ plant in standby) and $SU(t)$ the start-up binary variable ($SU(t)=0$ no start-up and $SU(t)=1$ start-up at time t) the constraints are the following

$$\delta(t)-\delta(t-1)-\gamma(t-1)-SU(t)\leq 0\,, \tag{4.15}$$

$$\delta(t)+\gamma(t)\leq 1\,, \tag{4.16}$$

$$\gamma(t)-\gamma(t-1)-\delta(t-1)\leq 0\,. \tag{4.17}$$

Eq. (4.15) imposes that only when the plant switches from off to on there is a start-up, Eq. (4.16) imposes that the system cannot be at the same time on and in standby mode, while Eq. (4.17) avoids that the system operating mode passes directly from off to standby. The operating ramps, which are impose to limit too fast load changes, in according to the dynamics of the plants, are imposed using the following constraints

$$P_{in}(t)-P_{in}(t-1)\leq r_{up}\,, \tag{4.18}$$

$$P_{in}(t)-P_{in}(t-1)\geq r_{down}\,. \tag{4.19}$$

Finally, a minimum UT and DT for each plant can be imposed, following the method presented in [96]. For sake of brevity, these constraints are omitted here.

Storages modeling: to model the storages, a linear model was used, that relates the energy stored at each time-step with the energy stored at the previous time-step using the following equation, which is valid for the energy carrier l:

$$E_{stor,l}(t) = \eta_{sd} E_{stor,l}(t-1) + \left(\eta_c P_{stor_{in,l}}(t) - \frac{P_{stor_{out,l}}(t)}{\eta_d} \right) \Delta t \,, \tag{4.20}$$

where $E_{stor,l}(t)$ is the energy stored at the current time-step, $E_{stor,l}(t-1)$ the energy stored at the previous time-step, η_{sd} is the self-discharge efficiency, $P_{stor_{in,l}}$ and $P_{stor_{out,l}}$ are the amount of power entering and exiting the storage at the current time-step, η_c is the charge efficiency and η_d is the discharge efficiency and Δt is the time-step length. Depending on the physics of the storage, different efficiencies can be used.

Energy balance equations: additional constraints which represent the energy balance for each energy carrier are set. When looking at Figure 4.4, each energy carrier is represented by an horizontal line, and the balance is made among input power flows to the line $P_{in,l}(t)$ and output power flows $P_{out,l}(t)$ at each time-step t. For the energy carrier l the constraint is the following:

$$\sum_{in=1}^{N_{in}} P_{in,l}(t) = \sum_{out=1}^{N_{out}} P_{out,l}(t) \,, \tag{4.21}$$

where N_{in} and N_{out} are the number of power flows entering and exiting the node.

Variable bounds: additional constraints regard the upper and lower bounds for the variables, which are set in according to the characteristics of the energy system. For instance, the input and output power to/from each plant are bounded between a minimum and a maximum value, the capacity of the storages is limited, as well as the amount of energy exchanged with storages and networks.

4.2 Application

This section presents the case study to which the novel MPC controller previously described was applied, and the characteristics of the simulations performed to test it.

4.2.1 Case study description

The case study analyzed consists of a PtG plant for the production of synthetic methane, starting from the renewable electricity generated by a wind farm. The system is integrated with a DHN through waste heat recovery from the exothermic components of the PtG plant. A schematic representation of the energy system is displayed in Figure 4.4 [97].

In Figure 4.4, all the energy flows involved are shown: the energy system is interconnected with both the electrical grid and the natural gas network, allowing for the exchange of electricity and gas through buying and selling energy. The electricity generated by the wind farm can be used to meet the electrical demands directly, it can be employed in the PEM electrolyzer (PEM) for hydrogen production, or finally consumed by both the methane compressor and the HP. The hydrogen produced by the PEM electrolyzer can be stored in the hydrogen storage (HS) for later use or directed employed in the methanation reactor. The methanation reactor produces methane at low pressure, specifically at 2.5 bar, and before storage or further use, this methane needs to undergo compression. Once compressed, the methane can serve various functions. It can be stored for future use, sold to the grid, or supplied to the boiler, which generates heat for the

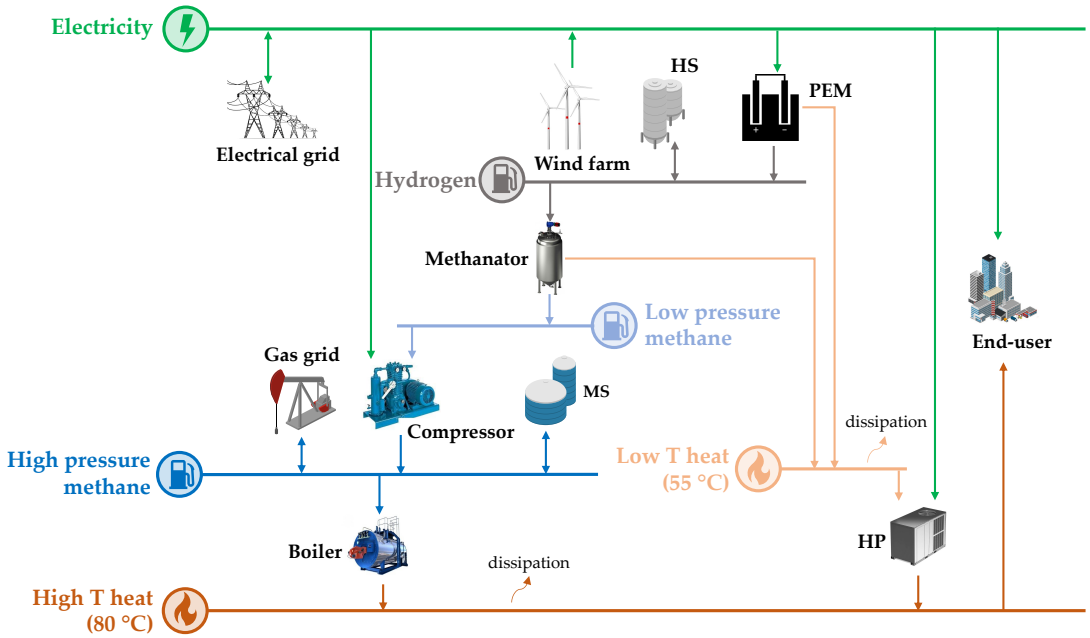

Figure 4.4: Schematization of the Multi-Energy System considered, which comprises the PtG and the DHN. (HS = Hydrogen Storage, MS = Methane Storage)

end-user's thermal demand. In addressing the thermal needs, the system relies on a gas-fueled boiler and the recovery of waste heat from the PtG plant.

Thermal energy recovery involves two distinct hot water circuits: the Heat Recovery Circuit (HRC) and the DHN. The HRC operates at lower temperatures, between 40 °C and 55 °C and, within this circuit, three heat exchangers recover waste heat from the PtG components, in particular from the electrolyzer (available at 55 °C), condenser (at 80 °C), and methanation reactor (at 290 °C). The DHN, on the other hand, operates at higher temperatures, ranging from 60 °C to 80 °C, and is used to provide heat directly to the end-user. An industrial heat pump (HP) bridges the two circuits by upgrading the heat from 55 °C to the required 80 °C for the DHN. The schematic representation of the novel heat recovery configuration is displayed in Figure 4.5. Here, the two water circuits can be seen, connected using the HP, together with the PtG components which are used for the heat recovery.

Table 4.1 contains a comprehensive presentation of the specifications of the system components.

4.2.2 Implementation

The main objective of this study is to test the novel MILP-based MPC and evaluate its potentials. In order to do that, it was compared using a MiL platform to a conventional rule-based strategy designed to run the PtG for producing methane when renewable electricity is available. Therefore, the MPC controller was applied to a so-called system digital twin, which is a dynamic model, built by means of connecting in a proper way the models of the single components

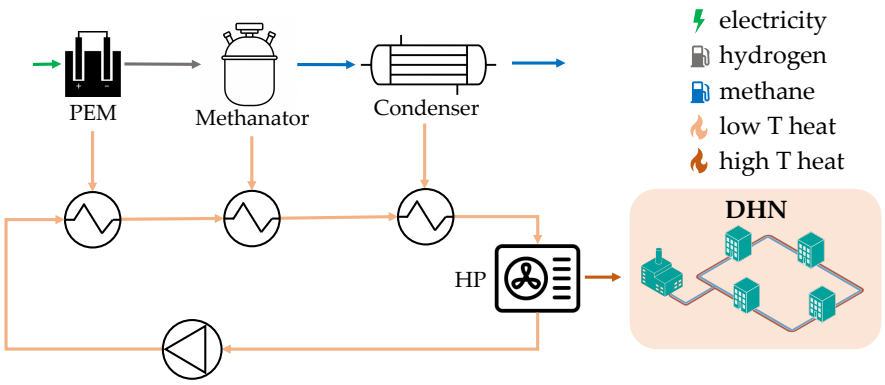

Figure 4.5: Schematization of the waste heat recovery from the Power-to-Gas plant.

Table 4.1: Characteristics of the plants involved.

Technology	Parameter	Value
Wind farm	Number of turbines (-)	4
	Nominal power (kW)	8000
Electrolyzer	Nominal inlet power (kW)	3750
	Nominal operating temperature (°C)	55
	Nominal operating pressure (bar)	35
Methanator	Nominal inlet power (kW)	2479
	Nominal operating temperature (°C)	290
	Nominal operating pressure (bar)	2.5
Boiler	Nominal inlet power (kW)	4000
	Nominal efficiency (%)	92.4
Heat pump	Nominal inlet power (kW)	380
H_2 storage	Volume (m^3)	100
	Maximum pressure (bar)	35
	Minimum pressure (bar)	2.5
Methane storage	Volume (m^3)	100
	Maximum pressure (bar)	7.5
	Minimum pressure (bar)	3.5

involved. The platform used for this application was developed in-house in the MATLAB®/Simulink® environment and its components are described in detail in [97, 98] and presented in the Appendix A of this thesis. A screenshot of the system digital twin is represented in Figure 4.6.

By testing a controller in a MiL configuration, it is possible to evaluate its benefits, without affecting the operation of a real system. The novel controller was implemented in the system as a supervisory controller, which gives the values of the control variables calculated by the optimization algorithm as input set-points to low-level controllers (e.g. PID controllers) already implemented in the system. The details regarding the application of the two control strategies is presented in the next paragraphs.

MPC control

The novel controller was applied to the model of the case study, as previously explained. At each time-step, the controller (i) gets the actual value of the system initialization variables, (ii) updates the forecast of the disturbances and the initial conditions and (iii) calls the MILP algorithm, which performs the optimization and returns the optimal values for the control variables as a result. A schematic

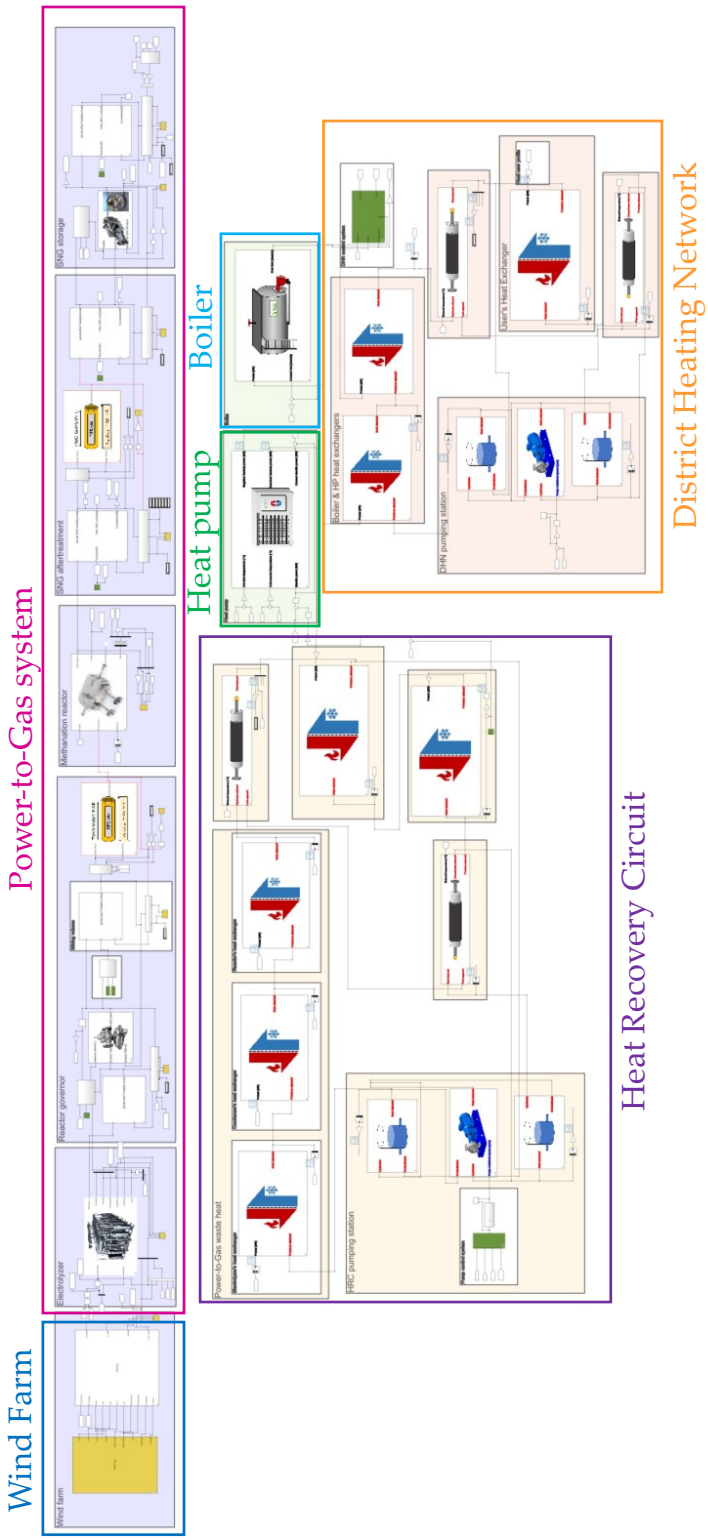

Figure 4.6: Simulink digital twin of the system analyzed.

representation of the MiL application is displayed in Figure 4.7. Here, the initialization and control variables, as well as the disturbances given to the algorithm and to the system model are specified. The prediction horizon set in the algorithm is two days, while to select the time-step length a sensitivity analysis was performed, the results of which are presented in the results section.

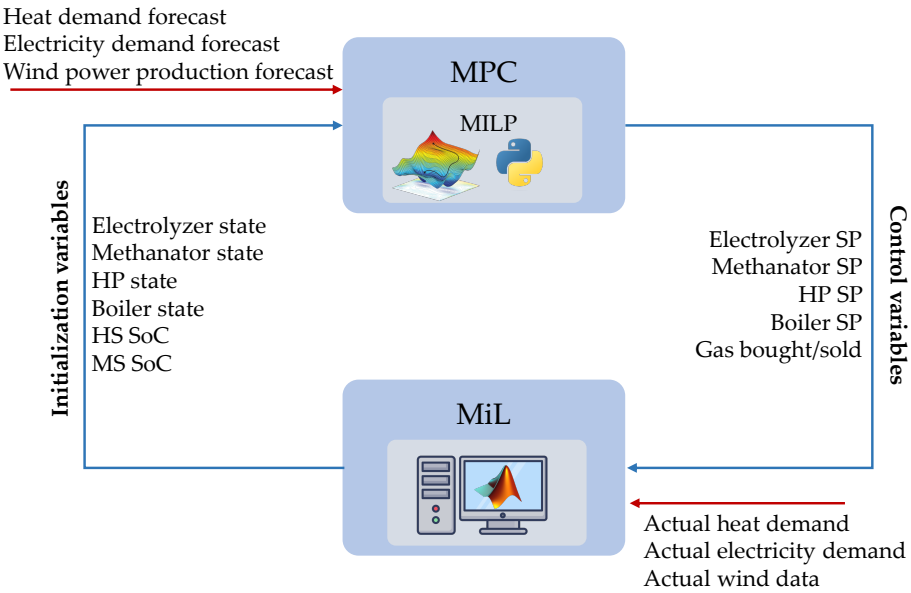

Figure 4.7: MPC setup in Model-in-the-Loop configuration. (SP = set-point, SoC = State of Charge)

The objective function implemented in the algorithm aims to maximize the overall operating margin, which encompasses the costs of purchasing and selling electricity and natural gas to and from the networks, as follows

$$\max f_{obj}\,, \tag{4.22}$$

with

$$f_{obj} = \sum_{t=1}^{N_t} \Big(c_{el,so}(t) P_{el,so}(t) + c_{ng,so}(t) P_{ng,so}(t) - c_{el,bo}(t) P_{el,bo}(t) - c_{ng,bo}(t) P_{ng,bo}(t) \Big) \Delta t\,, \tag{4.23}$$

where $P_{el,so}(t)$ and $P_{ng,so}(t)$ are the amount of electricity and natural gas sold to the networks at tome t, respectively, and $c_{el,so}(t)$, $c_{ng,so}(t)$ the revenues related to them, while $P_{el,bo}(t)$ and $P_{ng,bo}(t)$ are the amount of electricity and natural gas bought from the networks, with $c_{el,bo}(t)$ and $c_{ng,bo}(t)$ being their costs.

To achieve the optimization, the MILP algorithm described in Section 4.1.2

was adapted to the presented case study. The characteristics of the linearization process utilized to formulate the MILP algorithm are detailed in Table 4.2. This table provides information on whether piecewise linearization was conducted, the dimension of the linearization (linear, piecewise linearization 1D or piecewise linearization 2D), the number of intervals employed, and whether the UT, DT, and operating ramps were incorporated into the model. It also specifies which operating modes have been considered in the formulation.

Table 4.2: Features of the model linearization for MILP formulation. (pl = piecewise linearization)

Component	Method	Intervals	Parameters	UT/DT	Ramps	Op. modes
Electrolyzer	pl 1D	1x3	$P_{out_{H_2}}, P_{out_{th}} = f(P_{in_{el}})$	no	no	on/off/standby
Methanator	pl 1D	1x2	$P_{out_M}, P_{out_{th}} = f(P_{in_{H_2}})$	yes	yes	on/off/standby
Gas compressor	pl 2D	2x2	$P_{in_{el}} = f(P_{in_{ng}}, E_{stor_{ng}})$	no	no	on/off
Boiler	linear	1x1	$\eta_B = 92.2\,\%$	no	no	on/off
Heat pump	linear	1x1	$COP = 5.42$	no	no	on/off
H_2 storage	linear	1x1	$\eta_c = \eta_d = 95\,\%$	-	-	-
Methane storage	linear	1x1	$\eta_c = 95\,\%$, $\eta_d = 0.85\,\%$	-	-	-

Rule-based control

The degree of improvement resulting from the implementation of the MPC control strategy can vary depending on how the conventional control strategy is defined. To address this variability and ensure efficiency, a well-suited rule-based control strategy was developed. The set-points of the manipulated variables that were previously defined by the MPC are now calculated by using the control logic outlined in Table 4.3.

Table 4.3: Rule-based control strategy definition.

Variable	Condition	Set-point value
Electrolyzer SP	$SoC_{HS} \leq 80\,\%$	$\min\{P_{nom}, (P_{wind} - P_{el_{user}})\}$
	otherwise	0
Methanator SP	$SoC_{HS} > 60\,\%$ & $SoC_{MS} \leq 95\,\%$	P_{nom}
	$SoC_{HS} > 60\,\%$ & $SoC_{MS} > 95\,\%$	0.5 P_{nom}
	otherwise	0
Heat pump SP	PtG system ON & $P_{th_{user}} > 0$	P_{nom}
	otherwise	0
Boiler SP	–	–
Methane sold	$SoC_{MS} > 70\,\%$	1200 kW
	$30\,\% \leq SoC_{MS} \leq 70\,\%$	600 kW
	$SoC_{MS} < 30\,\%$	0 kW

This control strategy is designed to operate the PtG system, taking advantage of periods of renewable electricity availability. When renewable electricity is in

excess, the PtG plant is activated to produce gas. The resulting gas can be either stored for future use or sold to the network, depending on the current State of Charge (SoC) of the gas storages. Additionally, the waste heat is recovered as a by-product of the process when both the electrolyzer and methanator reactor are switched on, while when waste heat is not required, it is dissipated.

It is worth noting that this control logic does not calculate the set-point for the boiler. Instead, the input power for this component is regulated using a PI controller, which aims at maintaining the supply temperature of the DHN equal to 80 °C. Furthermore, the actual quantity of methane exchanged with the network is determined by subtracting the methane required for the boiler from the specified set-point for methane sold to the network.

4.2.3 Key Performance Indicators

To assess the outcomes achieved, an analysis of Key Performance Indicators (KPIs) related to the cumulative results of the simulations was conducted. The identified KPIs include:

- Operating Margin (EUR): this KPI measures the net revenue resulting from the exchange of electricity and methane with external networks. It quantifies the difference between the revenue generated from energy sales and the expenditure incurred from energy purchases over the simulated period.

- CO_2 Emissions (kg_{CO_2}): this KPI assesses the total carbon dioxide emissions associated with the operation of the energy system. It considers emissions related to both methane and electricity purchased from external networks. Emissions from renewable electricity generated by the wind farm and synthetic methane production via the PtG plant are assumed to be zero. Emissions from the electrical grid are calculated using a coefficient of 224 gCO_2/kWh [99], while emissions from the gas network are calculated using a coefficient of 200.8 gCO_2/kWh [100].

- RES Usage (%): this KPI represents the percentage of renewable electricity utilized within the system, thereby not sold to the electrical grid.

- Gas Production (kWh): this KPI quantifies the total amount of methane produced by the PtG system.

- Heat Recovered Share (%): this KPI measures the percentage of user thermal demand met using the heat recovered from the PtG plant.

4.3 Results

The simulations have been run with both control strategies previously presented and the results were analyzed. This paragraph exposes the main results obtained by this investigation: first, a sensitivity analysis is presented in which several time-steps for simulation are tested and compared, then the results and discussion on the management of the system with the two control strategies are explained.

4.3.1 Sensitivity analysis

A sensitivity analysis was carried out with the aim to find the most suitable time-step length for the current application. The simulations have been performed with a prediction horizon of two days and a varying time-step length (one hour, 30 minutes and 15 minutes) and with two different solvers: the open source solver CBC [22] and the commercial solver Gurobi [23]. In this way, by decreasing the time-step length, the optimization problem is increasingly complex since the number of time-steps in the prediction horizon increases, as well as the number of optimization variables, as shown in Table 4.4.

Table 4.4: Optimization details with different time-step length.

Time-step length	Prediction horizon	Number of time-steps	Number of variables
1 hour	2 days	49	4802
30 minutes	2 days	97	9506
15 minutes	2 days	193	18914

This study was performed since it is essential to consider the potential for future use in real-world applications when designing predictive controllers. Obtaining licenses for commercial solvers is straightforward for academics; however, when it comes to companies, this is not always the case. This is especially true due to the typically high costs associated with commercial solver licenses. Therefore, it becomes imperative to ensure that optimization tasks can also be effectively

carried out using open source solvers which are usually slower in terms of computational time [101]. The simulations have been run using a Core i7 system with 2.80 GHz CPU and 16 GB of RAM.

The controller was applied in MiL configuration as explained in section 4.2.2 and the time used to perform the optimization has been collected for every iteration during a one-day simulation. In Figure 4.8, the comparison of computational time employed with different time-step lengths is displayed, with the two aforementioned solvers in box plots.

A box plot is a graph that provides a visual indication of how the distribution of the 25th percentile, 50th percentile, 75th percentile, minimum, maximum, and outlier values of a data set are distributed. A brief explanation on how to read the graphs is presented below:

- The box is used to represent the interquartile range (IQR), or the 50 % of data points lying above the first quartile (Q1) and below the third quartile (Q3), in the given data set.
- The lower part of the box represents the first quartile (the 25th percentile) of the data, while the upper part of the box is the third quartile (the 75th percentile) of the data.
- The line in the middle of the box represents the median of the data, while the cross is the mean of the data.
- The vertical lines, also known as whiskers, are used to represent the variability of the minimum, maximum and any outlier data points in comparison to the IQR: the lower whisker shows the minimum data value and its variability in comparison to the IQR inside the range $(Q1 - 1.5 * IQR)$, while the upper whisker shows the maximum data value and its variability in comparison to the IQR inside the range $(Q3 + 1.5 * IQR)$.
- The dots outside the whiskers represent the outliers.

It can be noticed how the time needed to find an optimal solution changes with the two solvers, being considerably higher with the open source solver CBC. It needs to be mentioned that a time limit of 240 seconds (i.e. 4 minutes) was imposed for the solution of the optimization process with a time-step of 15 minutes. Indeed, if the optimization exceeds this time limit, it becomes impractical to implement the control action in a real application. However, by setting a time limit,

the optimal solution is not guaranteed, and the solver selects the best solution found before the stopping time, which can reveal to be sub-optimal.

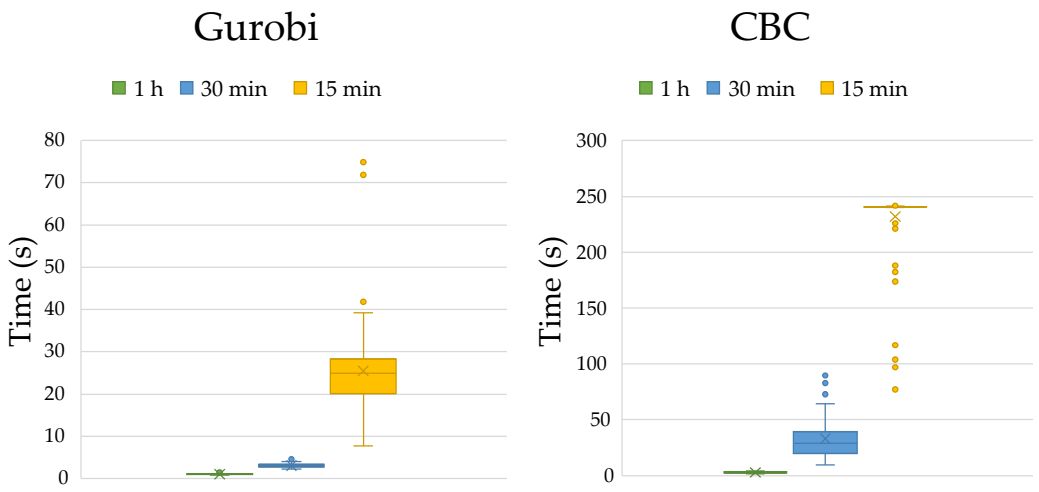

Figure 4.8: Time needed to find a solution with time-step length of 15 minutes, 30 minutes and 1 hour with Gurobi and with CBC solvers.

The same results are also shown in Figure 4.9, where the computational time is compared among the two different solvers, with same time-step length. With the Gurobi solver, the solution time is evidently shorter, and the difference in the solution time increases exponentially by decreasing the time-step length. With this solver, it is possible to obtain an optimal result in less than one minute also with time-step length of 15 minutes most of the time, and when using a time-step of one hour the solution can be found in around one second. With CBC, instead, the time-limit of 240 seconds is reached for almost all the calculations with time-step of 15 minutes, and when using a time-step of 30 minutes, the solution takes on average 30 seconds, but this time increased up to 90 seconds for some iterations. Instead, using one hour time-step, the solution is found in around 2.5 seconds, a time span that can increase up to 4 seconds.

Although the use of the commercial solver Gurobi demonstrated the ability to achieve optimal results within a reasonable time span even with shorter time-step length, it was chosen to adopt a one-hour time-step length for subsequent simulations. This decision was motivated by the desire to assess the advantages of the novel control strategy in scenarios where shorter time-steps might not be feasible because of the high computational time of open source solvers. Indeed, the aim of the investigation is to confirm whether the benefits of the novel control strategy could still be realized in real-world case studies, that may require open

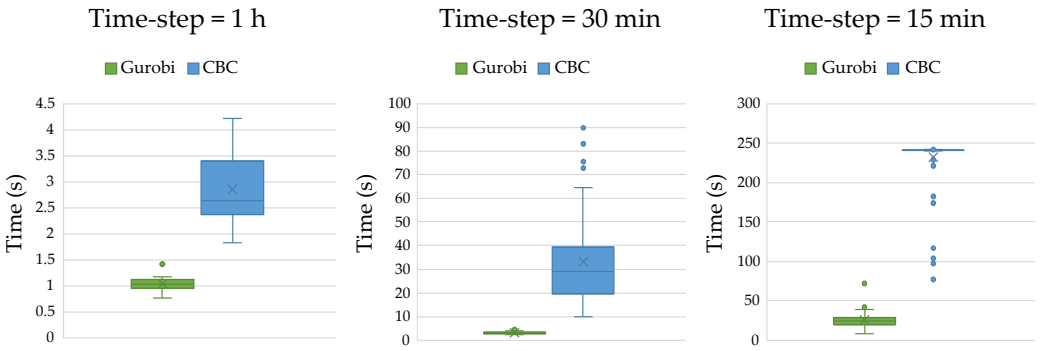

Figure 4.9: Time needed to find a solution with time-step length of 15 minutes, 30 minutes and 1 hour with Gurobi and with CBC solvers.

source solvers. In addition, not significant differences in the management of the system were evaluated, and therefore an increase in computational effort was not justified by a notable improvement on the solution.

It was decided to further extend this analysis, by testing the controller with different sampling intervals for the MPC. Specifically, attempts were made to execute the optimization process every 30 minutes or 15 minutes, but maintaining a time-step of one hour in the algorithm. This allows to have a computationally fast algorithm, as exposed above, since its time-step is of one hour, but to update the initialization variables and run it more frequently, since the sampling interval of the MPC is shorter.

The results obtained by this investigation are displayed in Figure 4.10, where 1 h - 1 h means time-step of one hour for the algorithm and sampling interval of one hour for the MPC, 1 h - 30 min stands for time-step equal to one hour for the algorithm and sampling interval of 30 minutes for the MPC, and 1 h - 15 min means time-step of one hour for the algorithm and sampling interval of 15 minutes for the MPC. It was found that the solutions obtained do not differ significantly in terms of KPIs and in particular the KPIs do not benefit from a decrease in the MPC sampling time; instead, better results are obtained by using a sampling time equal to one hour for most of the KPIs. In general, it was also evaluated that the management of the system did not present significant differences with different sampling times for the MPC controller.

For the aforementioned reasons, after performing the sensitivity analysis, it was decided to simulate the model with a time-step length of one hour for the optimization algorithm and a sampling time of one hour for the MPC. The results are presented in the following section.

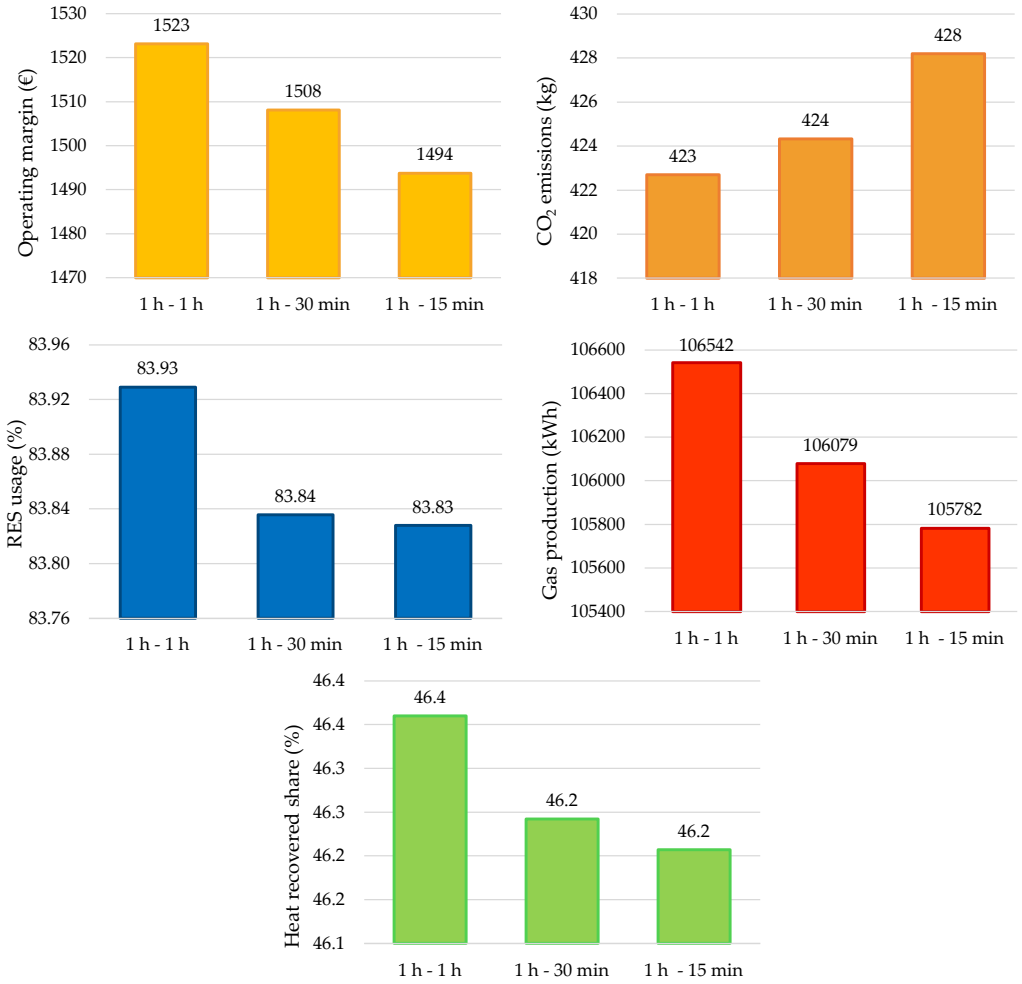

Figure 4.10: Value of KPIs by changing the digital-twin time-step and keeping the MILP time-step equal to one hour.

4.3.2 Simulation results

As previously mentioned, the purpose of the simulations is to assess the advantages of a novel controller utilizing the MPC technique for a PtG plant integrated with a DHN. To achieve this, the novel control approach was compared to a conventional rule-based method (refer to Section 4.2.2). The simulations were performed over a period of two days: nevertheless, the rule-based control strategy was employed in both simulations on the first day, in order to have the same initial conditions at the beginning of the second day, in which the two control strategies are compared. Consequently, the results were gathered exclusively during the second day, and the discussion will focus solely on the outcomes from this day.

The disturbances given to the MPC encompasses forecasts of end-user demands and electrical power generated by the wind farm, and they are illustrated in Figure 4.11 for the second simulated day. It is essential to emphasize that these forecasts differ from the disturbances imposed to the system digital-twin, which represent the actual disturbances and are obtained by applying random deviations to the ideal disturbances given to the controller. This methodology allows for the evaluation of the performances of the predictive controller with unexpected disturbances, a common occurrence in practical applications.

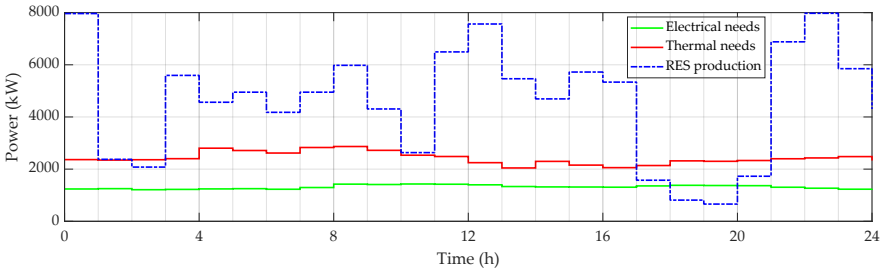

Figure 4.11: Forecasts of the disturbances given to the MPC controller for the second day.

Figure 4.12 displays how the electricity is managed with the two control strategies during the second day: in this figure, the energy balance among production, usage and exchange with the grid is shown. By comparing the management obtained with the two control strategies, it can be noticed that less electricity is exchanged with the grid using the MPC strategy, and it is possible to use more renewable electricity to work the electrolyzer and the HP for heat recovery.

This behavior can also be seen in Figure 4.13: here, the total amount of energy exchanged with the networks during the entire day is displayed, using the two different control strategies. In contrast, using the rule-based control logic, a greater quantity of electricity is exported to the grid, and the system simultaneously necessitates for a larger procurement of methane from the gas network. This is primarily due to the fact that during periods when the electrolyzer and methanation reactor are inactive, it becomes essential to purchase the required gas for operating the boiler, to meet the thermal demands of users. This outcome underscores that to have a cost-effective operation of the system it is better to exploit at the best way the self-generated energy resources and minimize the reliance on external energy networks. Additionally, such an approach serves to avoid grid unbalances and renewable energy resources curtailments.

Figure 4.14 presents both the set-point and the actual input power applied to

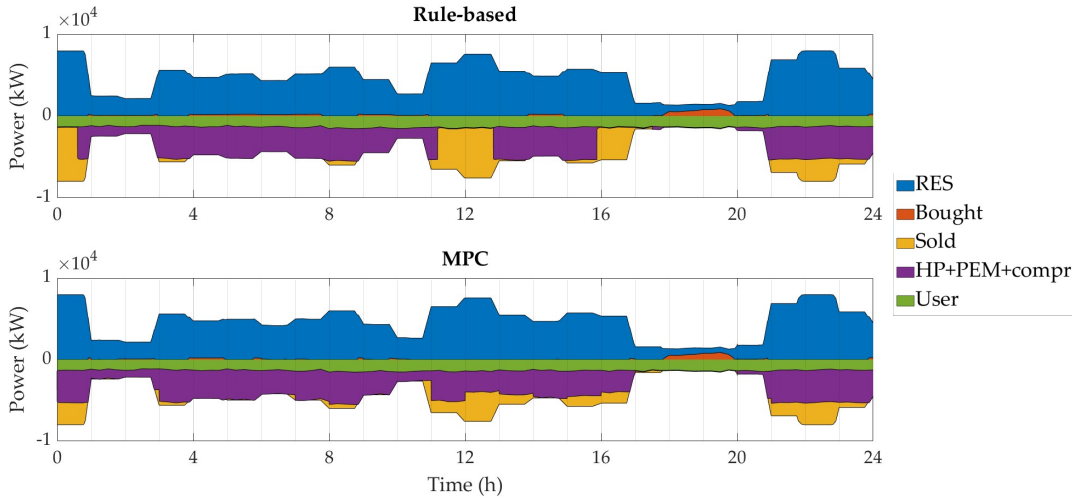

Figure 4.12: Energy balance at the electricity node. (RES = wind power produced, Bought/Sold = exchanges with the power grid, HP = heat pump, PEM = PEM electrolyzer, compr = compressor, User = user needs)

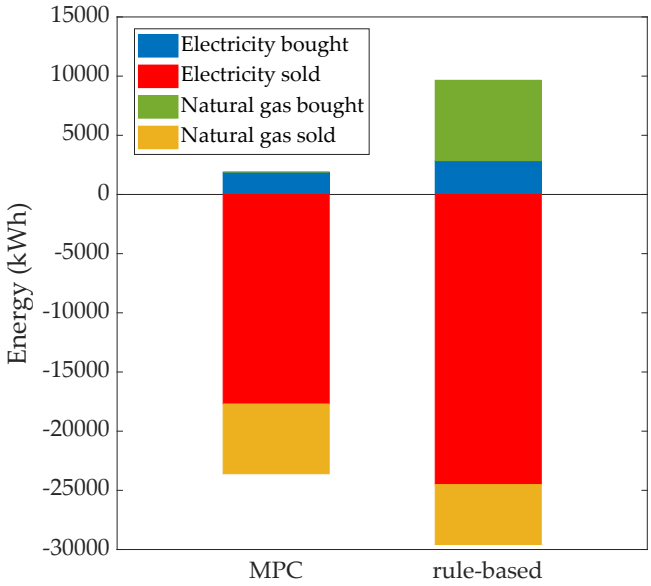

Figure 4.13: Bar plot with energy exchanged with the networks during the entire day.

the methanation reactor. It needs to be mentioned that the displayed set-point is the real one that emerges from the low-level proportional controller, and that takes into account also an adjustment based on the hydrogen storage SoC to prevent exceeding storage limits. The control strategies employed lead to notable

differences in the management of the methanation reactor. Specifically, under the rule-based control, the set-point remains predominantly constant at part load operation. In contrast, the MPC allows for the definition of a more precise set-point, enabling optimal system management to minimize the objective function.

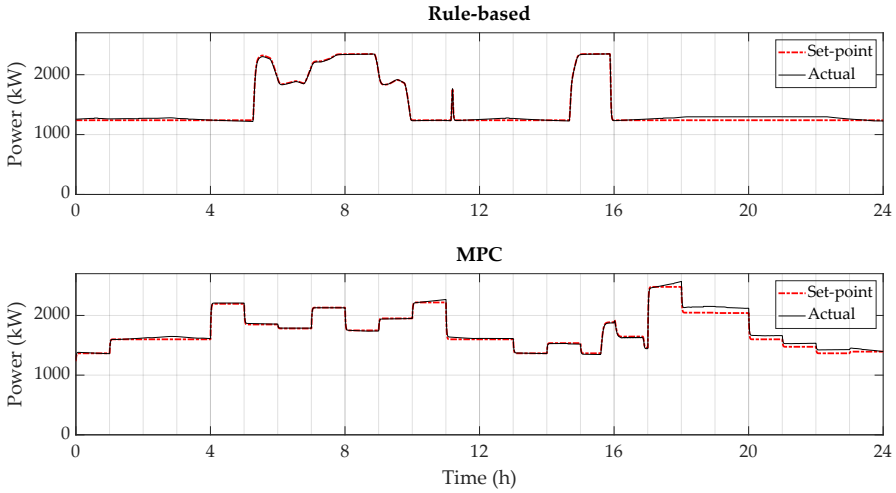

Figure 4.14: Input power set-point given to the methanation reactor with the two control strategies and realized one.

Figure 4.15 illustrates the real-time input power given to the electrolyzer with both control strategies and the hydrogen storage SoC. These two dimensions are closely interconnected: indeed, it is evident that under the rule-based control approach, there are periods in which the electrolyzer must be switched off due to hydrogen storage reaching its capacity limit (e.g. during hours 11 and 12). Conversely, this issue is not observed with the MPC, which can efficiently manage the operation of the electrolyzer, deactivating it only when the renewable generation is not enough, as depicted in Figure 4.11.

Table 4.5 presents the values obtained for the KPIs identified in paragraph 4.2.3. As expected, when using the MPC, the operating margin of the system is

Table 4.5: Values of the KPIs with the two control strategies.

Value	Rule-based control	MPC	Difference
Operating margin	996 EUR	1523 EUR	**- 527 EUR**
CO_2 emissions	2 004 kg_{CO_2}	423 kg_{CO_2}	**- 1 581** kg_{CO_2}
RES usage	77.7 %	83.9 %	**+ 6.2 %**
Gas production	89 483 kWh	106 541 kWh	**+ 17 103 kWh**
Heat demand met	41.8 %	45.6 %	**+ 3.8 %**

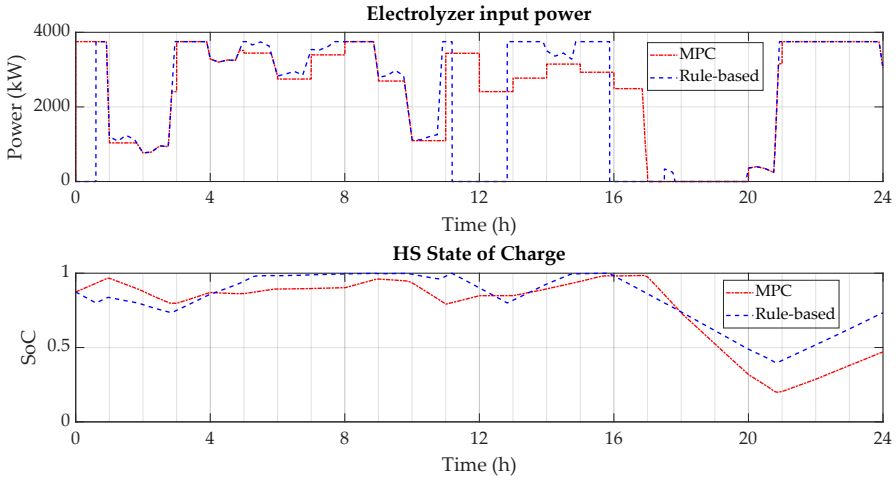

Figure 4.15: Actual input power of the electrolyzer and State of Charge of the hydrogen storage with the two control strategies.

notably greater, resulting in a 53 % improvement (approximately 527 EUR) over the course of a single day. Indeed, its maximization is the aim of the optimization performed in the controller. Additionally, the MPC control yields superior outcomes in terms of CO_2 emissions, achieving a reduction of over 50 % compared to those obtained using the rule-based control. Moreover, an examination of RES utilization reveals that the MPC enables a 6.2 % increase in the exploitation of renewable energy, consequently leading to higher methane production. Lastly, it is also obtained that the recovery of heat is more efficient with the MPC, and with this approach it is possible to meet 45.6 % of the thermal demand of the end-user (a 3.8 % improvement compared to the rule-based control).

Figure 4.16 illustrates how the heat demand is met over the second simulated day using the two different control strategies. Using the MPC strategy, the system efficiently fulfills the heat demand without the need to purchase gas from the network, relying solely on the heat recovered and the renewable gas produced by the PtG plant. Conversely, 10.6 % of the demand is satisfied by purchasing gas from the network when employing the rule-based controller. Furthermore, with the MPC controller, 45.6 % of the end-user heat demand is supplied through waste heat recovery, which is 3.8 % more than with the rule-based control. This outcome highlights the potential for full decarbonization of a small DHN with the integration of a properly sized and managed PtG system.

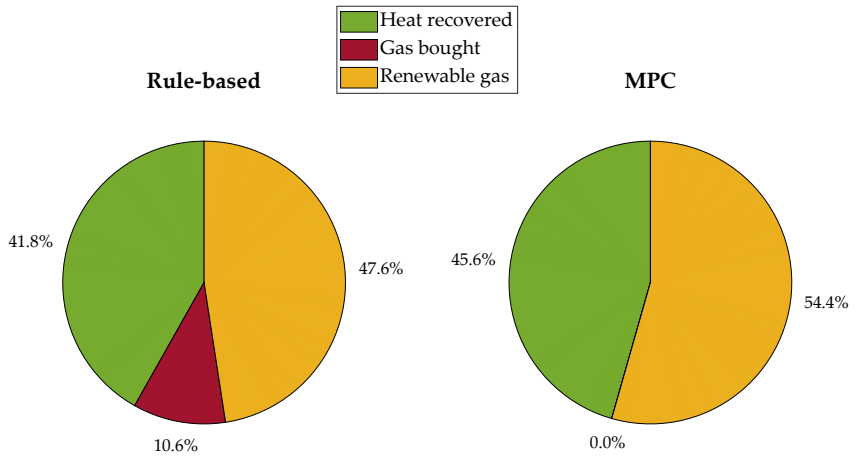

Figure 4.16: Fulfillment of the heat demand over the entire simulated day with the two control strategies.

4.4 Discussion

In this study, a PtG plant integrated with a DHN was analyzed, and the results of two control strategies, namely a novel MPC and a rule-based approach, were compared. The application involved a PtG plant that produces synthetic methane from renewable electricity generated by a wind farm. The system was integrated with a DHN, which make use of a gas-fueled boiler and of the waste heat recovered from the PtG plant to provide heat to end-users.

The two control strategies were compared by applying them in a MiL configuration. Overall, the MPC strategy demonstrated superior performance in terms of economic gains, carbon emissions reduction, renewable energy utilization, gas production, and heat demand fulfillment. It effectively optimized the operation of the PtG plant and DHN, highlighting its potential for decarbonization and efficient energy management in similar systems. These findings emphasize the benefits of advanced control strategies, such as MPC, in achieving more sustainable and economically viable energy systems, especially when integrating renewable energy sources with heat recovery and gas production components.

The development and validation of a MPC controller in a MiL environment paves the way for its real-world application, following the process outlined in Figure 4.17. In addition, as the optimization algorithm has been designed for a generic MES, the controller can be easily adapted to different case studies, and it can also help in testing various energy system configurations.

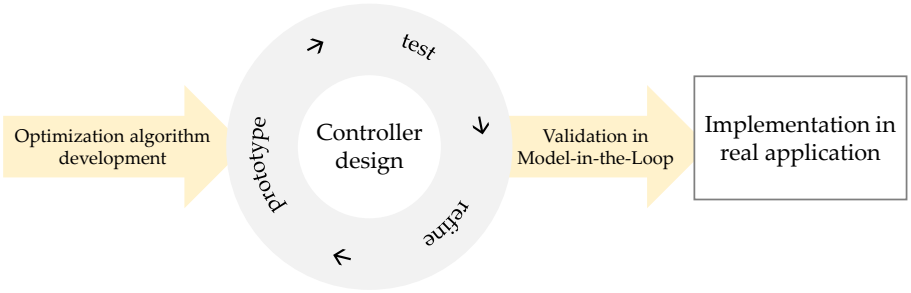

Figure 4.17: Procedure for development, validation and testing of controller prototype.

Once the controller has been validated within the MiL framework, its application to real-world case studies becomes a relatively straightforward process. Indeed, the optimal control has been tested to be viable even with open source solvers in adequate computational time. In addition, this can be achieved without the need for new hardware installation, since it only involves the modification of set-points within the existing low-level controllers in accordance with the MPC logic. A similar methodology was employed in the DISTRHEAT project [102], where an MPC controller was initially verified in a simulation platform and subsequently applied to a real-world case study, resulting in intelligent and efficient system management. This approach ensures that the operation of the real system is not negatively affected during the testing phase.

Chapter 5

Multi-temporal and multi-spatial Model Predictive Controller

In this chapter, the third outcome of this thesis is presented, which regards the development and validation of a multi-temporal and multi-spatial controller for the optimal management of a synthetic natural gas seasonal storage, which is shared among different energy systems. This application integrates the methods previously introduced in Chapters 3 and 4 to enhance their overall functionality and comprehensiveness.

First, the novel architecture is described, then an application is presented, in which the controller is applied to a case study and lastly the simulation results are presented for evaluation.

5.1 Method

As discussed in Paragraph 1.1, it is widely recognized that renewable fuels generated with PtG systems represent one of the most promising solutions for the growing need of seasonal storages. Nonetheless, the smart management of an energy system integrated with a seasonal storage is not straightforward: indeed, yearly dynamics related to renewable generation as well as energy demands must be taken into account. In addition, because of the high investments needed for large seasonal storages, they can serve multiple small PtG systems, that generate the fuel to be stored. When designing and developing smart controllers for such systems, these dynamics must be considered. Therefore, a novel control architecture that allows a shared natural gas seasonal storage to be optimally managed

was developed for this application. The control action is able to manage the day-ahead energy exchanges, by taking into account both daily and yearly dynamics. The control architecture is schematized in Figure 5.1 for a natural gas seasonal storage which is shared among three multi-energy systems.

The developed approach is multi-period and multi-spatial and it uses two different control levels, based on MPC strategy:

- **Supervisory long-term module**: this module is an MPC with a prediction horizon spanning a year and a time-step of one day. This setup enables the system to account for the seasonality in production and demand that occurs over the course of the year, as well as the management of seasonal energy storage. Regardless of the number of energy systems considered, the control architecture only necessitates one supervisory module, that regulates the entire system. This module uses a stochastic MILP algorithm to perform the optimization every day, taking into account the uncertainty in the disturbance forecasts.

- **Short-term modules**: these modules are repeated for each of the multi-energy systems in the application and they consider a prediction horizon of few days. As the supervisory module, they were developed as MPC controllers, and they use a detailed MILP algorithm for the optimization. They

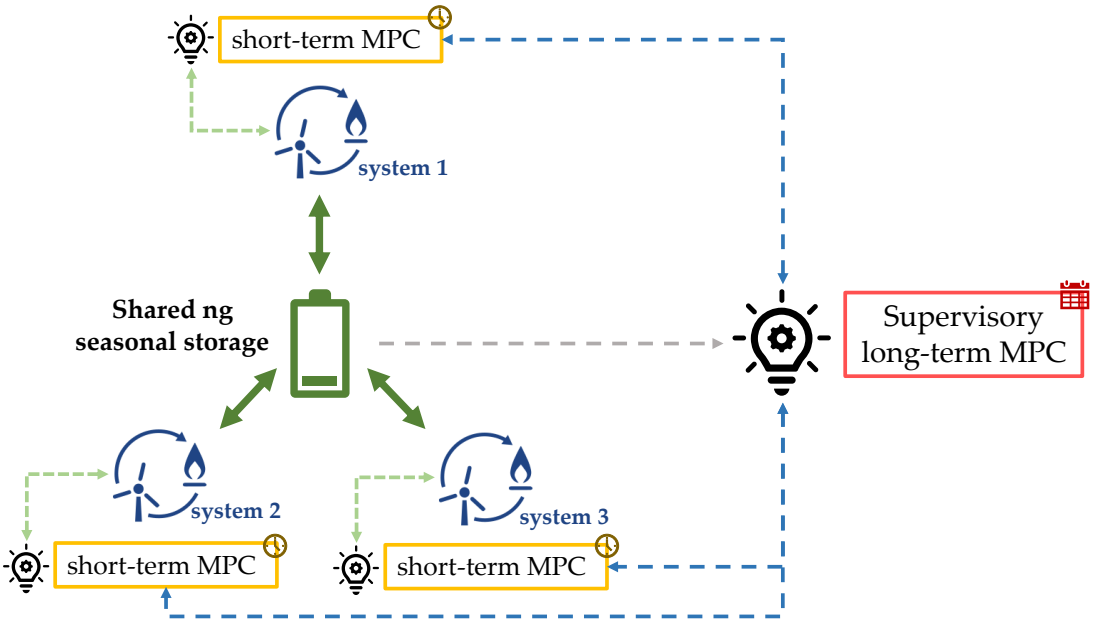

Figure 5.1: Multi-temporal and multi-spatial control architecture schematization.

do not optimize the seasonal storage management, but instead they receive additional information from the supervisory module regarding the amount of energy to exchange with it each day. This information is elaborated by the modules and transformed to *long-term constraints*.

In the following sections, the details regarding the architecture of the control approach and the MPC modules are described.

5.1.1 Supervisory module

As mentioned above, every day the supervisory module is run and calculates the amount of energy that the systems need to exchange with the seasonal storage each day of the prediction horizon. The algorithm used in this module is a stochastic MILP algorithm, as the one presented in Chapter 3. The uncertainties are modeled through the generation of several scenarios every day, starting from the future deterministic disturbances, using the roulette wheel mechanism, and the number of scenarios is reduced by employing the scenario reduction method proposed in 3.1.3.

The algorithm has been further refined to suit this particular application, allowing it to efficiently coordinate the management of multiple MES collectively. Basically, each MES is assumed to have its own energy carriers and cannot directly exchange energy with other MES. However, they are interconnected through the seasonal storage component, which enables every MES to exchange energy with it. The equation describing the behavior of the seasonal storage is as follows:

$$E_{stor}(t) = \eta_{sd} E_{stor}(t-1) + \sum_{i=1}^{N_z} \left(\eta_c P_{stor_{in,i}}(t) - \frac{P_{stor_{out,i}}(t)}{\eta_d} \right) \Delta t \,, \tag{5.1}$$

with N_z being the number of MES in the application, that can exchange energy with it. $E_{stor}(t)$ is the amount of energy stored at time-step t, $E_{stor}(t-1)$ the amount of energy stored at time-step $t-1$, η_{sd} is the self-discharge efficiency, η_c is the charge efficiency and η_d the discharge efficiency of the seasonal storage, while $P_{stor_{in,i}}(t)$ and $P_{stor_{out,i}}(t)$ are the power entering and leaving the storage, respectively, at time-step t for the MES i, and Δt is the time-step length. In addition, it was set that the amount of energy stored at the beginning of the prediction horizon must be equal to the energy stored at the end of the prediction horizon (i.e. one year). In this way, the algorithm is consistent with the idea of seasonal storage and prevents the system from using the storage to empty it in

order to increase the revenues without foreseeing what will happen the following year. Therefore, the following constraint was added for the seasonal storage, being N_t the total number of time-steps (i.e. 365 for daily time-step and one year of prediction horizon)

$$E_{stor}(0) = E_{stor}(N_t)\,, \tag{5.2}$$

with $t = 0$ being the current time-step and $t = N_t$ the last time-step of the prediction horizon.

The two-stage stochastic programming algorithm was configured such that the first-stage variables, namely the variables that present the same value for all the scenarios, were set as all the variables associated with the seasonal storage (i.e. the amount of natural gas entering and exiting the storage, and the energy stored in the storage). Instead, all the variables related to the other components were designated as second-stage variables, i.e. scenario specific. In this way, the management of the seasonal storage is robust against the future behavior of the uncertain parameters.

5.1.2 Short-term modules

The short-term modules have the same characteristics of the MPC module presented for the application in Chapter 4, and present hourly time-step with prediction horizon of two days. Nonetheless, they have also been enhanced for this application, making them able to consider the seasonal storage behavior. The difference for this application is that every day at midnight, when the long-term supervisory module is run, they receive information on the amount of energy to exchange with the seasonal storage during the next two days. Specifically, they use four values: $E_{day1_{in}}$, $E_{day1_{out}}$, $E_{day2_{in}}$ and $E_{day2_{out}}$, which are respectively the amount of energy to inject (in) and withdraw (out) from the storage during the first day of prediction horizon (day1) and during the second day of prediction horizon (day2). These are cumulative information over each day, and they cannot be used as such by the modules, that instead have a shorter time-step length. Therefore, they are elaborated and transformed into constraints for the problem, which were named *long-term constraints*.

In Figure 5.2, a visual representation of the process is presented. This diagram helps clarify the architecture: every day at midnight the long-term module supplies information for the subsequent two days to the short-term modules. This information is used differently by them depending on the time of the day. In-

deed, at the beginning of the day ($t = 0$), the prediction horizon contains all the time-steps of the two days, and therefore the value given from the long-term module is used to constrain all the time-steps (in day 1 and day 2). Instead, since the prediction horizon of the short-term module is of two days, when rolling the horizon, for constraining the time-steps in the first day, cumulative data on what happened during the past time-steps of the first day is needed. In addition, as time advances throughout the day, the prediction horizon extends into the third day, for which energy exchange information is unavailable. Nevertheless, it is believed that the absence of constraints on the time-steps entering the third day does not significantly impact the overall functionality of the control action. Indeed, with the MPC strategy, only the first signal is applied to the real system, which corresponds to the first time-step of the prediction horizon.

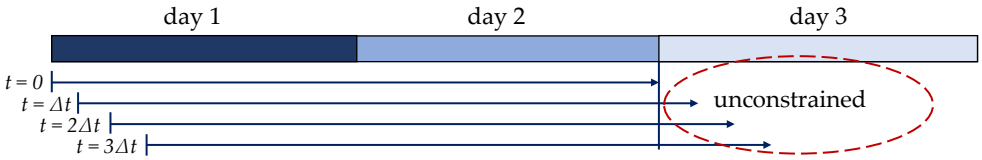

Figure 5.2: Schematization of how long-term constraints are given to the short-term modules and used by them.

The long-term constraints at time-step t are elaborated so that they impose that the amount of energy injected to the storage (or withdrawn from it) during each day must be equal to the amount of energy calculated by the long-term module +/- an ϵ term, always positive. In order to force the result to be obtained, the ϵ terms are inserted and minimized in the objective function. In this way, if the system is not able to fulfill the constraints, the problem does not become infeasible but instead these variables assume a value different than zero, making them *soft constraints*. The constraints are elaborated as follows for the first day of the prediction horizon

$$\sum_{\bar{t}=t}^{N_d-t} P_{stor_{in}}(\bar{t})\Delta t \leq E_{day1_{in}} - \sum_{\bar{t}=0}^{t-1} P_{stor_{in}}(\bar{t})\Delta t + \epsilon_{in_1} \,, \tag{5.3}$$

$$\sum_{\bar{t}=t}^{N_d-t} P_{stor_{in}}(\bar{t})\Delta t \geq E_{day1_{in}} - \sum_{\bar{t}=0}^{t-1} P_{stor_{in}}(\bar{t})\Delta t - \epsilon_{in_1} \,, \tag{5.4}$$

$$\sum_{\bar{t}=t}^{N_d-t} P_{stor_{out}}(\bar{t})\Delta t \leq E_{day1_{out}} - \sum_{\bar{t}=0}^{t-1} P_{stor_{out}}(\bar{t})\Delta t + \epsilon_{out_1} \,, \tag{5.5}$$

$$\sum_{\bar{t}=t}^{N_d-t} P_{stor_{out}}(\bar{t})\Delta t \geq E_{day1_{out}} - \sum_{\bar{t}=0}^{t-1} P_{stor_{out}}(\bar{t})\Delta t - \epsilon_{out_1} \,, \tag{5.6}$$

where $P_{stor_{in}}(\bar{t})$ and $P_{stor_{out}}(\bar{t})$ represent the power injected and withdrawn from the seasonal storage at time-step $\bar{t}$, $E_{day1_{in}}$ and $E_{day1_{out}}$ are the total amount of energy that the long-term module imposes to inject and withdraw from the seasonal storage during the first day, N_d is the number of time-steps in one day. Finally, ϵ_{in_1} and ϵ_{out_1} are the additional variables added to make these constraints soft. It is worth highlighting that the terms $\sum_{\bar{t}=0}^{t-1} P_{stor_{in}}(\bar{t})\Delta t$ and $\sum_{\bar{t}=0}^{t-1} P_{stor_{out}}(\bar{t})\Delta t$ represent the cumulative amount energy exchanged with the storage during the past time-steps of the day. These values are updated every time-step using actual data from the real system (or from the digital-twin of the system).

For the second day of the prediction horizon, the term related to the amount of energy already exchanged is not present because the current time never enters the second day. The constraints are the following

$$\sum_{\bar{t}=N_d-t+1}^{2N_d-t} P_{stor_{in}}(\bar{t})\Delta t \leq E_{day2_{in}} + \epsilon_{in_2} \,, \tag{5.7}$$

$$\sum_{\bar{t}=N_d-t+1}^{2N_d-t} P_{stor_{in}}(\bar{t})\Delta t \geq E_{day2_{in}} - \epsilon_{in_2} \,, \tag{5.8}$$

$$\sum_{\bar{t}=N_d-t+1}^{2N_d-t} P_{stor_{out}}(\bar{t})\Delta t \leq E_{day2_{out}} + \epsilon_{out_2} \,, \tag{5.9}$$

$$\sum_{\bar{t}=N_d-t+1}^{2N_d-t} P_{stor_{out}}(\bar{t})\Delta t \geq E_{day2_{out}} - \epsilon_{out_2} \,, \tag{5.10}$$

where symbols are identical to those used in the constraints for the first day, but they pertain to day 2 of the prediction horizon.

5.2 Application

The proposed approach was applied to a case study and its performance was evaluated by employing a MiL application. The case study and the implementation

are described in the following sections.

5.2.1 Case study description

The case study comprises three MES, in which synthetic natural gas is generated through a PtG process. Indeed, all the three systems comprise an electrolyzer for hydrogen generation and a methanation reactor for the production of synthetic natural gas. The generated natural gas can be then used internally in the systems, or otherwise stored in a shared natural gas seasonal storage. The overall architecture is schematized in Figure 5.1. The three systems have different architectures which are described in the following.

System 1: this energy system is schematized in Figure 5.3. Its architecture is the same as the energy system studied for the application described in Chapter 4, to which the reader can refer for more information. In this application, however, an additional component is added, which is the shared natural gas seasonal storage with which all the systems can exchange energy by injecting or withdrawing natural gas.

System 2: the architecture of this system is identical to that of system 1 (see Figure 5.3), but the sizes of the plants are obtained by multiplying the sizes of system 1 for a factor equal to 1.5. In this way, it was possible to validate the benefits of the control strategy also with larger energy systems.

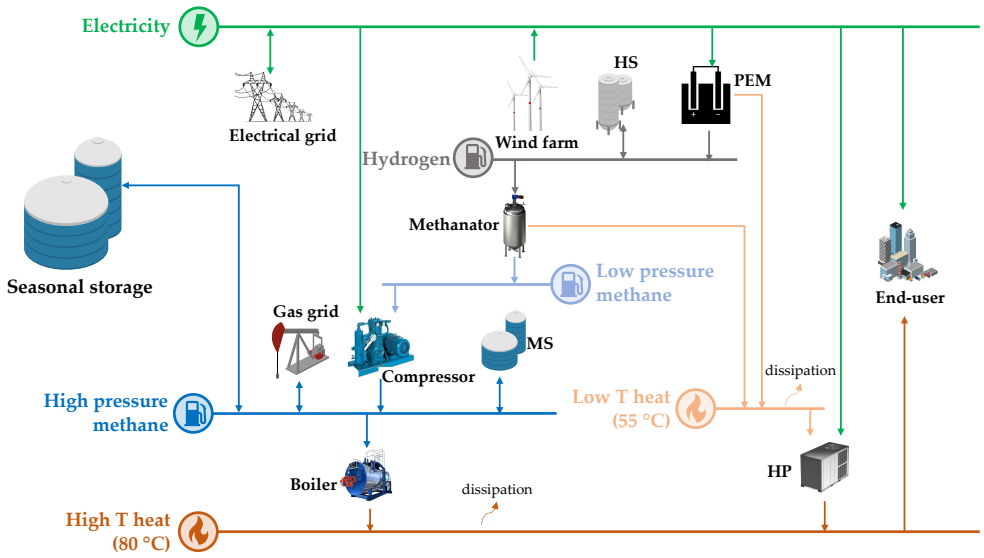

Figure 5.3: Schematization of systems one and two.

System 3: the third system considered differs from the other two, and its

architecture is presented in Figure 5.4. This system is connected both with the electrical and gas network and can exchange energy with them by buying or selling it, as the other two systems. Nevertheless, instead of having a wind farm for renewable energy generation, a photovoltaic plant is present. In addition, for this system the heat recovery from the PtG plant is not considered, as well as the internal storage for natural gas. Instead, there is a thermal energy storage (TES) for storing thermal energy in the form of hot water.

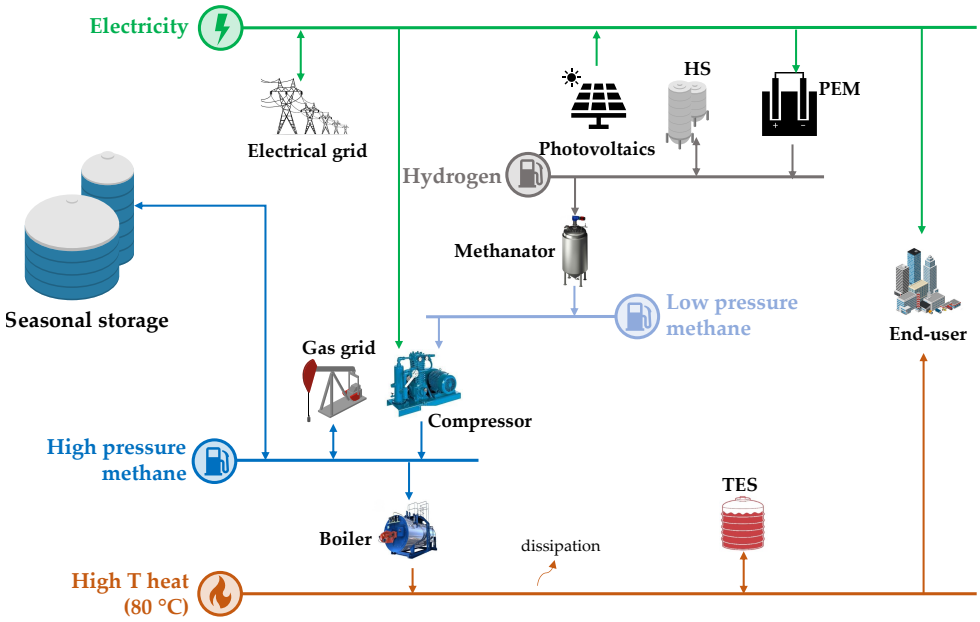

Figure 5.4: Schematization of the third system considered.

By considering systems with different sizes and architectures, the strategy is verified under different conditions that allow to evaluate the generality of the developed approach. The specifications on the systems are presented in Table 5.1

Technology	Parameter	System 1	System 2	System 3
Wind Farm	Nominal power (kW)	8000	12000	–
Photovoltaics	Nominal power (kW)	–	–	8000
Electrolyzer	Nominal inlet power (kW)	3750	5625	3750
	Nominal operating temperature (°C)	55	55	55
	Nominal operating pressure (bar)	35	35	35
Methanator	Nominal inlet power (kW)	2479	3718	2479
	Nominal operating temperature (°C)	290	290	290
	Nominal operating pressure (bar)	2.5	2.5	2.5
Boiler	Nominal inlet power (kW)	4000	6000	4000
	Nominal efficiency (%)	92.4	92.4	92.4
Heat Pump	Nominal inlet power (kW)	380	570	–
H_2 storage	Volume (m^3)	100	150	100
	Maximum pressure (bar)	35	35	35
	Minimum pressure (bar)	2.5	2.5	2.5
Methane storage	Volume (m^3)	100	150	–
	Maximum pressure (bar)	7.5	7.5	–
	Minimum pressure (bar)	3.5	3.5	–
Thermal energy storage	Maximum capacity (kWh)	–	–	12 000

Table 5.1: Characteristics of the components of three systems analyzed.

5.2.2 Implementation

The developed control architecture was tested by applying it in a MiL configuration. Similarly to what has been done in Chapter 4, a digital-twin of the case study was developed in the MATLAB®/Simulink® environment by using the in-house library of energy system components (refer to Appendix A for more details).

The schematization of the MiL application is represented in Figure 5.5. Every day, the long-term module (i) receives as initialization variables the SoC of all the storages in the system, (ii) it performs the stochastic optimization and (iii) returns to the short-term modules the amount of energy to exchange with the seasonal storage each day. The short-term modules, instead, are run every hour, and (i) they get as initialization variables the SoC of the storages in the systems (except from the seasonal storage), (ii) perform the optimization using the MILP algorithm and return the set-points calculated for the first time-step to the digital-twin: the set-points for the conversion units, the gas to exchange with the gas network and the gas to exchange with the seasonal storage.

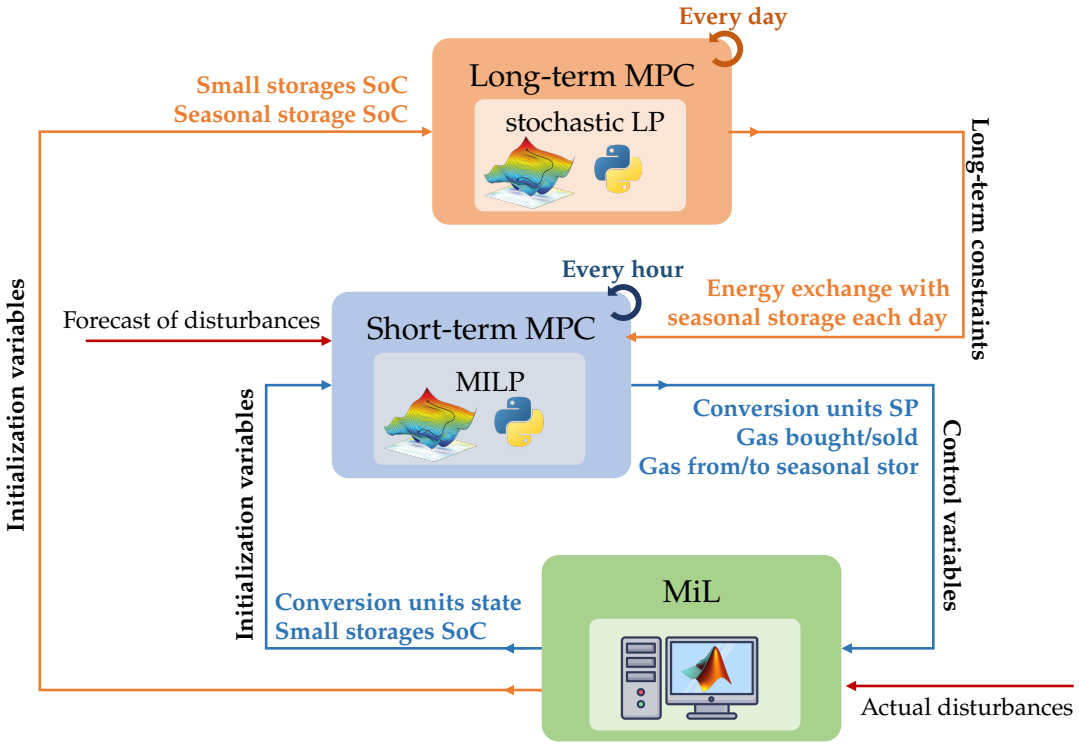

Figure 5.5: Schematization of the Model-in-the-Loop application of the control architecture. (SoC = State of Chrge, SP = set-point)

The long-term supervisory module was set with a prediction horizon of one year and daily time-step. Every day, 500 scenarios are generated for renewable energy production, electrical and thermal needs of the end-users, and these scenarios are reduced to the number of 30. The objective of the optimization is the minimization of the total CO_2 emissions, which are all the emissions related to the electricity and gas bought from the networks. The objective function is therefore the sum of the energy bought from the networks multiplied by the related emission factor, and it is expressed as follows

$$\min f_{obj_{LT}} \,, \tag{5.11}$$

with

$$f_{obj_{LT}} = \sum_{t=1}^{N_t} \sum_{s=1}^{N_{scen}} Pr(s) \Big(P_{el,bo,s}(t) e_{CO_2,el} + P_{ng,bo,s}(t) e_{CO_2,ng} \Big) \Delta t \,, \tag{5.12}$$

where N_t is the number of time-steps in the prediction horizon, N_{scen} is the number of scenarios considered, $Pr(s)$ is the probability of scenario ξ_s, $P_{el,bo,s}(t)$ and $P_{gn,bo,s}(t)$ are the amount of electricity and natural gas bought form the networks. The emissions related to the electrical grid are calculated using an emission factor equal to $e_{CO_2,el} = 224$ gCO_2/kWh [99], while for the gas network a coefficient of $e_{CO_2,ng} = 200.8$ gCO_2/kWh is used [100].

The short-term modules, instead, are set with a prediction horizon of two days, and an hourly time-step. The objective function implemented is the maximization of the total operating margin of the system, which encompasses the maximization of revenues minus costs. In the cost function, the minimization of the ϵ variables introduced for softening the long-term constraints is also added. The cost function is expressed by the following expression

$$\max f_{obj_{ST}} \,, \tag{5.13}$$

with

$$\begin{aligned} f_{obj_{ST}} = \sum_{t=1}^{N_t} \Big(& c_{el,so}(t) P_{el,so}(t) + c_{ng,so}(t) P_{ng,so}(t) - c_{el,bo}(t) P_{el,bo}(t) + \\ & - c_{ng,bo}(t) P_{ng,bo}(t) \Big) \Delta t - \Big(\epsilon_{in_1} + \epsilon_{in_2} + \epsilon_{out_1} + \epsilon_{out_2} \Big) \,, \end{aligned} \tag{5.14}$$

where $P_{el,so}(t)$ and $P_{ng,so}(t)$ are the amount of electricity and natural gas sold to the networks at time t, respectively, and $c_{el,so}(t)$, $c_{ng,so}(t)$ the revenues related to them, while $P_{el,bo}(t)$ and $P_{ng,bo}(t)$ are the amount of electricity and natural gas bought from the networks, with $c_{el,bo}(t)$ and $c_{ng,bo}(t)$ their costs at time t; ϵ_{in_1}, ϵ_{in_2}, ϵ_{out_1} and ϵ_{out_2} are the variables introduced for softening the long-term constraints and they are better explained in Paragraph 5.1.

To test the novel control architecture, it was decided to simulate two periods of the year with different weather conditions: five days in May and five days in November. It needs to be specified that for the simulations, the detailed digital-twin in Simulink® was built only for system 1. Instead, the operational characteristics of the other two systems were emulated using MILP models. These models were run on an hourly basis to ensure a complete representation of the system behavior. Additionally, a noise was added to the results, so that the amount of gas exchanged with the storages is not exactly the one calculated by the MILP algorithm. In this way, the model is closer to real-world applications since a level of unpredictability similar to practical situations is introduced. For this reason, only the results regarding system 1 will be shown. To calculate the renewable generation over the year, for the photovoltaic production data was taken from PVGIS [103], while for wind power generation the Wind Atlas website [104] was used. The user energy demands are instead estimated starting from historical data.

The deterministic forecasts of the disturbances given to the long-term supervisory module for system 1 over the course of the year are displayed in Figure 5.6. This figure represents the average daily energy needs and renewable produc-

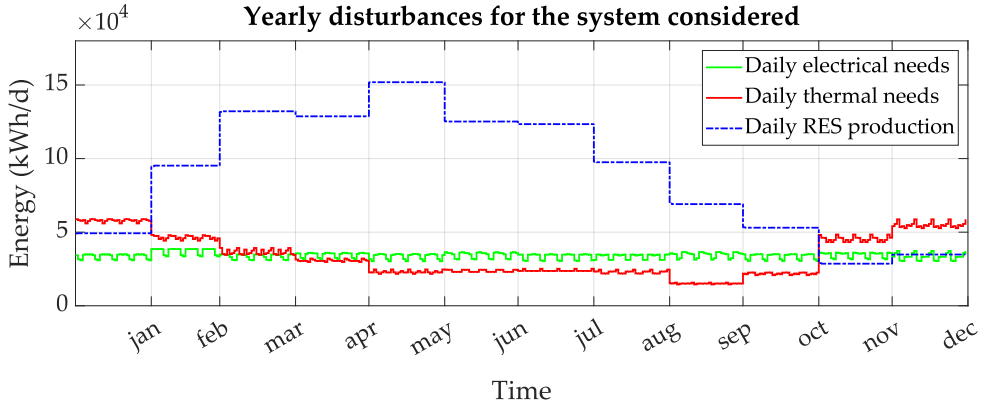

Figure 5.6: Forecast of yearly disturbances for system 1.

tion. Starting from the deterministic forecast, the scenarios used in the stochastic approach were generated.

While in the long-term module only the daily average values are needed, for the short-term module a more detailed forecast is used. The forecasts given to this module during the two simulated periods are displayed in Figure 5.7. It is notable that the disturbances in the two seasons change significantly. While in May the renewable energy is always in surplus with respect to the needs, in November it is almost always in deficit, and higher thermal needs are present in this season.

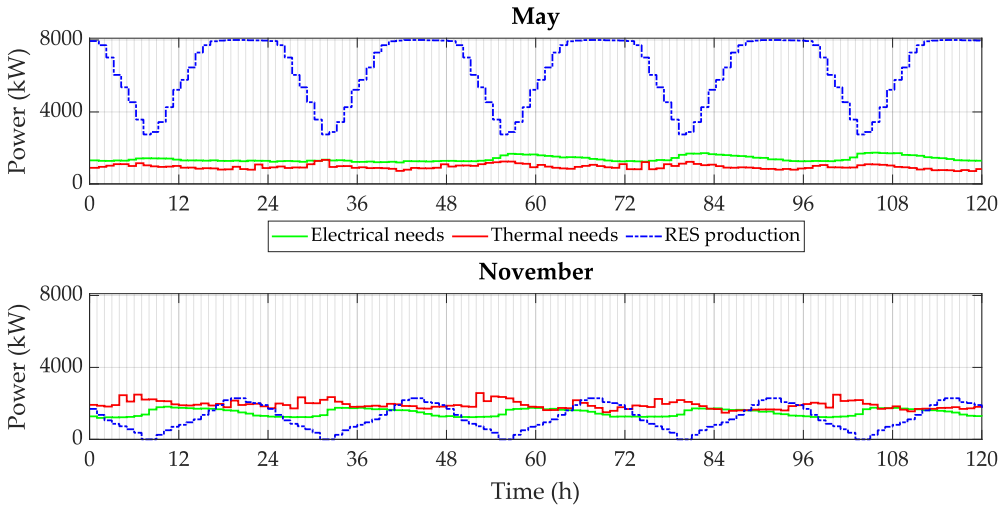

Figure 5.7: Forecast of disturbances given to the controller in the two simulated periods for system 1.

5.3 Results

The simulations have been run for the two periods of the year, i.e. May and November, and the results obtained were analyzed.

First, in Figure 5.8 the electricity balance is shown, being the positive values related to generation (RES and electricity bought) and the negative values related to consumption (user needs, electricity used by PtG system and electricity sold). It can be seen how the electricity is managed within the system during the two simulated periods: in May, since there is always a surplus renewable electricity, the system never buys electricity from the network, and it sells the surplus electricity generated. In November instead, the electricity needs to be bought

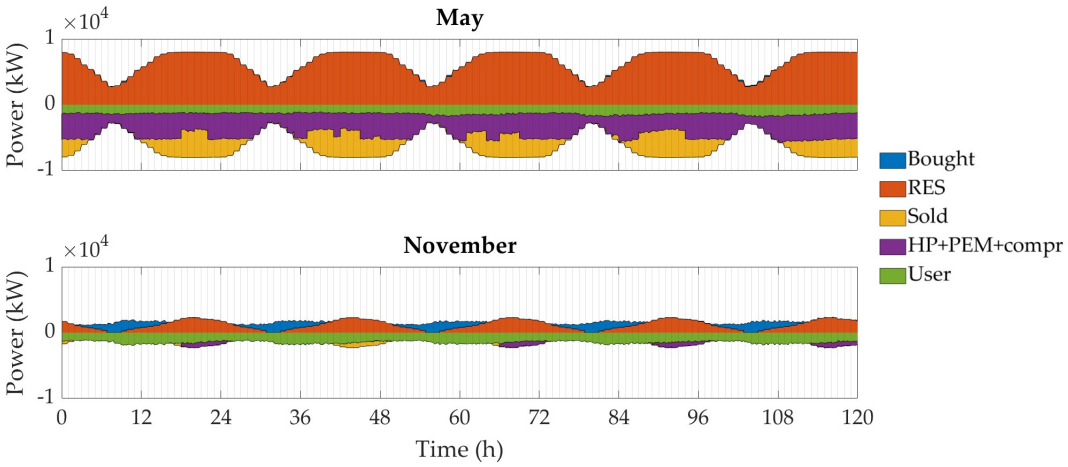

Figure 5.8: Electricity balance in the two simulated periods.

when it is in deficit, to fulfill the user needs, and it is almost never sold to the grid. How the electrolyzer is operated is displayed in Figure 5.9, together with the management of the hydrogen storage. Looking at the management during the spring period, in May, it can be noticed that, due to the large availability of renewable energy in this period, the electrolyzer is always switched on, and that the hydrogen storage is used to balance daily energy fluctuations. Instead, during November the electrolyzer is switched on only when there is a surplus electricity. Nevertheless, on the second day, the MPC decides to keep it off and sell the surplus electricity. As a matter of fact, switching on the electrolyzer also leads to additional start-up costs related to the time needed for the system to heat-up the electrolyzer stacks, and being the optimization based on economic cost minimization, it was not convenient for the system to switch it on during this day. Indeed, costs of purchasing and selling electricity and gas are variable during the five simulated days and depending on them, the production of gas can be more or less convenient using the PtG system. In addition, as shown in Figure 5.10, during November, the system uses the seasonal storage to withdraw natural gas, being the renewable generation in deficit compared to needs. This helps the system cover the thermal needs during the day and not need additional hydrogen generation.

In Figure 5.10, it can also be noticed that while in November the seasonal storage is only used to withdraw natural gas, the opposite situation happens in May, when the seasonal storage is only used by the system to inject the surplus natural gas generated. Even though simulating only five days for each season

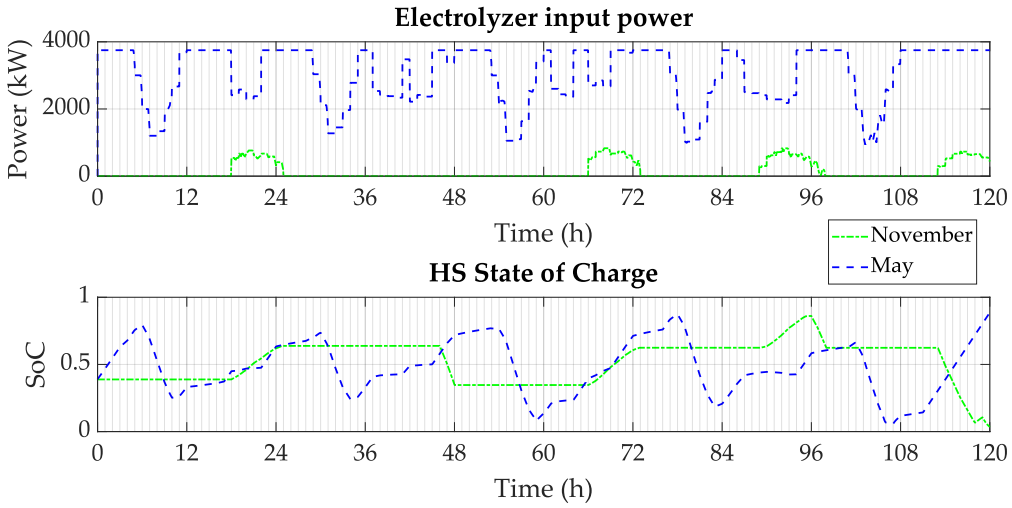

Figure 5.9: Electrolyzer and hydrogen storage management during the two simulated periods.

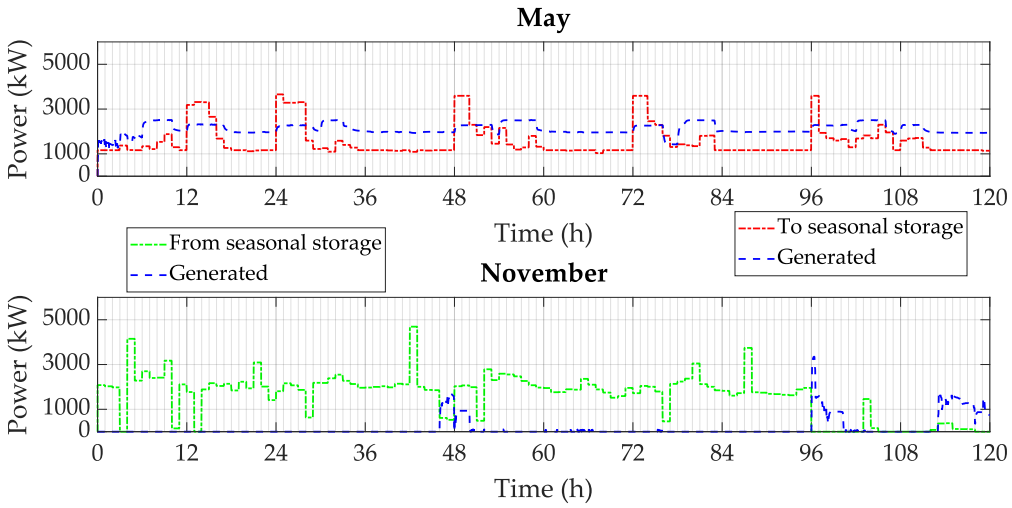

Figure 5.10: Amount of natural gas generated and exchanged with the seasonal storage during the two simulated periods.

could seem not representative of the whole yearly management of the seasonal storage, it is worth reminding that the long-term module has a yearly prediction horizon, and it is imposed that the amount of energy stored at the current time-step must be equal to the amount of energy stored at the end of the prediction horizon, as expressed in Eq. (5.2). This means that the energy exchanges with the storage are consistent to what happens during the rest of the year, and it is not unrealistic that in November a large amount of energy stored in the previous

months of the year is available. Additionally, the long-term module can adapt the management based on the availability of natural gas in the storage, since it receives as input the amount of energy stored in the seasonal storage each day.

How the thermal demand is fulfilled during the two seasons is displayed in Figure 5.11. It can be noticed that during May, all the thermal needs are satisfied using the renewable gas generated and the heat recovered from the PtG process only, and therefore a full decarbonization of the heating sector is obtained. Instead, in November part of the needs are fulfilled by using methane bought from the gas network, particularly the 16 % of the total demand. Only 1 % is fulfilled using the heat pump that recovers the waste heat from the PtG process, and 6 % by using renewable methane produced by the methanator. It is noteworthy that 76 % of the needs are covered using the gas withdrawn from the seasonal storage: also in this season the majority of thermal needs are fulfilled by using renewable energy, and this result would not be possible without the use of the seasonal storage. Indeed, the renewable generation was not enough to fulfill the thermal and electrical loads in this season, and thanks to the use of seasonal storage it was possible to utilize energy which was stored in periods of higher renewable production.

Even though Systems 2 and 3 were not simulated in detail, their management is updated every hour using the results of MILP algorithms, as mentioned in section 5.2.2, and it is taken into account in the long-term module and for the calculation of the energy stored in the seasonal storage. The amount of gas ex-

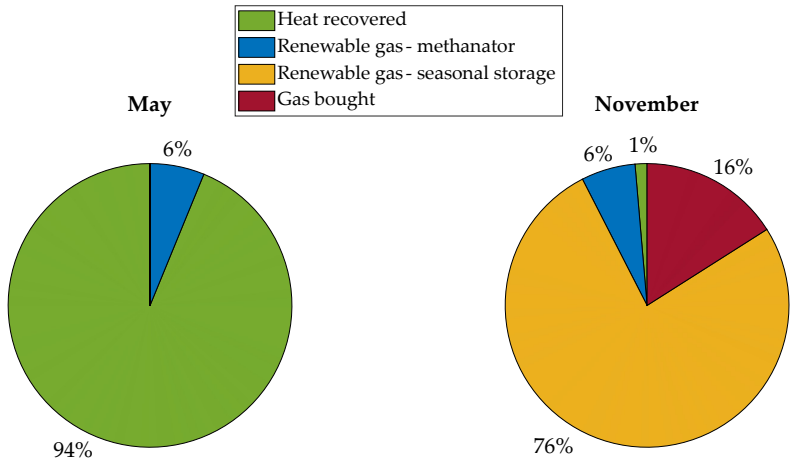

Figure 5.11: Pie with thermal demand fulfillment in the two simulated periods.

changed with the seasonal storage by the three systems during the two simulated periods is displayed in Figure 5.12. All the three systems use the seasonal storage to inject natural gas during May, and they withdraw it during November, to use it to cover the high thermal request in this season.

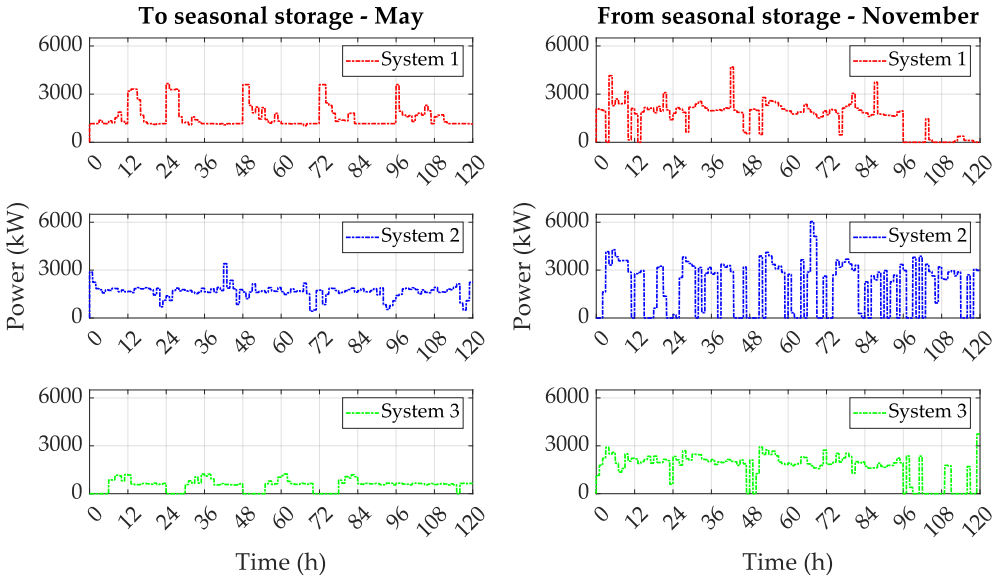

Figure 5.12: Power exchanges with the seasonal storage during the two simulated periods.

A complete fulfillment of the long-term constraints set by the long-term supervisory module was achieved across all three systems, confirming the effective performance of the control architecture. This is illustrated in Figure 5.13 for system 1, where the cumulative amount of gas exchanged with the seasonal storage (injected in May and withdrawn in November) is displayed, together with the long-term constraints (in gray), to be fulfilled each day.

The energy stored trend in the seasonal storage is shown in Figure 5.14. As expected, it increases in May, when higher renewable generation is available and part of it is stored, while it decreases during November, when the gas is used by the three systems.

Some numerical cumulative results over the five simulated days are presented in Table 5.2. It is worth highlighting that the operating margin, as expected, is negative in May, when large amount of renewable electricity is exported, and positive in November, when the system needs to buy part of the electricity to fulfill the internal needs. The CO_2 emissions, being related to the import of energy from the networks, are also higher during November. An important result concerns

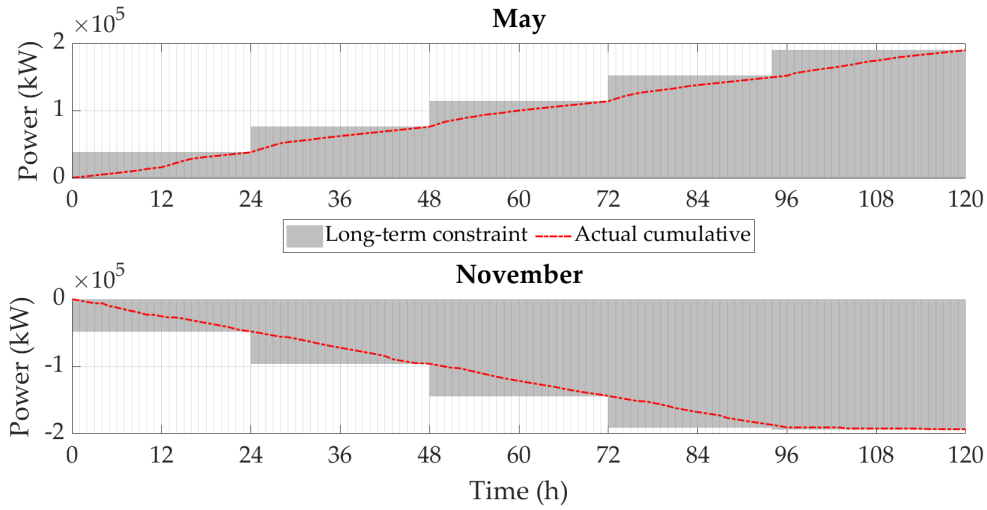

Figure 5.13: Fulfillment of long-term constraints by system 1.

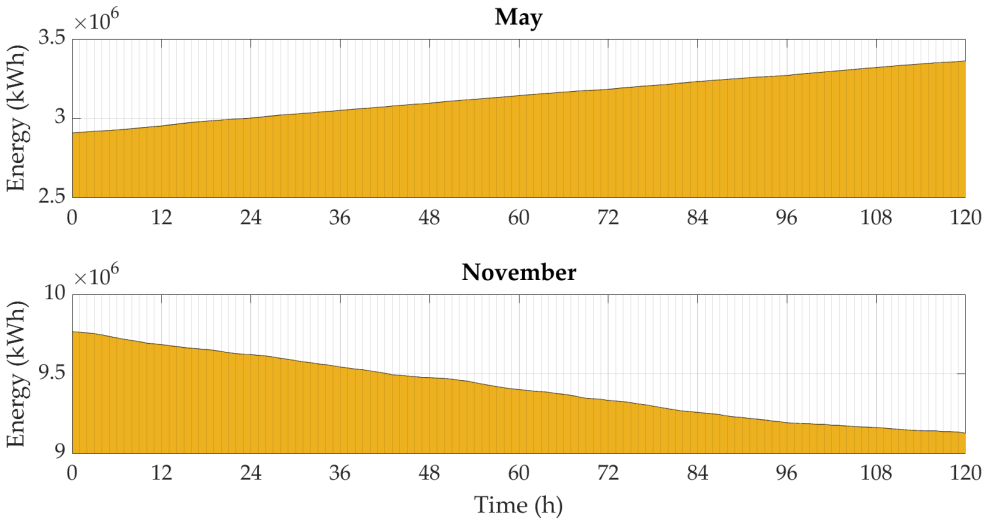

Figure 5.14: Energy stored in the seasonal storage during the two simulated periods.

the amount of renewable energy utilized by the system in the two periods, and therefore not injected into the electricity grid: in May, the 72 % of the RES production is used, and in November the 95 %, almost all of it. In general, the inclusion of a seasonal storage allows for a higher renewable energy utilization by the system, even in seasons with high surplus renewable generation. In addition, the amount of gas exchanged with the seasonal storage is displayed, and the fulfillment of the long-term constraints, which, as aforementioned, are fulfilled by 100 % in both seasons.

Table 5.2: Values of relevant indicators obtained in the two simulated periods.

Value	May	November
Operating margin	- 13 135 EUR	12 825 EUR
CO_2 emissions	2 101 kg_{CO_2}	22 586 kg_{CO_2}
RES usage	72 %	95 %
Gas to seasonal storage	189 720 kWh	–
Gas from seasonal storage	–	193 473 kWh
Long-term constraints fulfillment	100 %	100 %

5.4 Discussion

A novel hierarchical control architecture based on two MPC modules with different time- and space-scales was developed. The control architecture was developed for managing a natural gas seasonal storage, integrated in a case study comprising three different energy systems with integrated PtG solutions for the generation of synthetic natural gas. The simulations were conducted during two distinct periods of the year, May and November, providing valuable insights into the performance of the system. The results were discussed for one of the three systems considered.

The control strategy is particularly effective in managing the seasonal storage. In May, it enables the injection of renewable gas into the storage, taking advantage of excess renewable energy. In addition, by recovering the waste heat from the PtG process and using renewable gas generated, a full decarbonization of the heating sector in the simulated period was obtained. In November, instead, renewable electricity generation is not sufficient to meet the energy demand of the system. The control architecture allows the system to buy electricity and gas from the networks when necessary, optimizing its operating costs. Nevertheless, the seasonal storage plays a crucial role during this period, with a substantial portion of the thermal demand being fulfilled by utilizing gas withdrawn from storage, and only a small part being met using gas bought from the gas network.

The results highlight the effectiveness of the control architecture in optimally utilizing seasonal storage, effectively managing the fluctuations in renewable energy generation, and ensuring a reliable supply of renewable energy. The short-term modules effectively apply the long-term constraints imposed by the supervisory module and are able to completely fulfill them. Furthermore, the innovative control strategy, which views the entire system holistically, enables strategic decision-making regarding energy sales and purchases, taking into account mar-

ket conditions. This integrated approach to energy management is crucial for achieving sustainability and maximizing the use of renewable resources.

In conclusion, the control architecture showed its adaptability and effectiveness in managing energy systems with seasonal storage, providing flexibility to adapt to changing renewable generation and demand patterns. This study exemplifies the importance of multi-temporal and multi-spatial control strategies in energy systems to enhance sustainability and efficiency, and the research contributes to the development of more sustainable and efficient MES, paving the way for a cleaner and more resilient energy future.

Chapter 6

Conclusions

The primary objective of this thesis was to advance the research on future management strategies and novel solutions to address the increasing complexity of energy systems, aiming at the complete decarbonization of the energy sector, and it was achieved through the development of diverse smart management tools.

Concluding remarks

This thesis introduced innovative management and control tools, which were not only proposed but also tested on various case studies to validate their functionality. These tools are summarized below:

- *Long-term optimization*: a stochastic MILP algorithm was developed and applied to different case studies which comprised Power-to-Gas (PtG) solutions and hydrogen seasonal storage. The algorithm addresses the inherent uncertainty associated with future disturbances, such as energy demand, generation, and price, by employing a two-stage stochastic programming approach. Through testing it on diverse case studies, both grid-connected and positive energy districts, the algorithm demonstrated its ability to enhance optimization robustness compared to deterministic methods. Additionally, the incorporation of PtG solutions contributed to the energy security of these systems.

- *Short-term control*: a control strategy based on Model Predictive Control (MPC) was developed for the optimal management of Multi-Energy Systems (MES). The controller uses a MILP algorithm for the optimization and it was tested on a case study that comprises a PtG system for the

generation of synthetic natural gas from renewable electricity coupled with a district heating network through waste heat recovery. The control performances were compared to that obtained with a conventional rule-based strategy through simulations in Model-in-the-Loop environment. The novel smart controller has proven its superior performance in comparison to the conventional strategy, enabling for a full decarbonization of the heating sector and consistently cost and CO_2 emissions reduction.

- *Multi-temporal and multi-spatial control architecture*: a control architecture was introduced, which integrates the first two developed tools, creating a more comprehensive solution for handling the interaction among multiple MES that are connected via a shared natural gas seasonal storage. The smart system management approach was successfully implemented, and the controller efficiently regulated the system operation utilizing the seasonal storage to balance the seasonal mismatch between production and demand.

The developed tools were tested in this thesis on specific applications, but their utilization for different case studies is straightforward, as they were developed in a general way.

Limitations

Despite the tools were successfully verified giving promising results, this work presents some limitations. First, the MPC developed in this thesis were tested in a Model-in-the-Loop environment, but they were not applied on real-world case studies. Indeed, the transition from a simulation setting to actual operational conditions could lead to complexities which were not taken into account. In addition, the technologies and case studies examined in this research may not precisely represent the real-world scenarios in practical applications. Real applications often involve a multitude of additional factors, regulations, and constraints that could not be fully considered in this study. Furthermore, even if the controller was developed with the aim to define set-points for low-level controllers, some difficulties can emerge in real applications in the communications between controllers that could lead to reconsidering this setting. Another aspect is represented by the capital costs associated with these technologies. As a matter of fact, the thesis primarily focuses on evaluating the operating costs of PtG technologies and does not comprehensively assess their capital expenditures. While they are not relevant when operating an MPC controller, when setting up new

technologies in existing energy systems they become imperative. Therefore, a broader evaluation would provide a more complete understanding of the financial implications associated with the implementation of these technologies.

Future research

Future developments of this research will include the implementation and real-world application of the novel control strategies proposed in the thesis. By testing these strategies in real-world energy systems, it will be possible to evaluate their practicality, effectiveness, and adaptability to unpredictable environments. This empirical validation will offer valuable insights into the performance and robustness of the control systems under actual conditions.

In addition, the development of advanced design tools will be evaluated. Indeed, when integrating novel technologies in energy systems, it is crucial to enhance the sizing and selection of plants, considering not only their operational efficiency but also the capital expenditures associated with their components. By creating a comprehensive design tool, the selection of cost-effective, sustainable, and optimally-sized energy systems will be possible, contributing to more informed decision-making in the planning and implementation stages.

Future researches should also explore innovative methods for improving future disturbance forecasts, as well as online update of control parameters, taking into account the degradation of components. These methods should be capable of providing real-time updates at each control time-step. By incorporating more accurate and up-to-date disturbance prediction and parameter update, the controllers could respond to external events more effectively, enhancing the resilience of energy systems.

Finally, researchers should investigate multi-objective optimization approaches to address the complex and often conflicting goals within energy systems. This entails finding the right balance between efficiency, cost-effectiveness, sustainability, and reliability. This could help in simultaneously achieving multiple objectives, ensuring a more holistic approach to energy system management and control.

Appendix A: library of energy system components

This appendix reports the characteristics of the in-house libraries of energy system component models which were used to build the *digital-twins* of the case studies for the Model-in-the-Loop applications analyzed in the thesis. The libraries were developed in the MATLAB®/Simulink® environment and they are composed by single energy system component models, which if properly connected and sized, can be used to build the desired case study.

Each model has its own causality, and considers the physical inlet, outlet and stored flows. The governing equations that describe their behavior include mass and energy conservation and involve mass flow rate, temperature, composition and pressure. Two libraries of energy system components were created so far for modeling Multi-Energy Systems:

- **DHN library**: it is used for modeling district heating networks and it is described in detail in [98]. The library is composed of the pumping station blocks (pumps and expansion vassels), the thermal power unit blocks (boilers, heat exchangers, CHPs), the heating network blocks (pipelines) and the thermal energy storage (TES). This library was proved to be a reliable tool for model different case studies in previous works [98, 105].

- **Electricity and gas network library**: it is used for modeling integrated energy systems in which electricity and gas generation and usage are present. It is composed by a generation unit block (wind farm), Power-to-Gas system blocks (electrolyzer, methanation reactor), heat pump block, gas network blocks (pipelines, compressor, valve) and gas storage block. These components were developed for the applications described in this thesis and used for modeling Multi-Energy Systems, revealing to be efficient tools [97].

In the following, an overview of the main components of the electricity and gas network library is provided, while for the DHN library the reader can refer to [98]. The main features of all components are reported in Table 6.1, using the following characteristics:

- Algebraic/Dynamic: the component is algebraic (Al) if it can be modeled using algebraic relations, while it is Dynamic (Dy) if its behavior is described by differential equations and therefore it allows a storage term (i.e. state).
- Inputs, Outputs and States: they are defined based on the chosen causality.
- Main governing equations: they are the equations embedded in the blocks, and describe the physical behavior of the component.

Wind farm

The wind farm model is an algebraic model that calculates the output electrical power produced, using as input the undisturbed wind velocity module and direction $\mathbf{u}_0$, the geometry of the wind turbines and their position in the wind farm. The power generated by each turbine is calculated using the power curve of the turbine, given the velocity of the wind. The total electrical power generated by a wind farm with N wind turbines is calculated as

$$P_{el} = \sum_{i=1}^{N} C_p(u_{wind,i}) P_{wind,i} = \sum_{i=1}^{N} C_p(u_{wind,i}) A_{r,i} \rho u_{wind,i} \,, \tag{A.1}$$

where $P_{wind,i}$ is the wind power reaching the i-th turbine of the wind farm, $A_{r,i}$ is the area of the i-th turbine rotor, ρ is the air density and $C_p(u_{wind,i})$ is the power coefficient with a wind velocity equal to $u_{wind,i}$, which is the velocity of the wind reaching the i-th turbine, corrected by taking into consideration the wake effect. Indeed, in a wind farm with many turbines, the model considers the wake effect between turbines by applying the Jensen wake model [106]. Using this method, a correction is applied to the undisturbed wind velocity, to account for the wake effect, when the turbine is located behind other turbines. For each turbine i, the corrected wind velocity module $u_{wind,i}$ is calculated starting from the undisturbed wind velocity u_0 as follows

$$u_{wind_i} = u_0 - u_{mdef,i} = u_0 - \sqrt{\sum_{j=1}^{N} u_{def,ij}} \,, \tag{A.2}$$

where the velocity deficit $u_{def,ij}$ caused by the upstream turbine j on the downstream turbine i is calculated as

$$u_{def,ij} = u_0(1 - \sqrt{1 - C_{t,j}})\left(\frac{D_{r,i}}{D_{r,i} + 2k_{w,i}x_{ij}}\right)^2 \frac{A_{overlap,ij}}{A_{r,i}}\,, \tag{A.3}$$

with $D_{r,i}$ being the downstream turbine rotor diameter and $C_{t,j}$ the thrust coefficient of the upstream turbine. In addition, $k_{w,i}$ determines the size of the expanded wake behind the wind turbine, x_{ij} is the distance between the two turbines in the wind direction and $A_{overlap}$ is the overlap area between the expanded wake area of the upstream turbine and the rotor area of the downstream wind turbine $A_{r,i}$. The direction of the wind do not change because of the wake effect. Once the corrected wind velocity $\mathbf{u}_{wind,i}$ for each turbine of the wind farm is calculated, the model uses the power curve of the turbines to calculate the electricity generated [107].

PEM electrolyzer

The model of the PEM electrolyzer is an algebraic model that calculates the amount of hydrogen and the thermal power generated by the electrolyzer, given the electrical power supplied and the operating mode. It models three operating mode: on, off (i.e. no consumption, no production, cold start-up needed to switch on), standby (i.e. no production, consumption of a certain amount of nominal electrical power, warm start-up needed to switch on). The relation for the efficiency of the electrolyzer during the operation in production mode was derived by interpolating operating data taken form the literature [108]. The relationship obtained is the following

$$\eta = \rho_{H_2} HHV_{H_2} f(P_{el})\,, \tag{A.4}$$

and it is used to calculate the hydrogen flow rate produced with the formula

$$\dot{V}_{H_2} = \frac{1}{\rho_{H_2} HHV_{H_2}} \eta P_{el}\,, \tag{A.5}$$

where ρ_{H_2} is the gas density, HHV_{H_2} its high heating value of hydrogen and P_{el} the electric power in input. The thermal power generated is calculated using the following equation

$$P_{th} = (1 - \eta)P_{el} - P_{loss}\,, \tag{A.6}$$

where P_{loss} represents the heat that cannot be recovered and it is calculated as $P_{loss} = \alpha P_{nom} + (\beta P_{el} + \gamma P_{nom})$. The first term represents the losses due to the auxiliary systems, while the latter terms constitute the linear model of the power losses in the conversion from AC to DC.

Methanation reactor

The methanation reactor model is an algebraic model and correlates the input hydrogen flow to the output methane flow and thermal power generated. As for the electrolyzer, three operating modes are modeled: on, off and standby. During the operation in production mode, the output flow is calculated using the chemical reaction for methane generation starting from water and carbon dioxide

$$4H_2 + CO_2 \rightarrow yCH_4 + y2H_2O + (4 - 4y)H_2 + (1 - y)CO_2\,. \tag{A.7}$$

The yield of reaction y is calculated based on linear interpolation of experimental data taken from the literature [109], as follows

$$y = f(GHSV)\,, \tag{A.8}$$

where GHSV (gas hourly space velocity) is the rate between the total volumetric flow rate entering the reactor and the reactor volume, and evaluates the load of the reactor:

$$GHSV = \frac{\dot{m}_{H_2,in} + \dot{m}_{CO_2,in}}{V_{reactor}}\,. \tag{A.9}$$

Gas compressor

The compressor model is an algebraic model that calculates the output flow and the electrical power consumption, given as inputs the rotational speed, the input flow and the output desired pressure of the compressor. For the calculation of the corrected mass flow rate $\dot{m}$ and of the polytropic efficiency η_p the block employs the performance maps of turbocompressor (Figures 6.1 and 6.2), using the corrected rotational speed N_c and the pressure ratio Π as inputs. It is worth mentioning that the corrected mass flow rate and the polytropic efficiency have been considered constant in the choking area, since no data was available for that operating region.

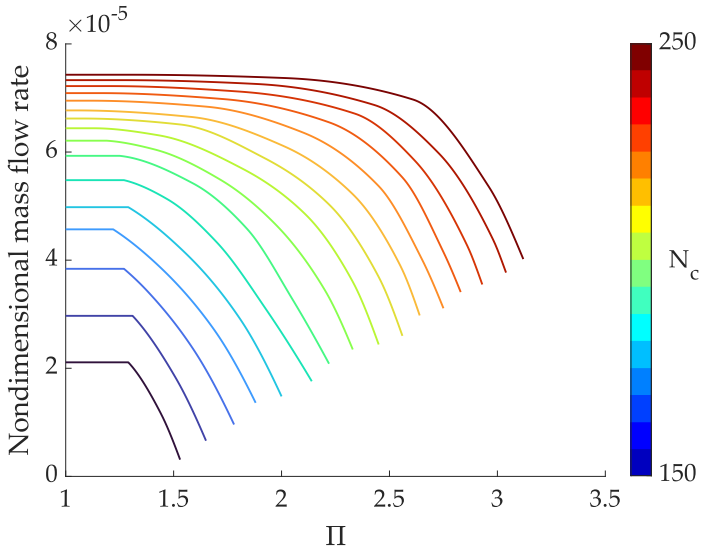

Figure 6.1: Turbocompressor performance map for mass flow rate.

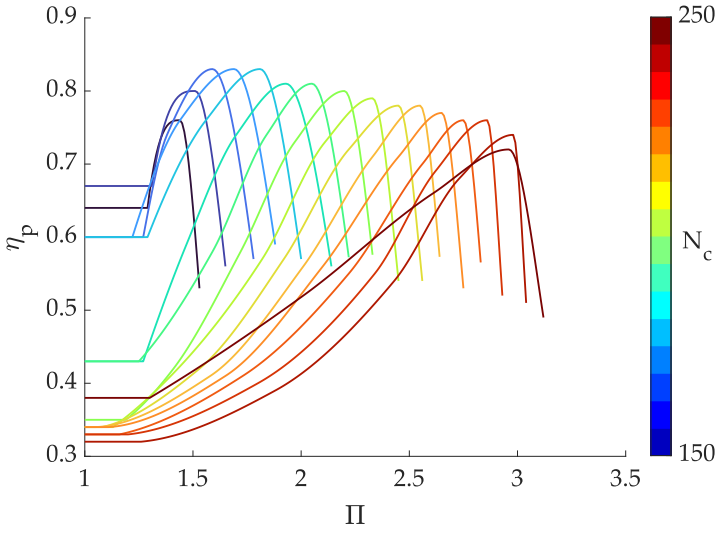

Figure 6.2: Turbocompressor performance map for polytropic efficiency.

Gas storage

The gas storage model is a dynamic model and it represents a node in which the input gas flow is mixed with the gas inside the storage. In terms of causality, incoming and outcoming flows are inputs to the model, and they are used to calculate the pressure, temperature and composition of the gas contained in the storage. The energy stored is estimated using the gas HHV and the gases are described using the perfect gas equation of state.

The mass balance equation for the gas is the following

$$\frac{dm_g}{dt} = \dot{m}_{g,in} - \dot{m}_{g,out}\,, \tag{A.10}$$

and it allows the calculation of the mass and molar composition of gases in the volume. The energy balance equation allows the calculation of the gas temperature and it is as follows

$$\frac{dT_g}{dt} = \frac{\Delta\dot{H}_g - c_v T_g \frac{dm_g}{dt} - m_g T_g \sum_i \frac{\partial c_v}{\partial w_i}\frac{dw_i}{dt}}{c_v m_g + m_g T_g \frac{\partial c_v}{\partial T}}\,, \tag{A.11}$$

with c_v being the specific heat of the gas at constant volume, w_i the mass fraction of the i-th gas species and $\Delta\dot{H}_g$ the power linked to the enthalpy flows of the gas phase species and it is calculated as

$$\Delta\dot{H}_g = \dot{H}_{g,in} - \dot{H}_{g,out} = \left[(\dot{m}_g c_p T)_{in} - (\dot{m}_g c_p T)_{out}\right]. \tag{A.12}$$

Finally, the partial pressure for each species is calculated as

$$p_i = \frac{m_i RT}{M_i V}\,. \tag{A.13}$$

Water condenser

The water condenser model is a dynamic model that calculates the pressure, temperature, amount of water condensed and composition of the gas exiting the condenser, using the incoming and outcoming flows. It models a wet mixture that enters the condenser, is cooled and therefore the steam condenses by accumulating liquid water at the base of a discharger. When the water reaches a certain level, the drain opens and the water flows out in a liquid state, while the dry gas mixture exits the condenser from another outlet.

The mass and molar composition of the gases in the volume are calculated using the mass balance equation for gases, as follows

$$\frac{dm_g}{dt} = \dot{m}_{g,in} - \dot{m}_{g,out} - \dot{m}_{H_2O,cond}\,, \tag{A.14}$$

the volume of the condensed water is calculated using the mass balance equation for the liquid water

$$\frac{dm_{h_2O}}{dt} = \dot{m}_{H_2O,cond} - \dot{m}_{H_2O,out}\,, \tag{A.15}$$

and the temperature of the gases in the condensate discharger is estimated using the energy balance equation for gases

$$\frac{dT_g}{dt} = \frac{\Delta\dot{H}_g - \dot{H}_{H_2O} - P - \dot{Q}_{sc} - c_v T_g \frac{dm_g}{dt} - m_g T_g \sum_i \frac{\partial c_v}{\partial w_i}\frac{dw_i}{dt}}{c_v m_g + m_g T_g \frac{\partial c_v}{\partial T}}\,, \tag{A.16}$$

where w_i is the mass fraction of the i-th gas species, P is the power due to the work related to the volume change

$$P = p\frac{dV_g}{dt}\,, \tag{A.17}$$

and $\Delta\dot{H}_g$ is the power linked to the enthalpy flows of the gas phase species. The latter is calculated as

$$\Delta\dot{H}_g = \dot{H}_{g,in} - \dot{H}_{g,out} = \dot{m}_g[(c_pT)_{in} - (c - pT)_{out}] + \dot{m}_{cond} r_v + [(\dot{m}_v c_p T)_{in} - (\dot{m}_v c_p T)_{out}]\,. \tag{A.18}$$

Finally, the Antoine's law is used to determine the water steam flow rate that condenses, using the saturation pressure value of water p_s

$$\log_{10} p_s = A - \frac{B}{T + C}\,, \tag{A.19}$$

where A, B, C are constants, experimentally obtained, and T is the temperature in degree Celsius. The partial pressure for each species is calculated as

$$\frac{dp_i}{dt} = \frac{RT}{M_i V}\sum_i \dot{m}_i - \frac{p_i}{V}\frac{dV}{dt} + \frac{p_i}{T}\frac{dT}{dt}\,. \tag{A.20}$$

Gas pipeline

The gas pipeline model is a dynamic model that returns the output mass flow rate and temperature of the gas, given the inlet pressure, temperature and composition, and the outlet pressure. The mass flow rate is calculated with the following equation

$$\dot{m} = sign(\Delta p)\sqrt{\frac{|\Delta p|\rho A_{in}}{\frac{fL}{D_{in}} + Z}}\,, \tag{A.21}$$

where Δp is the pressure drop in the pipeline, A_{in} the cross-section area of the pipeline, ρ the gas density, f the friction factor, L the pipe length, D_{in} the inner diameter, Z represents the total concentrated pressure drop. The governing

equation for the temperature is

$$\frac{dT_{out}}{dt} = \frac{1}{\rho c_v V}\left(\dot{m}\left[(c_p T)_{in} - (c_p T)_{out}\right] - \dot{Q}_w\right), \tag{A.22}$$

where c_p is the gas specific heat at constant pressure, c_v the average gas specific heat at constant volume, V the volume of the pipeline and $\dot{Q}_w$ the heat exchanged through the wall.

Heat pump

The heat pump model is an algebraic model that returns the thermal power absorbed and supplied by the heat pump, given the temperature of the cold and hot sources (T_{cold} and T_{hot}) and the electrical power used P_{el}. The actual COP is estimated using the following equation

$$COP = \frac{COP_{nom}}{C_c(1-(1-C_c)}\frac{P_{el,nom}}{P_{el}}, \tag{A.23}$$

where C_c is a correction factor, which is usually declared by the manufacturer, $COP_{nom} = \frac{COP_{max}}{\eta_{II}}$ and η_{II} is the second principle efficiency and it is calculated using a lookup table with $\eta_{II} = f(T_{cold}, T_{hot})$.

Gas pressure reduction valve

The gas pressure reduction valve model is an algebraic model that returns the mass flow rate through the valve, using as inputs the income and outcome pressure, temperature and composition of the gas, and the opening ratio of the valve. The mass flow rate is estimated using the expansion factor Y, which can be calculated as

$$Y = 1 - \frac{1}{3}\left(\frac{X}{F_k X_T}\right), \tag{A.24}$$

where

$$X = \frac{\Delta p}{p_{in}}, \tag{A.25}$$

F_k is the ratio between the k of the gas and the k of air $F_k = k/k_{air}$ and X_T is the value of X when Y reaches its minimum value ($Y = 2/3$).

Then, if $\frac{2}{3} \leq Y \leq 1$, namely when the gas is in sub-critical conditions, the

mass flow rate is calculated as

$$\dot{m} = N_x c_v Y \sqrt{X p_{in} \rho_{in}}\,, \tag{A.26}$$

where N_x is a coefficient introduced to match the measurement units used. When $Y = \frac{2}{3}$, instead, the fluid is in super-critical conditions and, being $X = X_T$, the mass flow rate equation becomes

$$\dot{m} = N_x c_v \frac{2}{3} \sqrt{X_T p_{in} \rho_{in}}\,. \tag{A.27}$$

Component	Al/Dy	Inputs	Outputs	States
Wind farm	Al	$\mathbf{u}_{wind}$	P_{el}	-
Electrolyzer	Al	P_{el}	$\dot{m}_{out}, T_{out}, x_{out}, p_{out}$	-
		Op. mode	$\dot{m}_{H_2O}$, P_{th}, P_{loss}	
Methanation reactor	Al	$\dot{m}_{in}, T_{in}, x_{in}$	$\dot{m}_{out}, T_{out}, x_{out}$	-
		Op. mode	P_{th}, P_{loss}	
Gas compressor	Al	n, $p_{in}, p_{out}, T_{in}, x_{in}$	$\dot{m}, T_{out}, x_{out}$, P_{el}	-
Gas storage	Dy	$\dot{m}_{in}, T_{in}, x_{in}$	$p_{stor}, T_{stor}, x_{stor}$	$p_{stor}, T_{stor}, x_{stor}$
Gas pipeline	Dy	$p_{in}, T_{in}, x_{in}, p_{out}$	$\dot{m}_{out}, T_{out}, x_{out}$	T_{pipe}
Heat pump	Al	T_{hot}, T_{cold}, P_{el}	$P_{th_{out}}$, $P_{th_{in}}$	-
Gas pressure reduction valve	Al	p_{in}, T_{in}, x_{in}	$\dot{m}_{out}, T_{out}, x_{out}$	-
		$p_{out}, T_{out}, x_{out}$		
		ϕ		
Water condenser	Dy	$\dot{m}_{in}, T_{in}, x_{in}$	$p_{node}, T_{node}, x_{node}$	$p_{node}, T_{node}, x_{node}$
Boiler	Al	$\dot{m}_f$	P_{th}	-
Pump	Al	n, H	$\dot{m}_w$	-
Expansion vessel	Dy	$\dot{m}_{in}$, $\dot{m}_{out}$	p_w	V_w
Water pipeline	Dy	$\dot{m}_{w,in}$, $T_{w,in}$, p_{out}	$\dot{m}_{w,out}$, $T_{w,out}$	$T_{w,pipe}$
Heat exchanger	Dy	$\dot{m}_{w,in}$, $T_{w,in}$, $p_{w,in}$, P_{th}	$p_{w,out}$, $T_{w,out}$	T_w

Table 6.1: System components summary. (Al = Algebraic, Dy = Dynamic, Op. mode = Operating mode)

Bibliography

[1] A. Berjawi, S. Walker, C. Patsios, and S. Hosseini, "An evaluation framework for future integrated energy systems: A whole energy systems approach," *Renewable and Sustainable Energy Reviews*, vol. 145, p. 111163, 2021.

[2] M. Hasanuzzaman, U. S. Zubir, N. I. Ilham, and H. Seng Che, "Global electricity demand, generation, grid system, and renewable energy polices: a review," *Wiley Interdisciplinary Reviews: Energy and Environment*, vol. 6, no. 3, p. e222, 2017.

[3] M. S. Lester, R. Bramstoft, and M. Münster, "Analysis on electrofuels in future energy systems: A 2050 case study," *Energy*, vol. 199, p. 117408, 2020.

[4] A. Goldmann, W. Sauter, M. Oettinger, T. Kluge, U. Schröder, J. R. Seume, J. Friedrichs, and F. Dinkelacker, "A study on electrofuels in aviation," *Energies*, vol. 11, no. 2, p. 392, 2018.

[5] E. Marzi, M. Morini, and A. Gambarotta, "Analysis of the status of research and innovation actions on electrofuels under horizon 2020," *Energies*, vol. 15, no. 2, p. 618, 2022.

[6] B. Xiong, J. Predel, P. C. del Granado, and R. Egging-Bratseth, "Spatial flexibility in redispatch: Supporting low carbon energy systems with power-to-gas," *Applied Energy*, vol. 283, p. 116201, 2021.

[7] G. A. Powerfuels, "Powerfuels: Missing link to a successful global energy transition," 2019.

[8] W. E. Council, "E-storage: Shifting from cost to value: Wind and solar applications," 2016.

[9] S. Schiebahn, T. Grube, M. Robinius, V. Tietze, B. Kumar, and D. Stolten, "Power to gas: Technological overview, systems analysis and economic assessment for a case study in germany," *International journal of hydrogen energy*, vol. 40, no. 12, pp. 4285–4294, 2015.

[10] Q. I. Roode-Gutzmer, D. Kaiser, and M. Bertau, "Renewable methanol synthesis," *ChemBioEng Reviews*, vol. 6, no. 6, pp. 209–236, 2019.

[11] M. Götz, J. Lefebvre, F. Mörs, A. M. Koch, F. Graf, S. Bajohr, R. Reimert, and T. Kolb, "Renewable power-to-gas: A technological and economic review," *Renewable energy*, vol. 85, pp. 1371–1390, 2016.

[12] H.-I. Ji, J.-H. Lee, J.-W. Son, K. J. Yoon, S. Yang, and B.-K. Kim, "Protonic ceramic electrolysis cells for fuel production: a brief review," *Journal of the Korean Ceramic Society*, vol. 57, pp. 480–494, 2020.

[13] Z. Zakaria and S. K. Kamarudin, "A review of alkaline solid polymer membrane in the application of aem electrolyzer: Materials and characterization," *International Journal of Energy Research*, vol. 45, no. 13, pp. 18337–18354, 2021.

[14] C. Li and J.-B. Baek, "The promise of hydrogen production from alkaline anion exchange membrane electrolyzers," *Nano Energy*, vol. 87, p. 106162, 2021.

[15] G. Soloveichik, "Electrochemical synthesis of ammonia as a potential alternative to the haber–bosch process," *Nature Catalysis*, vol. 2, no. 5, pp. 377–380, 2019.

[16] P. Mancarella, "Mes (multi-energy systems): An overview of concepts and evaluation models," *Energy*, vol. 65, pp. 1–17, 2014.

[17] C. Klemm and P. Vennemann, "Modeling and optimization of multi-energy systems in mixed-use districts: A review of existing methods and approaches," *Renewable and Sustainable Energy Reviews*, vol. 135, p. 110206, 2021.

[18] C. Papadimitriou, M. Di Somma, C. Charalambous, M. Caliano, V. Palladino, A. F. Cortés Borray, A. González-Garrido, N. Ruiz, and G. Graditi,

"A comprehensive review of the design and operation optimization of energy hubs and their interaction with the markets and external networks," *Energies*, vol. 16, no. 10, p. 4018, 2023.

[19] P. C. Blaud, P. Haurant, F. Claveau, B. Lacarrière, P. Chevrel, and A. Mouraud, "Modelling and control of multi-energy systems through multi-prosumer node and economic model predictive control," *International Journal of Electrical Power & Energy Systems*, vol. 118, p. 105778, 2020.

[20] L. Zhang, W. Dai, B. Zhao, X. Zhang, M. Liu, Q. Wu, and J. Chen, "Multi-time-scale economic scheduling method for electro-hydrogen integrated energy system based on day-ahead long-time-scale and intra-day mpc hierarchical rolling optimization," *Frontiers in Energy Research*, vol. 11, p. 1132005, 2023.

[21] L. Taccari, E. Amaldi, E. Martelli, and A. Bischi, "Short-term planning of cogeneration power plants: a comparison between minlp and piecewise-linear milp formulations," in *Computer Aided Chemical Engineering*, vol. 37, pp. 2429–2434, Elsevier, 2015.

[22] CBC Solver website. Url: https://github.com/coin-or/Cbc.

[23] Gurobi Optimization website. Url: https://www.gurobi.com/.

[24] The Community Research and Development Information Service. Url: https://cordis.europa.eu/.

[25] Fuel Cells and Hydrogen Joint Undertaking website. Url: https://www.fch.europa.eu/.

[26] ERA-Net Smart Energy Systems website. Url: https://www.eranet-smartenergysystems.eu/.

[27] F. Dolci, D. Thomas, S. Hilliard, C. F. Guerra, R. Hancke, H. Ito, M. Jegoux, G. Kreeft, J. Leaver, M. Newborough, *et al.*, "Incentives and legal barriers for power-to-hydrogen pathways: An international snapshot," *international journal of hydrogen energy*, vol. 44, no. 23, pp. 11394–11401, 2019.

[28] I. Sorrenti, T. B. H. Rasmussen, S. You, and Q. Wu, "The role of power-to-x in hybrid renewable energy systems: A comprehensive review," *Renewable and Sustainable Energy Reviews*, vol. 165, p. 112380, 2022.

[29] E. Guelpa, A. Bischi, V. Verda, M. Chertkov, and H. Lund, "Towards future infrastructures for sustainable multi-energy systems: A review," *Energy*, vol. 184, pp. 2–21, 2019.

[30] A. Barbaresi, M. Morini, and A. Gambarotta, "Review on the status of the research on power-to-gas experimental activities," *Energies*, vol. 15, no. 16, p. 5942, 2022.

[31] M. Bailera, P. Lisbona, L. M. Romeo, and S. Espatolero, "Power to gas projects review: Lab, pilot and demo plants for storing renewable energy and co2," *Renewable and Sustainable Energy Reviews*, vol. 69, pp. 292–312, 2017.

[32] S. Clegg and P. Mancarella, "Integrated modeling and assessment of the operational impact of power-to-gas (p2g) on electrical and gas transmission networks," *IEEE Transactions on Sustainable Energy*, vol. 6, no. 4, pp. 1234–1244, 2015.

[33] W. Liu, F. Wen, and Y. Xue, "Power-to-gas technology in energy systems: current status and prospects of potential operation strategies," *Journal of modern power systems and clean energy*, vol. 5, no. 3, pp. 439–450, 2017.

[34] Y. Chen, Z. Yuan, and B. Chen, "Process optimization with consideration of uncertainties—an overview," *Chinese journal of chemical engineering*, vol. 26, no. 8, pp. 1700–1706, 2018.

[35] P. Gabrielli, F. Fürer, G. Mavromatidis, and M. Mazzotti, "Robust and optimal design of multi-energy systems with seasonal storage through uncertainty analysis," *Applied energy*, vol. 238, pp. 1192–1210, 2019.

[36] Z. Wang, J. Hu, and B. Liu, "Stochastic optimal dispatching strategy of electricity-hydrogen-gas-heat integrated energy system based on improved spectral clustering method," *International Journal of Electrical Power & Energy Systems*, vol. 126, p. 106495, 2021.

[37] J. Duan, Y. Yang, and F. Liu, "Distributed optimization of integrated electricity-natural gas distribution networks considering wind power uncertainties," *International Journal of Electrical Power & Energy Systems*, vol. 135, p. 107460, 2022.

[38] B. Liu and Y. Wang, "Energy system optimization under uncertainties: A comprehensive review," *Towards Sustainable Chemical Processes*, pp. 149–170, 2020.

[39] Z. Zheng, X. Li, J. Pan, and X. Luo, "A multi-year two-stage stochastic programming model for optimal design and operation of residential photovoltaic-battery systems," *Energy and Buildings*, vol. 239, p. 110835, 2021.

[40] M. Farrokhifar, F. H. Aghdam, A. Alahyari, A. Monavari, and A. Safari, "Optimal energy management and sizing of renewable energy and battery systems in residential sectors via a stochastic milp model," *Electric Power Systems Research*, vol. 187, p. 106483, 2020.

[41] Y.-H. Huang, J.-H. Wu, and Y.-J. Hsu, "Two-stage stochastic programming model for the regional-scale electricity planning under demand uncertainty," *Energy*, vol. 116, pp. 1145–1157, 2016.

[42] A. Nazari and R. Keypour, "A two-stage stochastic model for energy storage planning in a microgrid incorporating bilateral contracts and demand response program," *Journal of Energy Storage*, vol. 21, pp. 281–294, 2019.

[43] S. Lin, C. Liu, Y. Shen, F. Li, D. Li, and Y. Fu, "Stochastic planning of integrated energy system via frank-copula function and scenario reduction," *IEEE Transactions on Smart Grid*, vol. 13, no. 1, pp. 202–212, 2021.

[44] N. Eghbali, S. M. Hakimi, A. Hasankhani, G. Derakhshan, and B. Abdi, "Stochastic energy management for a renewable energy based microgrid considering battery, hydrogen storage, and demand response," *Sustainable Energy, Grids and Networks*, vol. 30, p. 100652, 2022.

[45] X. Song, C. Lin, R. Zhang, T. Jiang, and H. Chen, "Two-stage stochastic scheduling of integrated electricity and natural gas systems considering ramping costs with power-to-gas storage and wind power," *Frontiers in Energy Research*, p. 289, 2020.

[46] M. Rahimi, F. J. Ardakani, and A. J. Ardakani, "Optimal stochastic scheduling of electrical and thermal renewable and non-renewable resources in virtual power plant," *International Journal of Electrical Power & Energy Systems*, vol. 127, p. 106658, 2021.

[47] I. Gomes, R. Melicio, and V. Mendes, "A novel microgrid support management system based on stochastic mixed-integer linear programming," *Energy*, vol. 223, p. 120030, 2021.

[48] A. S. Farsangi, S. Hadayeghparast, M. Mehdinejad, and H. Shayanfar, "A novel stochastic energy management of a microgrid with various types of distributed energy resources in presence of demand response programs," *Energy*, vol. 160, pp. 257–274, 2018.

[49] V. Shabazbegian, H. Ameli, M. T. Ameli, and G. Strbac, "Stochastic optimization model for coordinated operation of natural gas and electricity networks," *Computers & Chemical Engineering*, vol. 142, p. 107060, 2020.

[50] S. F. Zandrazavi, C. P. Guzman, A. T. Pozos, J. Quiros-Tortos, and J. F. Franco, "Stochastic multi-objective optimal energy management of grid-connected unbalanced microgrids with renewable energy generation and plug-in electric vehicles," *Energy*, vol. 241, p. 122884, 2022.

[51] J. Aghaei, T. Niknam, R. Azizipanah-Abarghooee, and J. M. Arroyo, "Scenario-based dynamic economic emission dispatch considering load and wind power uncertainties," *International Journal of Electrical Power & Energy Systems*, vol. 47, pp. 351–367, 2013.

[52] C. A. Correa-Florez, A. Gerossier, A. Michiorri, and G. Kariniotakis, "Stochastic operation of home energy management systems including battery cycling," *Applied energy*, vol. 225, pp. 1205–1218, 2018.

[53] T. M. Alabi, F. D. Agbajor, Z. Yang, L. Lu, and A. J. Ogungbile, "Strategic potential of multi-energy system towards carbon neutrality: A forward-looking overview," *Energy and Built Environment*, vol. 4, no. 6, pp. 689–708, 2023.

[54] Y. Zong, W. Su, J. Wang, J. K. Rodek, C. Jiang, M. H. Christensen, S. You, Y. Zhou, and S. Mu, "Model predictive control for smart buildings to provide the demand side flexibility in the multi-carrier energy context:

Current status, pros and cons, feasibility and barriers," *Energy procedia*, vol. 158, pp. 3026–3031, 2019.

[55] Y. Xu, A. Parisio, and Z. Ding, "Hierarchical model predictive control for energy efficient buildings with multi-energy storage systems," in *2020 IEEE Power & Energy Society General Meeting (PESGM)*, pp. 1–5, IEEE, 2020.

[56] D. Zhang, X. Han, and C. Deng, "Review on the research and practice of deep learning and reinforcement learning in smart grids," *CSEE Journal of Power and Energy Systems*, vol. 4, no. 3, pp. 362–370, 2018.

[57] R. Nian, J. Liu, and B. Huang, "A review on reinforcement learning: Introduction and applications in industrial process control," *Computers & Chemical Engineering*, vol. 139, p. 106886, 2020.

[58] D. Görges, "Relations between model predictive control and reinforcement learning," *IFAC-PapersOnLine*, vol. 50, no. 1, pp. 4920–4928, 2017.

[59] A. Turk, Q. Wu, and M. Zhang, "Model predictive control based real-time scheduling for balancing multiple uncertainties in integrated energy system with power-to-x," *International Journal of Electrical Power & Energy Systems*, vol. 130, p. 107015, 2021.

[60] M. B. Abdelghany, M. F. Shehzad, V. Mariani, D. Liuzza, and L. Glielmo, "Two-stage model predictive control for a hydrogen-based storage system paired to a wind farm towards green hydrogen production for fuel cell electric vehicles," *International Journal of Hydrogen Energy*, vol. 47, no. 75, pp. 32202–32222, 2022.

[61] D. Fischer, F. Kaufmann, R. Hollinger, and C. Voglstätter, "Real live demonstration of mpc for a power-to-gas plant," *Applied Energy*, vol. 228, pp. 833–842, 2018.

[62] C. Huang, Y. Zong, S. You, and C. Træholt, "Economic model predictive control for multi-energy system considering hydrogen-thermal-electric dynamics and waste heat recovery of mw-level alkaline electrolyzer," *Energy Conversion and Management*, vol. 265, p. 115697, 2022.

[63] C. Huang, Y. Zong, S. You, C. Træholt, Y. Zheng, J. Wang, Z. Zheng, and X. Xiao, "Economic and resilient operation of hydrogen-based microgrids:

An improved mpc-based optimal scheduling scheme considering security constraints of hydrogen facilities," *Applied Energy*, vol. 335, p. 120762, 2023.

[64] H. Böhm, S. Moser, S. Puschnigg, and A. Zauner, "Power-to-hydrogen & district heating: Technology-based and infrastructure-oriented analysis of (future) sector coupling potentials," *International Journal of Hydrogen Energy*, vol. 46, no. 63, pp. 31938–31951, 2021.

[65] J. Ikäheimo, "Power-to-gas plants in a future nordic district heating system," *Energy procedia*, vol. 135, pp. 172–182, 2017.

[66] R. Weiss, H. Saastamoinen, J. Ikäheimo, R. Abdurafikov, T. Sihvonen, and J. Shemeikka, "Decarbonised district heat, electricity and synthetic renewable gas in wind-and solar-based district energy systems," *Journal of Sustainable Development of Energy, Water and Environment Systems*, vol. 9, no. 2, pp. 1–22, 2021.

[67] G. Darivianakis, A. Eichler, R. S. Smith, and J. Lygeros, "A data-driven stochastic optimization approach to the seasonal storage energy management," *IEEE control systems letters*, vol. 1, no. 2, pp. 394–399, 2017.

[68] B. Thaler, S. Posch, A. Wimmer, and G. Pirker, "Hybrid model predictive control of renewable microgrids and seasonal hydrogen storage," *International Journal of Hydrogen Energy*, 2023.

[69] S. O. Weber, M. Oei, M. Linder, M. Böhm, P. Leistner, and O. Sawodny, "Model predictive approaches for cost-efficient building climate control with seasonal energy storage," *Energy and Buildings*, vol. 270, p. 112285, 2022.

[70] M. Petrollese, L. Valverde, D. Cocco, G. Cau, and J. Guerra, "Real-time integration of optimal generation scheduling with mpc for the energy management of a renewable hydrogen-based microgrid," *Applied Energy*, vol. 166, pp. 96–106, 2016.

[71] É. Cuisinier, P. Lemaire, B. Penz, A. Ruby, and C. Bourasseau, "New rolling horizon optimization approaches to balance short-term and long-term decisions: An application to energy planning," *Energy*, vol. 245, p. 122773, 2022.

[72] A. F. Castelli, L. Moretti, G. Manzolini, and E. Martelli, "Robust optimization of seasonal, day-ahead and real time operation of aggregated energy systems," *International Journal of Electrical Power & Energy Systems*, vol. 152, p. 109190, 2023.

[73] E. Marzi, M. Morini, C. Saletti, S. Vouros, V. Zaccaria, K. Kyprianidis, and A. Gambarotta, "Power-to-gas for energy system flexibility under uncertainty in demand, production and price," *Energy*, p. 129212, 2023.

[74] PuLP library documentation. Url: https://coin-or.github.io/pulp/.

[75] S. Mohammadi, S. Soleymani, and B. Mozafari, "Scenario-based stochastic operation management of microgrid including wind, photovoltaic, microturbine, fuel cell and energy storage devices," *International Journal of Electrical Power & Energy Systems*, vol. 54, pp. 525–535, 2014.

[76] L. Wu, M. Shahidehpour, and T. Li, "Stochastic security-constrained unit commitment," *IEEE Transactions on power systems*, vol. 22, no. 2, pp. 800–811, 2007.

[77] M. Friman, 2020. Techno-economic analysis of solar powered hydrogen production in vicinity of Swedish steel industries.

[78] Mälarenergi AB. Kraftvärmeverket Västerås.
Url: https://www.malarenergi.se/om-malarenergi/framtidens-samhalle/vara-anlaggningar/kraftvarmeverket-vasteras/.

[79] Mälarenergi AB. A combined heat and power plant under constant development. Url: https://www.malarenergi.se/globalassets/dokument/anlaggningar/kraftvarmeverk_utv_eng.pdf.

[80] A. Buttler and H. Spliethoff, "Current status of water electrolysis for energy storage, grid balancing and sector coupling via power-to-gas and power-to-liquids: A review," *Renewable and Sustainable Energy Reviews*, vol. 82, pp. 2440–2454, 2018.

[81] S. Mekhilef, R. Saidur, and A. Safari, "Comparative study of different fuel cell technologies," *Renewable and Sustainable Energy Reviews*, vol. 16, no. 1, pp. 981–989, 2012.

[82] C. Arpagaus, F. Bless, M. Uhlmann, J. Schiffmann, and S. S. Bertsch, "High temperature heat pumps: Market overview, state of the art, research status, refrigerants, and application potentials," *Energy*, vol. 152, pp. 985–1010, 2018.

[83] D. Steen, M. Stadler, G. Cardoso, M. Groissböck, N. DeForest, and C. Marnay, "Modeling of thermal storage systems in milp distributed energy resource models," *Applied Energy*, vol. 137, pp. 782–792, 2015.

[84] P. Gabrielli, M. Gazzani, E. Martelli, and M. Mazzotti, "Optimal design of multi-energy systems with seasonal storage," *Applied Energy*, vol. 219, pp. 408–424, 2018.

[85] J. Andersson and S. Grönkvist, "Large-scale storage of hydrogen," *International journal of hydrogen energy*, vol. 44, no. 23, pp. 11901–11919, 2019.

[86] H. Bahlawan, E. Losi, L. Manservigi, M. Morini, P. R. Spina, and M. Venturini, "Analysis of a multi-generation renewable energy system with hydrogen-fueled gas turbine," *Journal of Engineering for Gas Turbines and Power*, 2022.

[87] A. Gröngröft, G. C. de Paiva, S. Hauschild, D. Matschegg, D. J. Spekreijse, A. Sagani, V. Tzelepi, and D. Kourkoumpas, "Report on the case study of swedish biofuels," *Swedish Biofuel*, 2021.

[88] T. Broberg, E. Dijkgraaf, and S. Meens-Eriksson, "Burn or let them bury? the net social cost of producing district heating from imported waste," *Energy Economics*, vol. 105, p. 105713, 2022.

[89] Nord Pool Website. Url: https://www.nordpoolgroup.com/en/.

[90] M. Jangsten, P. Filipsson, T. Lindholm, and J.-O. Dalenbäck, "High temperature district cooling: challenges and possibilities based on an existing district cooling system and its connected buildings," *Energy*, vol. 199, p. 117407, 2020.

[91] C. Saletti, M. Morini, and A. Gambarotta, "Smart management of integrated energy systems through co-optimization with long and short horizons," *Energy*, vol. 250, p. 123748, 2022.

[92] M. Ellis, H. Durand, and P. D. Christofides, "A tutorial review of economic model predictive control methods," *Journal of Process Control*, vol. 24, no. 8, pp. 1156–1178, 2014.

[93] A. Bischi, L. Taccari, E. Martelli, E. Amaldi, G. Manzolini, P. Silva, S. Campanari, and E. Macchi, "A detailed milp optimization model for combined cooling, heat and power system operation planning," *Energy*, vol. 74, pp. 12–26, 2014.

[94] L. Maier, M. Schönegge, S. Henn, D. Hering, and D. Müller, "Assessing mixed-integer-based heat pump modeling approaches for model predictive control applications in buildings," *Applied Energy*, vol. 326, p. 119894, 2022.

[95] C. D'Ambrosio, A. Lodi, and S. Martello, "Piecewise linear approximation of functions of two variables in milp models," *Operations Research Letters*, vol. 38, no. 1, pp. 39–46, 2010.

[96] M. Carrión and J. M. Arroyo, "A computationally efficient mixed-integer linear formulation for the thermal unit commitment problem," *IEEE Transactions on power systems*, vol. 21, no. 3, pp. 1371–1378, 2006.

[97] A. Gambarotta, F. Ghionda, E. Marzi, M. Morini, and C. Saletti, "Optimal integration of power-to-gas and district heating through waste heat recovery from electrofuel production," in *10.52202/069564-0221*, ECOS2023 - 36th International Conference on efficiency, cost, optimization, simulation and environmental impact of energy systems, 2023.

[98] A. De Lorenzi, A. Gambarotta, M. Morini, M. Rossi, and C. Saletti, "Setup and testing of smart controllers for small-scale district heating networks: An integrated framework," *Energy*, vol. 205, p. 118054, 2020.

[99] Statista 2023 – Carbon intensity of the power sector in Italy from 2000 to 2021. Url: https://www.statista.com/statistics/1290244/carbon-intensity-power-sector-italy/.

[100] Specific carbon dioxide emissions of various fuels. Url: https://www.volker-quaschning.de/datserv/CO2-spez/index_e.php.

[101] B. Meindl and M. Templ, "Analysis of commercial and free and open source solvers for linear optimization problems," *Eurostat and Statistics Nether-*

lands within the project ESSnet on common tools and harmonised methodology for SDC in the ESS, vol. 20, 2012.

[102] DISTRHEAT - Digital Intelligent and Scalable Control for Renewables in Heating Networks - project website. Url: https://www.distrheat.eu/.

[103] Photovoltaic Geographical Information System (PVGIS). Url: https://re.jrc.ec.europa.eu/pvg_tools/en/.

[104] Global Wind Atlas. Url: https://globalwindatlas.info/en.

[105] A. De Lorenzi, A. Gambarotta, E. Marzi, M. Morini, and C. Saletti, "Predictive control of a combined heat and power plant for grid flexibility under demand uncertainty," *Applied Energy*, vol. 314, p. 118934, 2022.

[106] N. O. Jensen, *A note on wind generator interaction*, vol. 2411. Citeseer, 1983.

[107] K. Yang, G. Kwak, K. Cho, and J. Huh, "Wind farm layout optimization for wake effect uniformity," *Energy*, vol. 183, pp. 983–995, 2019.

[108] M. Kopp, D. Coleman, C. Stiller, K. Scheffer, J. Aichinger, and B. Scheppat, "Energiepark mainz: Technical and economic analysis of the worldwide largest power-to-gas plant with pem electrolysis," *International Journal of Hydrogen Energy*, vol. 42, no. 19, pp. 13311–13320, 2017.

[109] O. Lemaire. Liten Ceatech - two key technologies for power-to-gas, compact methanation reactors. Url: https://www.cea.fr/ceatech/english/Documents/CEA_Tech_Japan/COMPILATION%20LITEN.pdf.